World Scientific Series in Contemporary Chemical Physics – Vol. 20

TOWARDS A NONLINEAR QUANTUM PHYSICS

J R Croca

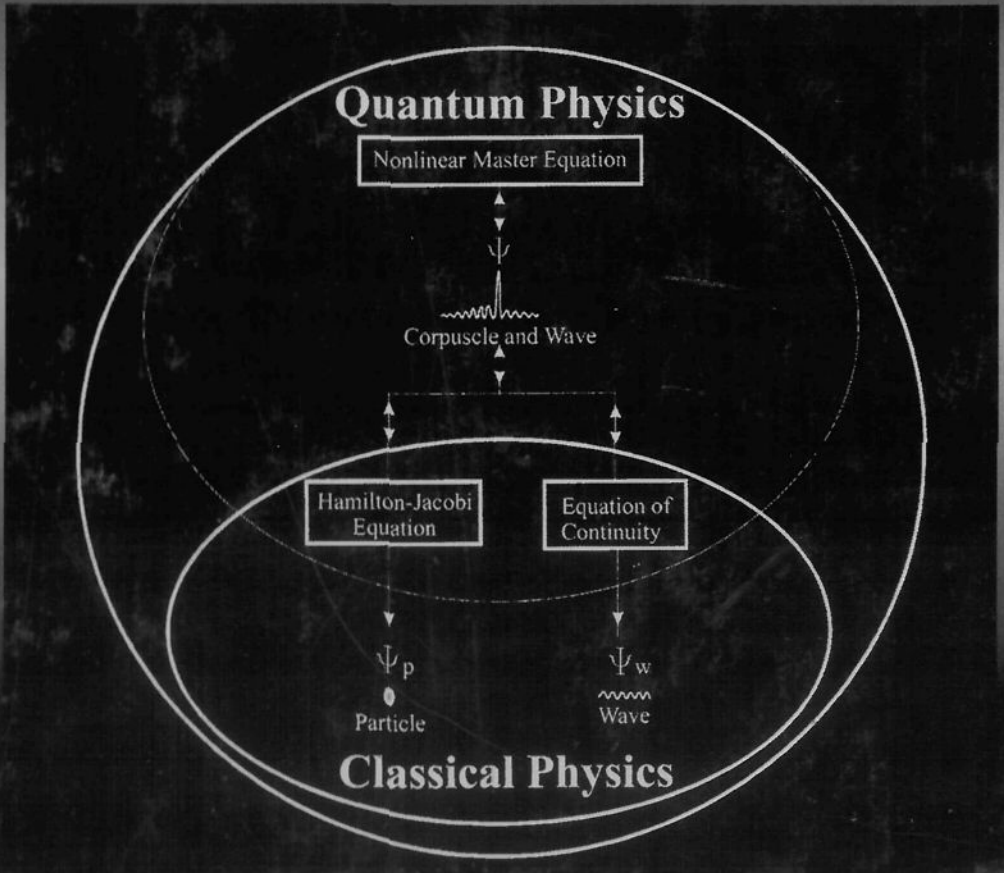

TOWARDS A NONLINEAR QUANTUM PHYSICS

SERIES IN CONTEMPORARY CHEMICAL PHYSICS

Editor-in-Chief: M. W. Evans *(AIAS, Institute of Physics, Budapest, Hungary)*

Associate Editors: S Jeffers *(York University, Toronto)*
D Leporini *(University of Pisa, Italy)*
J Moscicki *(Jagellonian University, Poland)*
L Pozhar *(The Ukrainian Academy of Sciences)*
S Roy *(The Indian Statistical Institute)*

Vol. 1 The Photon's Magnetic Field — Optical NMR Spectroscopy
by M. W. Evans and F. Fahari

Vol. 2 Beltrami Fields in Chiral Media
by A. Lakhtakia

Vol. 3 Quantum Mechanical Irreversibility and Measurement
by P. Grigolini

Vol. 4 The Photomagneton and Quantum Field Theory: Quantum Chemistry, Vol. 1
by A. A. Hasanein and M. W. Evans

Vol. 5 Computational Methods in Quantum Chemistry: Quantum Chemistry, Vol. 2
by A. A. Hasanein and M. W. Evans

Vol. 6 Transport Theory of Inhomogeneous Fluids
by L. A. Pozhar

Vol. 7 Dynamic Kerr Effect: The Use and Limits of the Smoluchowski Equation and Nonlinear Inertial Responses
by J.-L. Dejardin

Vol. 8 Dielectric Relaxation and Dynamics of Polar Molecules
by V. I. Gaiduk

Vol. 9 Water in Biology, Chemistry and Physics: Experimental Overviews and Computational Methodologies
by G. W. Robinson, S. B. Zhu, S. Singh and M. W. Evans

Vol. 10 The Langevin Equation: With Applications in Physics, Chemistry and Electrical Engineering
by W. T. Coffey, Yu P. Kalmykov and J. T. Waldron

Vol. 11 Structure and Properties in Organised Polymeric Materials
eds. E. Chiellini, M. Giordano and D. Leporini

Vol. 12 Proceedings of the Euroconference on Non-Equilibrium Phenomena in Supercooled Fluids, Glasses and Amorphous Materials
eds. M. Giordano, D. Leporini and M. P. Tosi

Vol. 13 Electronic Structure and Chemical Bonding
by J.-R. Lalanne

Vol. 14 Dialogues on Modern Physics
by M. Sachs

Vol. 15 Phase in Optics
by V. Peřinova, A. Lukš and J. Peřina

Vol. 16 Extended Electromagnetic Theory: Space Charge in Vacuo and the Rest Mass of the Photon
by S. Roy and B. Lehnert

Vol. 17 Optical Spectroscopies of Electronic Absorption
by J.-R. Lalanne, F. Carmona and L. Servant

Vol. 18 Classical and Quantum Electrodynamics and the B(3) Field
by M. W. Evans and L. B. Crowell

Vol. 19 Modified Maxwell Equations in Quantum Electrodynamics
by H. F. Harmuth, T. W. Barrett and B. Meffert

World Scientific Series in Contemporary Chemical Physics – Vol. 20

TOWARDS A NONLINEAR QUANTUM PHYSICS

J R Croca

University of Lisbon, Portugal

World Scientific

New Jersey • London • Singapore • Hong Kong

Published by

World Scientific Publishing Co. Pte. Ltd.

5 Toh Tuck Link, Singapore 596224

USA office: Suite 202, 1060 Main Street, River Edge, NJ 07661

UK office: 57 Shelton Street, Covent Garden, London WC2H 9HE

British Library Cataloguing-in-Publication Data

A catalogue record for this book is available from the British Library.

TOWARDS A NONLINEAR QUANTUM PHYSICS

Copyright © 2003 by World Scientific Publishing Co. Pte. Ltd.

All rights reserved. This book, or parts thereof, may not be reproduced in any form or by any means, electronic or mechanical, including photocopying, recording or any information storage and retrieval system now known or to be invented, without written permission from the Publisher.

For photocopying of material in this volume, please pay a copying fee through the Copyright Clearance Center, Inc., 222 Rosewood Drive, Danvers, MA 01923, USA. In this case permission to photocopy is not required from the publisher.

ISBN 981-238-210-0

This book is printed on acid-free paper.

Printed in Singapore by Mainland Press

To my wife

Maria Adelaide

This page is intentionally left blank

ACKNOWLEDGEMENTS

I would like to thank Professor Franco Selleri for his friendship and constant support in the vicissitudes of the hard battle to recover causality. No less significant was his constant assistance in practical academic matters since anyone who seeks for the truth has to face not only the inherent difficulties of scientific research but also the strong prejudices of the established scientific community. Now as ever, anyone who dares to have opinions in science and seeks truly innovative approaches to understand Nature questioning the sacrosanct established ideas is to be stopped at any cost. Among the same type of original daring men stands Professor Myron Evans, who besides his highly innovative work has also devoted his activities, as a scientific editor, to promote new ideas thus helping the researchers to diffuse their scientific ideas. To him my most deep gratitude for having invited me to write this book for his series. Probably, without his kind encouragement this book would never have been written.

I also would like to thank the one I always see as my master, Professor J. Andrade e Silva, who initiated me not only in this fascinating field of the foundations of quantum physics, but also in the ways of true, free responsible science where personal intellectual courage plays a significant role. To my dear friends, Professors Rui Nobre Moreira, Amaro Rica da Silva and J. Sousa Ramos, my gratitude for the very interesting and helpful discussions in our meetings along the years which much contributed to the shaping of this book.

I take the opportunity to express my appreciation to Professor J. Sousa Lopes and his group, to Professor Antonio Vallera, Professor L. Mendes Victor, Professor Eduardo Ducla Soares and all other colleagues for the support they gave me when the hardships and prejudices of the established scientific community have fallen upon the author.

I wish to express my gratitude for all his friendship and enthusiasm to Professor Antonio Ribeiro, who in the field of Geology fights a war similar to mine in Physics. To Dr. J. Alexandre Croca, my son, for the interesting and helpful discussions and permanent support my most sincere appreciation. To Professor J.P. Marvão, for the help in the final preparation of the manuscript both in correcting my bad English and for the very interesting suggestions that much improved the final form of the book, my many thanks.

Finally, I want to express my gratitude and support to all those in the world who, with the risk of loosing or stagnating in their careers, dare to have scientific opinions and, against all odds, keep fighting for the truth.

CONTENTS

Acknowledgements vii

1 Introduction 1

2 Complementarity Principle and the Nonlocal Fourier Analysis 7
- 2.1 Introduction 7
- 2.2 Fourier nonlocal analysis 8
  - 2.2.1 The quantum operators P_x and X 13
- 2.3 The measurement and the collapse of the wave train 16
  - 2.3.1 Measurement without physical interaction 21
- 2.4 Heisenberg uncertainty relations and the complementarity principle 23
  - 2.4.1 Other derivations of Heisenberg's uncertainty relations 28
  - 2.4.2 Meaning of the uncertainty relations 34
- 2.5 References 37

3 New Generation of Microscopes 39
- 3.1 Introduction 39
- 3.2 The common Fourier microscopes 40
- 3.3 Tunneling super-resolution microscope 49
  - 3.3.1 Measurements of first and second kind 51
- 3.4 Apertureless optical microscope 53
- 3.5 References 56

4 Beyond Heisenberg's Uncertainty Relations 57
- 4.1 Introduction 57

4.2 Wavelet local analysis 59
4.3 Some elements of the causal theory of de Broglie 65
4.4 A nonlinear Schrödinger equation 71
4.4.1 Derivation of the nonlinear master Schrödinger equation 72
4.4.2 Some particular solutions of the nonlinear Schrödinger equation 80
4.4.3 A mathematical model for the quantum particle 82
4.4.4 An example of the application of the model 87
4.5 Local Paradigm in place of the nonlocal Fourier Paradigm 90
4.6 Derivation of a more general set of uncertainty relations 94
4.7 Experiments to test the general validity of the usual uncertainty relations 109
4.7.1 Photon Ring Experiment 109
4.7.2 Limitless Expansion of Matter Wave packets 112
4.8 An Example of a Concrete Measurement that goes beyond Heisenberg's Uncertainty Relations 120
4.9 References 128

5 The Meaning of the Wave Function 131
5.1 Introduction 131
5.2 A causal interpretation for the two-slit experiment 133
5.3 Experiments to test the nature of the wave function 135
5.4 Experiments on the collapse of the wave function 136
5.4.1 Generator of theta waves 136
5.4.2 Direct detection of the theta waves 140
5.4.3 Detection with coherent sources 142
5.4.4 Detection with incoherent sources 144
5.4.4.1 Experiment with correction for synchronization 151
5.4.4.2 Mandel's experiment 157

5.5 Experiments based on the complex interaction process of the causal quantum particles 164
5.5.1 Experimental test of the tired light model of de Broglie for the photon and its implications on the Cosmological expanding model of the Big Bang for the Universe 169
5.6 References 178

6 Interference Without Superposition of the Wave Packets 181
6.1 Introduction 181
6.2 Interferometric experiments without overlapping of the wavepackets 182
6.3 Orthodox interpretation 185
6.4 Causal explanation 198
6.5 Experimental test for the two approaches 205
6.6 Franson type experiments 208
6.7 References 210

Author Index 211

Subject Index 213

CHAPTER 1

INTRODUCTION

The aim of this book is to present a local causal epistemology as a more general alternative to the orthodox nonlocal and nontemporal Copenhagen paradigm for quantum phenomena. The development of this general local causal paradigm was possible thanks to the recent breakthrough in mathematics, related with local analysis by wavelets. It is now finally possible to answer, in the framework of a local causal epistemology, the old question of how to conciliate the two apparently contradictory properties exhibited by quantum entities. These two opposite characteristics result from the known facts that in certain experiments those strange quantum entities behave like waves or like corpuscles. That is, they must have extended properties but also need to be localized. We know that Bohr had already answered this question with the help of his complementarity principle. The price to pay for this early nonlocal orthodox synthesis for quantum phenomena was the denial of the observer independent reality and consequently the abandon of the concepts of space and time as basic tools to assist us in the understanding of Nature. Since then many efforts to restore the locality and causality were made by other researchers that never accepted this rejection of the external objective reality. Nevertheless, all those attempts were naturally fated to fail because they all were made in the mathematical framework of nonlocal and nontemporal Fourier analysis. As long as one does not get rid of Fourier analysis, which from one among other mathematical processes for composing and decomposing functions was promoted by Bohr to the status of ontological self-evident truth for physics, no satisfactory locality is ever possible. This ontology states that any finite sign, any finite observable wave, is in reality composed of a large number of infinite harmonic plane waves. The harmonic plane wave is the only entity, in this approach, that can have a perfect, single, pure frequency. As a consequence, any representation of a reasonable localized particle needs to include all space, all time and necessarily all possible energies and frequencies. This is a simple corollary of the fact that the wave packets, which represent the particle, are, in last instance, nothing more than the sum

of many infinite harmonic plane waves. Since each of these waves has a well-defined frequency it implies that what, in this paradigm, we call particle, needs to have a multiplicity of energies. Still, the real observable particles do have a precise energy. As a natural consequence of these assumptions before the observation no real particle with a single energy does really exist. All we have is a bunch of potentialities out of which a single one can be made real by the act of measurement. Once engaged in this path no real objective locality is ever possible or makes sense anymore. The quantum systems are, in this nonlocal paradigm, necessarily spread over all space and time.

In order to develop a sound local causal model for describing quantum reality it is necessary to assume as a fundamental ontologic statement that, as common observation teaches us, it is definitely possible to conceive a single real finite wave with a well-defined frequency. This assumption, which in a first look may seem innocuous, represents indeed an important conceptual change in the way we look at Nature. In fact we have to accept, contrary to what is stated in Bohr's Fourier paradigm, that the tuning fork when strike does indeed emit a finite real sound wave with a well-defined frequency. Furthermore this physical wave of a well-defined frequency has a beginning and certainly an end. The mathematical tool that allows us to make up this important epistemological revolution is wavelet local analysis. This local analysis must, in this context, be promoted to the status of basic mathematical representation for the present and future quantum physics replacing in this way the nonlocal and nontemporal Fourier analysis. Needless to say that this more general local causal paradigm for describing Nature contains formally, in the linear approach, the old one, the orthodox Copenhagen model, rooted in Fourier analysis, as a particular case.

The physical implications resulting from the use of local analysis as the basic mathematical tool to describe reality, instead of the nonlocal and nontemporal Fourier analysis, are the necessity to change from a linear approach to a nonlinear theory with all its mathematical difficulties. Yet the beauty of this nonlinear approach lies in the fact that it allows a general unitary causal local synthesis between classical and quantum physics. This new integrated picture results directly from the known fact that we do observe reality by scales, that is, by levels of understanding. The change between each stage of reality depends on the precision of the physical sensors and of course on the available theoretical tools. In such circumstances, any significative physical model for description of Nature needs also to follow, as close as possible, the same pattern. In such

circumstances, for each stage of reality we need to have an adequate special description. This more general integrated approach contains in itself the seeds for the diverse levels of description that are properly interconnected among them.

In this work we are concerned with two realms or levels of description of reality: The classical, associated with the macroscopic world, and the quantum domain.

The level of classical physics, the macroscopic world, is related with two main fundamental areas, which, at this level of description, are assumed to be independent.

One of these areas deals with localized systems. In this approach for the description of reality we are concerned with entities whose position is assumed to be perfectly determined, the particles. The behavior, the interaction among these particles is thus described by classical mechanics.

The other important area is related with extended systems. Here we are mainly interested in the physical extended systems like waves, which cannot to be described as point-like entities.

At the level of classical physics, for the description of reality, the particle like and the wavelike extended systems are treated as separate independent entities. Discrete and continuum are assumed as entirely different ontological concepts, which cannot be reconciliated. In this classical picture, at this level of understanding of Nature, one thing is a well-localized particle, another an extended wave. These independent systems, particles and waves, with diverse properties are, naturally, described by different differential equations.

At the quantum level things are rather different. The two seemingly independent realms wave-like and particle-like of classical physics melt into a single complex reality. Quantum beings have, at the same time, extended and localized properties.

Therefore, in the general synthesis proposed in this work, we can simply say that quantum physics is nothing more than classical physics where the extended and the localized properties need to be integrated into a single complex entity.

For the same token, we can say, symmetrically, that classical physics is no more than a derivation, a particular case, of a more general theory, nonlinear quantum physics, when we start describing the extended undulatory and the corpuscular localized properties as two well independent separate realities.

In the fourth chapter it will be shown how starting from the nonlinear master equation for quantum phenomena, with solutions that have at the same time extended and localized properties, it is possible to arrive, by imposing the need of separating the local from the extended properties, at the two fundamental equations of classical physics. Inversely, it is also shown, how starting from these two fundamental classical equations, the Hamilton-Jacobi and the continuity equation, by their fusion, and assuming naturally that they both share the same solution, we can arrive at the quantum nonlinear master equation. This nonlinear master equation for local causal quantum physics in certain conditions approaches the common linear Schrödinger equation.

Stemming directly from the fact that the basic mathematical tool, in this new causal paradigm, is the local analysis by wavelets, instead of the nonlocal and nontemporal Fourier analysis, and also from the fact that the fundamental equation to describe quantum phenomena needs to be intrinsically a nonlinear equation we are lead at many discrepancies with the orthodox Copenhagen paradigm for quantum physics.

From among these discrepancies we may refer the natural direct and implicit conclusion that the sacrosanct Heisenberg uncertainty relations, revered until now by almost every one, as the most profound and final statement ever produced by the human mind, are not, in reality, so general as it is claimed by the orthodox followers. Indeed, starting from this general local causal paradigm we derive a more general set of uncertainty relations that contains the old orthodox ones as a particular case. Furthermore we present experimental evidence confirming that these orthodox uncertainty relations have, as expected, a limited universe of applicability. We show that there are practical concrete measurements, done everyday, which are not described by the orthodox Heisenberg uncertainty relations. These measurements are done with the super-resolution microscopes of the new generation. The principal feature of these new imaging devices is their high-resolution power. The resolution of these microscopes can be much greater than the resolution of the familiar Fourier microscopes, which, as we know since Abbe, is of about half wavelength. These very particular types of concrete measurements are naturally integrated and described by the new more general local causal uncertainty relations.

Furthermore, we also present other particular types of measurements that can test the general applicability of the old orthodox Heisenberg uncertainty relations.

The problem of how to decide, experimentally, on the real nature of quantum waves is fully discussed in chapter five. The question is to know whether quantum waves, solution to the common Schrödinger equation, are mere probability waves, devoid of any physical meaning or are, indeed, real physical waves. The local causal model, even at the linear approach, sustains that quantum waves are real waves while orthodox theory claims that they are mere probability waves devoid of any physical meaning. Diverse proposals of experiments based on the collapse of the wave function are presented. A concrete experimental realization of one of these experiments is also fully discussed. Other type of experiments, based on a different approach, for inquiring on the nature of the entity we call photon are also discussed. The problem, in last instance, could be summarized in the question of whether the photon has indeed an inner complex structure or is a single undivided eternal entity as is assumed by the majority of the researchers. In fact an experiment that could clarify this question is discussed in the same chapter. Furthermore, as a side effect, this experiment could test the habitual Doppler interpretation for the observable cosmologic redshift that stands as the basic experimental proof argued in favor of the Big Bang model for the universe.

The sixth and last chapter is dedicated to a full discussion of some strange experiments that are, in general, presented in scientific literature with big fanfare. These experiments according to those authors are no more than concrete examples where the weirdness, the magic of orthodox quantum mechanics is put into action. We shall see that all these claims are no more than a show off. A complete misunderstanding of the objective facts, and even more, in some cases, bad use of the orthodox Copenhagen approach. These experiments in which, according to those authors, there are actions in the past, retroactions in time, are perfectly understood in the conceptual framework of the more general local causal paradigm. It is perfectly possible to interpret these strange quantum experiments in an intuitive natural way without need to summon, retroaction in time, miracles, magic, or any other similar mysteries far beyond the creative rational mind of man.

The work was planned so that the second and third chapters act as an introduction to the fourth chapter that constitutes the kernel of the book. The fifth and sixth chapters are devoted to more practical matters such as experiments, applications and implications.

One important objective of this book is to present these naturally complex matters, dealing with the foundations of quantum mechanics, in a twofold way: One dedicated to the expert on the fundaments of quantum

physics that can follow and even improve the calculations; the other to the open minded reader, familiar with the rudiments of science, mainly interested in conceptual problems posed by quantum physics. To accomplish this objective, whenever possible, the matters discussed have intelligible introductions, so that the learned reader can perfectly get along and fully understand the problems under discussion without need to follow, step by step, the more or less detailed mathematics.

Other, non-less central, purpose of this work is to contribute to the development of the new more general local paradigm. This local causal approach has allowed us to demolish and go beyond the conceptual boundaries built by the old orthodox paradigm as unsurpassable limits for the human possibility to comprehend reality. This local causal paradigm opens entire new realms, new universes for the understanding of Nature. In this local causal framework there are thus far many important problems waiting to be solved and the main consequences are yet to be discovered both at the theoretical, experimental and technological levels...

CHAPTER 2

COMPLEMENTARITY PRINCIPLE AND THE NONLOCAL FOURIER ANALYSIS

2.1 INTRODUCTION

As is well known, during the heroic years of the construction of quantum mechanics, the scientists faced the hard task of conciliating the two apparently contradictory manifestations of quantum beings. In certain experiments quantum entities showed a corpuscular nature while in other experimental setups the same quantum beings exhibited undulatory properties. This problem was made even more acute when in 1926 two theories were developed to try to explain the experimental results at the atomic and molecular level. One of these approaches was matrix mechanics, created by Heisenberg. The matrix mechanics is based on the corpuscular properties of the quantum entities. The other approach was wave mechanics, developed by Schrödinger. Schrödinger elaborated his wave mechanics inspired in the fundamental relation of de Broglie, relating the undulatory characteristic of matter. Wave mechanics emphasized the undulatory characteristics of the quantum entities. In March of the following year, 1927, Heisenberg was able to derive the mathematical uncertainty relations that later got his name. He tried to interpret those inequalities in accordance with his most dear idea that quantum beings had essentially a corpuscular nature. Here he enters in clash with Niels Bohr. Bohr believed that a complete quantum theory, able to explain in a coherent way the new phenomena, at the atomic and molecular level, ought to contemplate this intrinsically dual nature of the quantum entities, i.e. the two apparently opposed properties of being waves and particles. Bohr spent the vacations of that year pondering very hard on the problem. In September he reached a solution for the big question: How to conciliate those two fundamental antagonistic properties of matter? He presented his ideas to the scientific community, for the first time, at the Volta conference held at the lake Di Como, in Italy in September 1927. Before an audience of the most prominent physicists of the time he

stated that it is possible to explain the whole experimental evidence if one assumes that Nature has a dual or complementary essence. That is, in certain experiments matter shows corpuscular properties, while in other displays undulatory characteristics. These two properties never manifest themselves clearly at the same time. The more distinctly the corpuscular nature shows, in an experiment, the more cloudy the undulatory aspect appears, and vice versa. The mathematical tool to express this very basic characteristic of Nature is nonlocal Fourier analysis. The relations derived by Heisenberg are a single and very clear manifestation of those facts.

Since Fourier nonlocal analysis plays such an important role in the conceptual and formal structure of quantum mechanics, let us now have a closer look at it.

2.2 FOURIER NONLOCAL ANALYSIS

When Fourier, in the first quarter of the XIX century, discovered that any well-behaved function could be represented by an infinite sum of sine and cosine functions he, for sure, could not have guessed the paramount importance of his discovery for either the technology and the basic science of the twentieth century. In fact, from communication technology, from pure and applied mathematics, to the very foundations of quantum mechanics, it plays a key role which importance is not easy to grasp even today.

What Joseph Fourier discovered, when studying heat diffusion, was that any well-behaved function could be represented as a sum of sine and cosine functions. In the case of a periodic function his representation in terms of sine and cosine functions can be written,

$$f(\xi) = \frac{1}{2} A_0 + \sum_{m=1}^{\infty} (A_m \cos m\eta\xi + B_m \sin m\eta\xi), \qquad (2.2.1)$$

with ξ standing for the variable x or t, and η, the conjugate of ξ, representing either the spatial frequency, $\eta = k = 2\pi/\lambda$, or temporal frequency $\eta = \omega = 2\pi/T$; λ, as usual, is the wavelength and T the period. The decomposition coefficients A_m and B_m assume the form:

$$A_m = \frac{2}{\lambda}\int_0^{\lambda} f(\xi)\cos m\eta\xi \, d\xi \,, \tag{2.2.2}$$

$$B_m = \frac{2}{\lambda}\int_0^{\lambda} f(\xi)\sin m\eta\xi \, d\xi \,. \tag{2.2.3}$$

In the case of a non-periodic function the discrete decomposition or synthesis turns into a continuous sum,

$$f(\xi) = \int_{-\infty}^{+\infty} g(\eta) e^{i\eta\xi} d\eta \tag{2.2.4}$$

where $e^{i\eta\xi} = \cos\eta\xi + i\sin\eta\xi$ is the kernel of the transformation and the coefficient function $g(\eta)$, also called Fourier transform of $f(\xi)$, has the form

$$g(\eta) = \int_{-\infty}^{+\infty} f(\xi) e^{-i\eta\xi} d\xi \,, \tag{2.2.5}$$

expression which is sometimes called analysis of signal $f(\xi)$.

Summarizing: Usually in Fourier analysis one starts from a function that represents the information available on a physical situation, the signal function. The next step is to make the analysis, that is, the decomposition in terms of sine and cosine functions, which amounts to find the coefficients for the sines and cosines or, in the case of a non-periodic function, the coefficient function $g(\eta)$. After that, once those coefficients are known, one normally makes the synthesis of the initial function also called reconstruction.

$$f(\xi) \xrightarrow{\text{Analysis or Decomposition}} g(\eta) \xrightarrow{\text{Synthesis or Reconstruction}} f(\xi)$$

Since an harmonic plane wave may be written in the form

$$\psi = A\, e^{i\eta\xi} \,,$$

where A is the constant amplitude and $\eta\xi$ the phase, the previous results indicate that any regular function, containing the information on a physical

situation, can be expressed as a sum of harmonic plane waves, that is, in terms of sine and cosine functions.

Let us now suppose that we want to apply Fourier analysis to a rectangular function representing, for instance, the region of space where the particle can be localized or simply a bit of information.

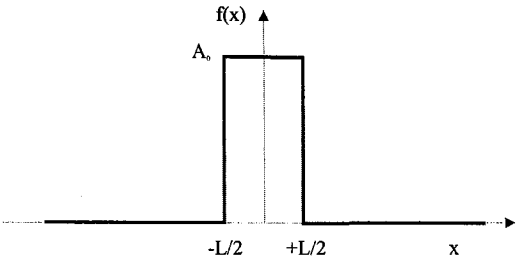

Fig.2.1 – Rectangular function.

This function can also be expressed analytically

$$f(x)=\begin{cases} A_0, & |x|\le L/2, \\ 0, & |x|> L/2. \end{cases} \tag{2.2.6}$$

The Fourier transform of this function, that is, the function coefficient *g(k)*, that allows the reconstruction of *f(x)* in term of sine and cosine functions is obtained with the help of expression (2.2.5) and leads to the well known formula

$$g(k) = A_0 L\,\mathrm{sinc}(kL/2), \tag{2.2.7}$$

where, as usual the "sinc" function stands for

$$\mathrm{sinc}(kL/2)=\frac{\sin(kL/2)}{(kL/2)}$$

whose graphical representation is,

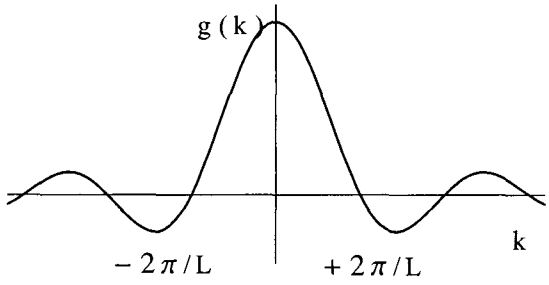

Fig.2.2 – Fourier transform of rectangular function.

from which it is possible to see that as the width of the rectangular function $\Delta x = L$ increases, the width of the main bulk of *g(k),* limited by $-2\pi / L$ and $+2\pi / L$, given by $\Delta k = 4\pi / L$, decreases and vice-versa. Later, it will be shown that this property of the Fourier transform was extremely important for the conceptual and formal development of quantum mechanics. From the knowledge of the coefficient function *g(k),* and with the help of the formula (2.2.4) it would be possible to reconstruct the initial function.

The title of this section was chosen Fourier nonlocal analysis just to emphasize the nonlocal or global character of this kind of analysis discovered by Joseph Fourier more than a century ago. This basic property of the Fourier analysis is a direct consequence of two main reasons connected in a certain sense.

1 – The first reason why Fourier analysis ought to be called nonlocal or global is because its bricks, its building bocks, are harmonic plane waves. These harmonic plane waves are no more than sine and cosine functions, which, as we know, are defined in whole space and in whole time. These harmonic plane waves have constant amplitude everywhere. That is, the amplitude of these waves is constant at any point of space and time.

2 – The second reason is because this kind of analysis has nonlocal or global implications. In order to understand the meaning of this statement let us look at Fig.2.3, where two particles are represented graphically against a homogeneous background.

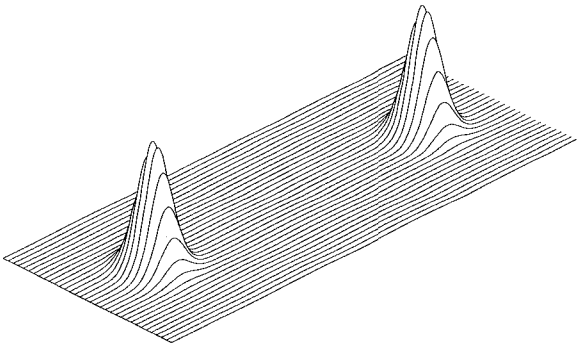

Fig.2.3 – Graphical representation of two particles.

In order to Fourier represent the first particle one has to add an infinity of harmonic plane waves, defined in all space and time, that is sine and cosine functions, so that these waves interfere negatively in all space except in the region where the particle is localized. The same statement is also true for representing the second particle. This means that in terms of Fourier representation any particle somehow occupies all space and time. Indeed the waves that sum up to represent the particle occupy all space and time. Therefore the two particles even if in a first approach look as well separate entities in terms of Fourier representation are composed by the same infinite harmonic plane waves. Under these conditions their separation is only apparent because intrinsically they are made of the same waves. Therefore, in this sense, they are the same extended entity occupying all space and time. As a consequence of this interpretation the separability of the quantum entities is only an illusion. If one moves one of the particles, for instance the first one, to the right, while the other remains at the same position, as shown in Fig.2.4,

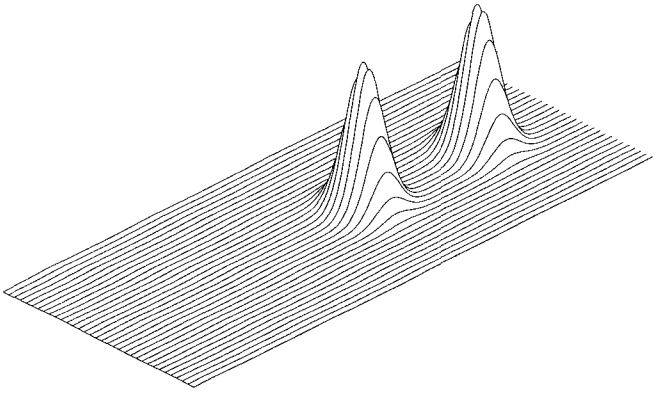

Fig.2.4 – The particle of the left is moved to the right.

it is necessary to change the relative amplitude and phase of the harmonic plane waves so that their interference is only constructive at the region where the first particle now stands. But when the change is made in the waves that sum up to make the first particle, one also changes the waves that made the second particle because they are the same. Thus, in this sense, the two particles are never truly separate. Indeed in terms of Fourier analysis they make a whole nonlocal entity.

2.2.1 The Quantum Operators P_x and X

In the formal construction of quantum mechanic measurement theory the operators play a major role. If one wants to perform a measurement, in quantum mechanics, it is necessary to perform the initial following steps:

1 – First it is necessary to know the classical function $A(q,p,t)$ corresponding to the physical quantity we wish to determine.

2 – This classical function needs to be written in cartesian coordinates.

3 – Applying the operatorial correspondence rules on the classical function one builds the quantum operator $O(A)$.

$$A(q,p) \xrightarrow{\text{Correspondence rules}} O(A)$$

This step is not so straightforward as it seems. In reality the problem of writing a quantum operator from the knowledge of the classical expression is not so simple as is usually supposed. As shown by many authors, namely by Temple, there are no perfect correspondence rules. In certain cases, starting from the same classical expression, and following the usual correspondence rules one obtains different operators. A perfect rule would allow a one-to-one correspondence, for the writing of the quantum operators. Apart from these minor points, which concern only few special cases, in general, there are fair simple rules to build the quantum operators. The simplest way consists in substituting, in the classical expression, the classic basic variables x and p_x by its corresponding quantum operators,

$$\begin{aligned} x &\rightarrow x. = X \\ p_x &\rightarrow -i\hbar\frac{\partial}{\partial x} = P_x \end{aligned} \tag{2.2.8}$$

When these simple rules conduce to different quantum operators, the next step in order to reduce the ambiguity is to apply the substitution (2.2.8) to the symmetrised product of the classical relation thus getting a one-to-one relation.

4 – Once in possession of the quantum operator, corresponding to the physical quantity one wants to make a measurement of, it is necessary to find its eigenfunctions. The eigenvalues are the possible results of the quantum measurement. For that it is necessary to solve the eigenvalues equation for the non-null solutions

$$A\varphi = a\varphi, \tag{2.2.9}$$

where A represents a generic operator, φ its eigenfunction and a the corresponding eigenvalue.

The most common observables are the position and the momentum. The other observables can in general be expressed as a function of both. In such conditions it is useful to look a little more into these two basic observables.

From quantum mechanics we know that to the observable position and momentum correspond the following operators:

$$X \to x.$$
$$P_x \to -i\hbar \frac{\partial}{\partial x} \tag{2.2.10}$$

The eigenfunction of the momentum operator is the kernel of the Fourier transform

$$P_x = -i\hbar \frac{\partial}{\partial x} \xrightarrow{\text{Eigenfuncion}} e^{\frac{i}{\hbar} p_x x} = e^{ik_x x}. \tag{2.2.11}$$

While the eigenfunction of the position operator is the well-known Dirac delta function.

At this point it is worth to recall that the Dirac delta function can be written as an infinite sum of eigenfunctions of the momentum operator

$$\delta(x) = \frac{1}{2\pi} \int_{-\infty}^{+\infty} e^{ikx} dk. \tag{2.2.12}$$

In quantum measurement theory, as we have seen, the quantum operators position and momentum play a key role in the construction of all quantum operators. This is a consequence of the fact that all quantum operators can be expressed as a function of these two operators. In view of this and since even the position eigenfunction can be represented as a combination of eigenfunctions of the momentum operator it follows that any well-behaved eigenfunction is also, in last instance, to be represented as a combination of the eigenfunctions of the momentum operator. In this perspective every regular quantum eigenfunction is no more than a combination eigenfunctions of the momentum operator $(e^{ik_x x})$, which is a combination of sine and cosine functions $(e^{ik_x x} = \cos k_x x + i \sin k_x x)$.

Those facts show how basic and important is Fourier analysis for the very roots of the quantum measurement theory and consequently for all quantum physics.

2.3 THE MEASUREMENT AND THE COLLAPSE OF THE WAVE TRAIN

Before further tracking the deep relations between nonlocal Fourier analysis and quantum measurement theory I shall discuss, as an introduction to the subject, a most fundamental experiment that has played, and still plays, a key role in the conceptual foundations of quantum theory.

It is the double slit experiment with a single quantum particle. Let us consider this fundamental experiment, sketched in Fig.2.5.

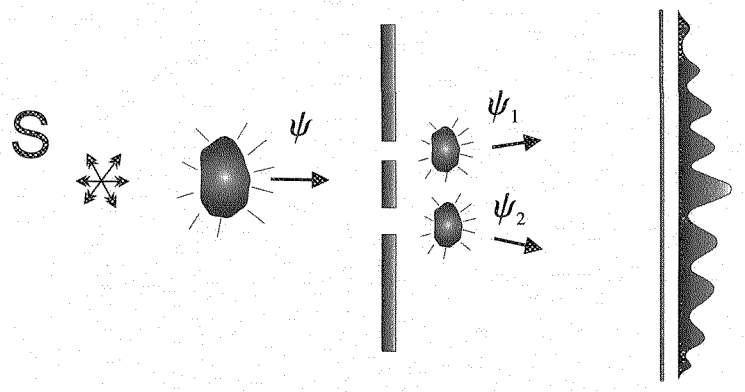

Fig.2.5 – Sketch of the double slit experiment.

where a single particle source S, emitting quantum particles, one at a time, is seen. Let us suppose that, in this particular case, the quantum particles, emitted one at a time by the source, are electrons. The entire reasoning would stand as well for any other quantum particle. In fact double slit experiments have already been performed with atoms, neutrons, protons, electrons and photons, and always with the same result. The electron in its way encounters a screen with two slits. If one places a detector right behind each slit what is to be expected?

It happens that sometimes one detector is triggered and at other times it is the second detector that is activated. In any case, and here stands the point, it never happens the two detectors being activated at the same time. Naturally this situation can never occur since we are dealing with one single electron at a time. On the whole apparatus, for each event, there is only one

single quantum particle. If this basic conceptual and practical requirement is not met the experiment is meaningless. On the other hand a simultaneous detection on the two detectors would imply that the quantum particle would have split into two and consequently half electron would go through each slit. This is a completely impossible situation! Until today, no one has seen say, half electron, half proton, half neutron, and so on. Therefore from this first analysis the observer would conclude that the electron would go through one slit or the other.

If one removes the two detectors from the slits, and places a large array of detectors sufficiently far away in the route of the particles that went through the slits, what is to be expected? What shall be the distribution of impacts of the electrons on the array of detectors?

If one maintains the previous affirmation that the electron went by only one of the slits, then one would expect a continuous gaussian distribution of impacts on the detector. This distribution would result from the contribution of electrons that sometimes come from one slit plus the contribution of the particles that, at other times, come from the second slit.

Still, experimental evidence clearly shows that instead of a continuous gaussian pattern, what in fact is observed is an interferometric pattern as shown in Fig.2.5.

In order to explain the observed interference pattern one has to assume that the quantum particle, in this case the electron, has somehow gone both ways. An interference pattern is always a result of the superposition of more than one wave. This means that what we call an electron went through both slits. Under these conditions we have to conclude that the electron must be a wave.

Now we have a problem!

The first experiment, with the detectors placed just behind the two slits, indicates that the electron is a particle that went though one slit or through the other.

The second experiment leads us to conclude that the electron is a wave because it went through both slits at the same time giving origin to an interference pattern.

Therefore the quantum entity we call electron must have a very weird behavior: It has to pass through one slit **or** the other and also must go, at the same time, through **both** slits.

Summarizing: In the single particle double slit experiment the quantum particle must pass:

1 – through one slit **or** the other slit.

2 – through one slit **and** the other slit

It was precisely to face this very complex problem, to conciliate the two apparently contradictory affirmations, that Niels Bohr developed his famous principle of complementarity that states that a quantum particle has a dual nature. Sometimes it shows its undulatory nature at other times its corpuscular properties. The two properties never showing at the same time.

According to these views, in the double slit experiment those two properties of quantum systems manifest clearly one at a time: When the detectors are placed in front of the slits and only one of the two is triggered the quantum particle exhibits its corpuscular nature. With the detectors removed the electron passes through the two slits showing the undulatory characteristic in order to produce the observable interference pattern.

Therefore in the Copenhagen, or borhean, interpretation of the quantum physics the double slit experiment can be interpreted in a general conceptual framework in the following way:

The quantum particle is to be described by a probability wave ψ, containing all information on the quantum system. This wave goes in direction of a screen with two slits. There the initial wave splits into two probability waves ψ_1 and ψ_2

$$\psi = \psi_1 + \psi_2 . \tag{2.3.1}$$

These two waves, coming from the slits, are directed to the detection region where they overlap. The detection region is usually composed of a large array of detectors. When the composite wave $(\psi = \psi_1 + \psi_2)$ arrives at the detection zone one small detector from the array is triggered. The distribution of the clicks, corresponding to the successive arrivals of electrons, follows an interference pattern distribution given by the squared modulus of the wave

$$I = |\psi|^2 = |\psi_1 + \psi_2|^2 = |\psi_1|^2 + |\psi_2|^2 + 2|\psi_1||\psi_2|\cos\delta , \tag{2.3.2}$$

where δ is the phase difference between the two waves.

If these two waves were not assumed to exist simultaneously, then we would expect no interference, since only one, either ψ_1 or ψ_2 would exist at one time. In such circumstances they would not mix, so the interference term $(|\psi_1||\psi_2|\cos\delta = 0)$ would be zero, and consequently no interference pattern would ever be seen. In order to account for the observable single quantum particle interference pattern the two waves $\psi_1$and ψ_2 must exist at the same time.

In general to make a real quantum measurement, after having followed the exposed preceding initial steps, it is further necessary:

5 – The knowledge of the state of the quantum system, i.e. its wave function psi.

6 – Next, we decompose the psi function, containing all information we have on the quantum system under study, as a sum of eigenfunctions of the operator corresponding to the physical property we want to measure

$$\psi = c_1\varphi_1 + c_2\varphi_2 + c_3\varphi_3 + \cdots + c_n\varphi_n + \cdots \tag{2.3.3}$$

In such case the squared modulus of the coefficients of the decomposition $|c_n|^2$ give the probability of finding, in an actual measurement, a concrete value, p_n.

To clear a little more this issue let us consider a concrete situation. Suppose that one wants to make a measurement of the linear momentum of a quantum particle, an electron for instance. In order to perform the actual measurement we must possess an analyzer. This analyzer, depending on the concrete measurement to be performed, can be a crystal, a diffraction grating, an electromagnetic field, or any other suitable device. The ψ function that, according to the copenhagen interpretation of quantum theory, contains all the information we can have on the electron, is directed to the analyzer which splits this probability wave into many probability waves φ_n that are precisely the eigenfunctions of the momentum operator. The number of probability waves φ_n depends on the number of possible outcomes of the measurement. This situation is sketched graphically in the Fig.2.6

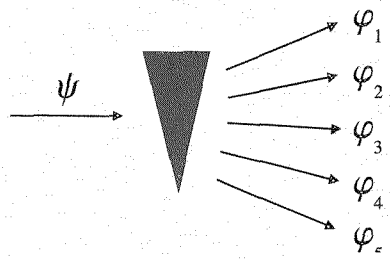

Fig.2.6 – Graphical representation of the decomposition, by the action of the analyzer, of the wave function in eigenfunctions of the operator corresponding to the classic observable.

where for the sake of simplicity we have represented only five possible outcomes. The action of the physical analyzer on the quantum system is described, in quantum formalism, by the operator applied to the state function decomposing it in eigenfunctions, as many as the possible outcomes of the measurement. Recalling the eigenfunctions of the operator momentum, given by (2.2.11), it is possible to rewrite the generic expression (2.3.3) for this particular case

$$\psi(x) = c_1 e^{\frac{i}{\hbar}p_1 x} + c_2 e^{\frac{i}{\hbar}p_2 x} + c_3 e^{\frac{i}{\hbar}p_3 x} + \cdots + c_n e^{\frac{i}{\hbar}p_n x} + \cdots \qquad (2.3.4)$$

which shows that, as expected, the action of the analyzer on the quantum system is described according to Fourier analysis. In the other cases the relation is not so direct, but by the nature of Fourier analysis, any well-behaved eigenfunction can always be written in terms of sine and cosine functions. These facts further emphasize the supreme importance of nonlocal Fourier analysis on formal orthodox quantum mechanics.

When one of the detectors from the array, placed in front of the analyzer, is triggered we get a value for the momentum, say p_3. This means that the probability wave φ_3 materializes itself at that position. Under such conditions all probability waves $(\varphi_1, \varphi_2, \varphi_3, \cdots \varphi_n, \cdots)$ instantly collapse into φ_3. In other words, before the interaction with the detector all functions φ_n do exist, when the actual measurement is done all the waves collapse instantly into a single one.

At first sight this statement may look a little out of place. It appears that we could instead say that the analyzing device had transformed the initial state wave function into φ_3, which existence was put in evidence by the click

of the corresponding detector. So, in such circumstances, the so-called collapse of the wave function would be nothing more than a figure of speech without any physical significance.

Had the latter statement any grounds then it would be impossible to explain the double slit interference with a single particle. We have just seen that the two waves must exist at the same time, before the interaction with the detector, otherwise no interference would be observed. Therefore to be consistent the theory must assume that before the interaction all waves $(\varphi_1, \varphi_2, \varphi_3, \cdots \varphi_n, \cdots)$ do exist. At the precise instant of the measurement all probability waves collapse instantly into a single one. Therefore any quantum measurement, in the bohrean conception, implies the reduction or collapse of the wave packet.

2.3.1 Measurement Without Physical Interaction

In the previous section we have seen that the collapse of the wave function was a result of the interaction with a physical device, in that case the detector. Now we are going to see situations were the collapse of the wave packet is accomplished without any detectable physical interaction.

This strange situation of interaction free measurement was studied by Renninger. Consider the following experiment sketched in Fig.2.7.

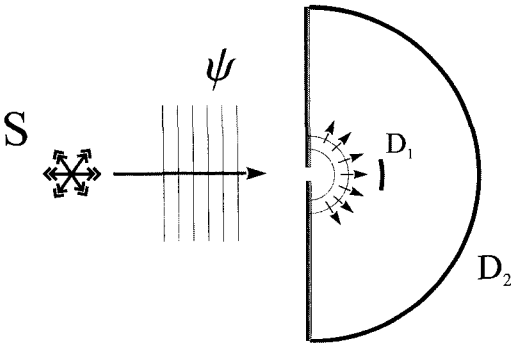

Fig.2.7 – Renninger experiment.

This experiment, as usual, is composed of a source emitting one single particle at a time, a screen with a hole, a small detector D_1, near the screen, and a very large hemispheric detector D_2 placed far away. The wave ψ

coming from the monoparticle source, arrives at the screen with the hole. From the hole emerges a spherical wave that in its way may trigger the small detector D_1 at a time t_1. If this detector is not activated, it means that later, at time t_2, the large detector D_2 shall be triggered. This situation can be described in the following way: the initial probability wave ψ upon arriving at the screen is split into two probability waves ψ_1 and ψ_2

$$\psi = \psi_1 + \psi_2 .$$

The squared modulus of the first, $p_1 = |\psi_1|^2$, represents the probability of the particle being registered at detector D_1, while $p_2 = |\psi_2|^2$ corresponds to a later detection by the large hemispheric detector placed very far from the hole. Naturally the sum of the two probabilities is one, $P_1 + P_2 = 1$.

Until now everything seems all right, the situation being similar to any other quantum measurement. Nevertheless, if one looks a little deeper into it a strange situation arises. Let us suppose that a quantum particle enters the hole made on the screen. We wait until time t_1, necessary for the particle to eventually be registered at the detector D_1, but it happens that no click is produced. Then we immediately make $p_1 = 0 \Rightarrow \psi_1 = 0$ and conclude that $p_2 = 1$, which means that the particle will be registered later at the detector D_2. If, conceptually, this detector D_2 is placed at an astronomical distance then this later may mean thousands of years after time t_1. The collapse of the wave function, that is the transformation of the initial function ($\psi = \psi_1 + \psi_2$) into one of its components ($\psi \rightarrow \psi_2$) occurs, in this particular and very special case, without any physical interaction. This is precisely the reason why such types of measurements are called negative measurements, or interaction free measurements. No physical interaction with the measuring apparatus was detected and yet the collapse of the wave function was accomplished. This collapse was a consequence of our previous knowledge of conservation of probability ($P_1 + P_2 = 1$) and of the fact that the detector D_1, was not triggered at the right time. If the first detector were activated, at time t_1, then the collapse of the wave function ($\psi \rightarrow \psi_1$) would be due to a physical observable interaction. But since, in the considered case, no physical interaction occurred and the wave function still collapsed into one of its components, what is the cause for such transformation? According to London and Bauer, this transformation, this collapse of the wave function, just like any other quantum collapse, is due, in last instance, to the

consciousness of the Observer. It is in the mind of the observer that in reality the collapse of the wave function occurs and not from any physical interaction.

Recently other researchers have developed other kinds of quantum measurements without physical interaction. Later, at the six chapter, when studying the so-called nonlocal interference we shall retake this problem.

2.4 HEISENBERG UNCERTAINTY RELATIONS AND THE COMPLEMENTARITY PRINCIPLE

We have seen previously that Bohr, in his 1927 summer holidays, solved the duality problem integrating it into a very beautiful and general conceptual framework.

Basically the idea of Bohr is the following:

From Fourier analysis it is known that when one wants to represent a localized function, for instance, a rectangular function, like the one discussed before, the more localized is the function the larger is the bandwidth needed for the synthesis. That means that the more localized is the function to be analyzed the more monochromatic harmonic plane waves it's necessary to add in order to build up the initial function and vice-versa.

The next step is to associate the probability of finding the particle with the squared modulus of the wave function psi. This step was inspired in the former work of Max Born in the quantum theory of measurement. Under this conditions the squared modulus of the wave function represents the region where the particle can be localized in a measurement process. The smaller the width of the function, Δx smaller, the more precise one knows the position of the quantum particle and consequently, according to Fourier analysis, more waves are necessary to include for the synthesis of the wave function. Since to each wave corresponds a well-defined wave number, that is velocity, it means that our knowledge of the velocity of the particle decreases.

The previous situation is sketched in the following schemes, Fig.2.8, where $f(x)$, the function to be Fourier analyzed, representing the region where the particle can be localized, the squared modulus of the wave function, is a

gaussian. The first column represents the width of the function $f(x)$ and the second the function coefficient, that is, the bandwidth of the waves necessary to synthesize $f(x)$. As can be seen the smaller Δx, the more localized the particle, the larger is the distribution of the velocities. At the limit the position of the particle is known without error, $\Delta x = 0$, and the function $f(x)$ assumes the form of a Dirac delta function. In this extreme case, of no error in the position, the number of waves necessary to make the Fourier synthesis of the wave function is infinity. This means that when $\Delta x = 0$, all waves, each one with its particular velocity and with the same weight, are necessary to reconstruct $f(x)$. Therefore an absolute knowledge of the position of the particle leads to a total ignorance of its velocity, $\Delta x = 0, \Rightarrow \Delta v = \infty$.

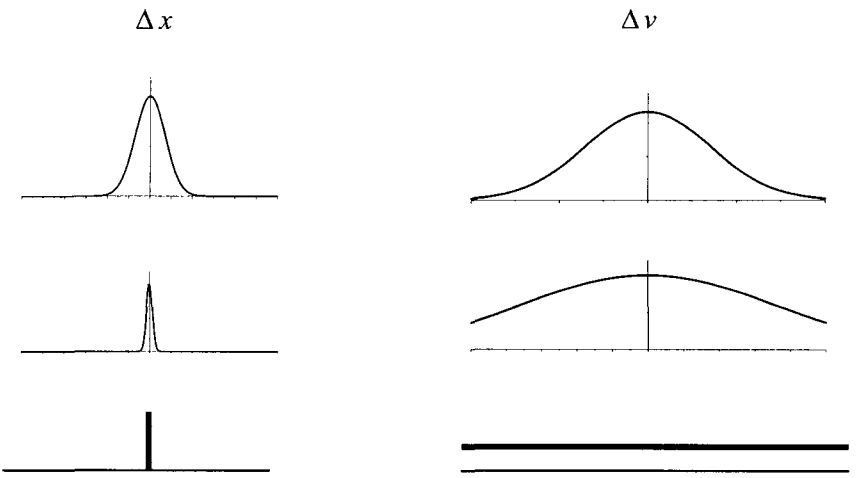

Fig.2.8 – Function $f(x)$ and its Fourier transform. As the width of $f(x)$ decreases the width of its Fourier transforms increases.

Symmetrically, Fig.2.9, if the width of $f(x)$ increases, which corresponds to an increase in the error of the position, the bulk of its Fourier transform decreases. In the limiting case when the velocity of the particle is known with absolute precision $\Delta v = 0$, the function coefficient is a Dirac delta function. In this situation the position of the particle is completely unknown

$\Delta x = \infty$. Therefore an absolute knowledge of the velocity of the particle leads to a total ignorance of its position, $\Delta v = 0, \Rightarrow \Delta x = \infty$.

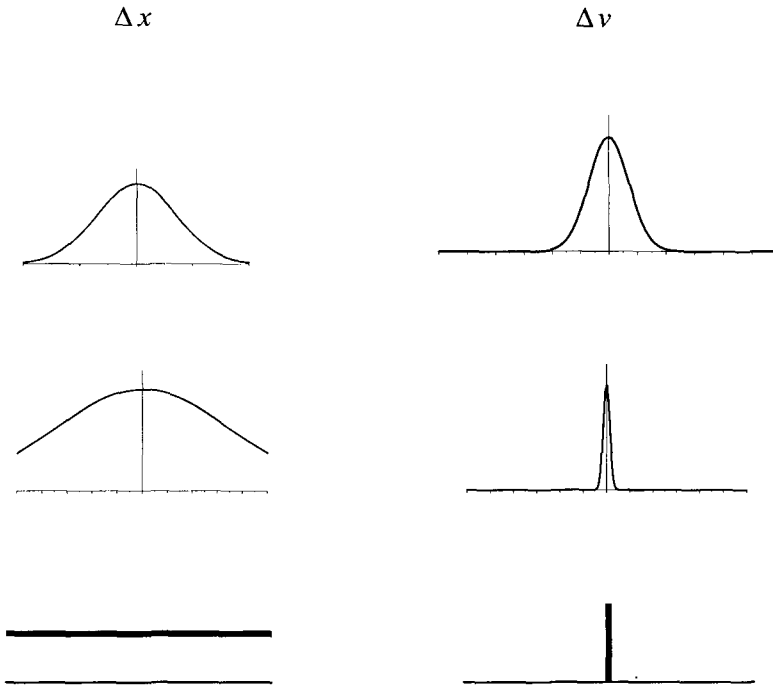

Fig.2.9 – Function $f(x)$ and its Fourier transform. As the width of $f(x)$ increases the with of its Fourier transforms decreases.

So at the end, summarizing these two cases, it is possible from these extreme situations to establish an inverse relation between the two observables position and velocity

$$\Delta x = 0, \quad \Leftrightarrow \quad \Delta v = \infty$$
$$\Delta x = \infty, \quad \Leftrightarrow \quad \Delta v = 0$$

This statement is precisely one form of enunciating the principle of complementarity. In words it reads:

"The more we know on the position of a particle the less we known about its velocity and vice-versa".

This line of descriptive reasoning can be made more precise in mathematical terms.

From Fourier analysis, and following Niels Bohr as close as possible, it is possible to represent a well-behaved function, representing the region where the particle can be localized, as an infinite sum of monochromatic plane waves

$$f(x) = \int_{-\infty}^{+\infty} g(\sigma) e^{i\sigma x} d\sigma \tag{2.4.1}$$

where $\sigma = 1/\lambda$, represents the wave number and $g(\sigma)$ the coefficient function that it is assumed to have a gaussian form

$$g(\sigma) = e^{-\frac{\sigma^2}{2(\Delta\sigma)^2}}. \tag{2.4.2}$$

By substitution of the coefficient function into (2.4.1)

$$f(x) = \int_{-\infty}^{+\infty} e^{-\frac{\sigma^2}{2(\Delta\sigma)^2}} e^{i\sigma x} d\sigma \tag{2.4.3}$$

and integration one has

$$f(x) = \sqrt{2\pi}\Delta\sigma\, e^{-\frac{x^2}{2/(\Delta\sigma)^2}}. \tag{2.4.4}$$

Meaning that, as is very well known, the Fourier transform of a gaussian is also a gaussian. From (2.4.4) one concludes that

$$\Delta x \Delta\sigma = 1, \tag{2.4.5}$$

expression establishing the relation between the width of the functions $f(x)$ and $g(\sigma)$. In the case of temporal information on the particle one gets, following the same steps, the corresponding temporal relation,

$$\Delta t \, \Delta \nu = 1 . \tag{2.4.6}$$

Remembering the fundamental relations of quantum mechanics, Plank-Einstein and de Broglie equations

$$E = h\nu ; \qquad p = \frac{h}{\lambda} = h\sigma$$

and by substitution in (2.4.5) and (2.4.6) one finally gets

$$\begin{aligned} \Delta x \, \Delta p_x &= h \\ \Delta t \, \Delta E &= h \end{aligned} \tag{2.4.7}$$

expressions that express the relations between the two most important conjugate pairs of quantum uncertainties.

In this way, particularly simple and elegant, Niels Bohr was able to derive the Heisenberg's uncertainty relations as a direct consequence of Fourier nonlocal analysis. Thus, from single mathematical relations, these formulas assume the deep ontological status of expressing, in an extremely condensed way, an aspect of the Principle of Complementarity of Niels Bohr. For this reason even if it was Heisenberg who derived those relations for the first time it was nonetheless Bohr the person first to understand their importance and to give them the status they have enjoyed in science during the twentieth century. Therefore it would be quite fair to call them Heisenberg-Bohr's relations, because even if Heisenberg had the privilege of discovering them it was in fact Bohr the one that understood the deep meaning of these relations.

In this demonstration we have followed Niels Bohr, who made $\sigma = 1/\lambda$. Nevertheless, the most common way when dealing with Fourier transforms is to have $\sigma = k = 2\pi/\lambda$, due to the usual and convenient use of radian for the angular unit. In this case a complete wavelength corresponds to an argument in the circular function of 2π. It means that when the argument of the circular function corresponds to a complete cycle $\sigma x = 2\pi$ we have $x = \lambda$. Under these conditions the value of the parameter is fixed and consequently we must have $\sigma = 2\pi/\lambda$, that is $\sigma = k$. Had we used degrees as unit of the circular function then we would write $\sigma x = 360$, and for the

complete cycle $x = \lambda$ got $\sigma = 360/\lambda$. The choice of Bohr is very elegant because it corresponds to choosing an angular unit such that the entire circle corresponds to one, $\sigma x = 1$ that for the complete cycle $x = \lambda$ gives $\sigma = 1/\lambda$.

For the common choice of radian as the unit for the argument of the circular function the expression (2.4.5) would become

$$\Delta x \, \Delta k = 1, \quad k = \frac{2\pi}{\lambda} = \frac{2\pi}{h} p$$

and the uncertainty relation would be

$$\Delta x \Delta p_x = \frac{h}{2\pi},$$

the same happening with the temporal relation

$$\Delta t \Delta E = \frac{h}{2\pi}.$$

This numerical discrepancy, depending on the chosen unit for the argument of the circular function, may look a little bizarre in a formula so fundamental as the uncertainty relations, nevertheless we must recall that Bohr always assumed them as estimate relations and not as absolute numerical relations. Some people may argue that there are other more rigorous mathematical forms for the uncertainty relations such as the one by Robertson expressed in terms of the operators.

2.4.1 Other Derivations of Heisenberg's Uncertainty Relations

In this section we refer to the works of Hilgevoord and Uffink, Max Jammer, and others that exhaustively discuss the posterior derivations of the uncertainty relations, their implications and validity.

In the same year, 1927, that Heisenberg presented his relations Kennard derived the well-known formula

$$\Delta q\ \Delta p \geq \tfrac{1}{2}\hbar\,, \tag{2.4.8}$$

in which Δ, represents here and only in this section, the standard deviation squared root,

$$(\Delta q)^2 = \overline{(q-\overline{q})^2} = \overline{q^2} - \overline{q}^2, \quad (\Delta p)^2 = \overline{(p-\overline{p})^2}\,. \tag{2.4.9}$$

Elsewhere Δ stands for the quantum uncertainty, equivalent to the general bulk of the probability function. This broad bulk, containing most of the area of the probability function is, as we shall see, in general, very different from the standard deviation squared root.

The next important contribution was given in 1929 by Robertson who derived the following expression for the uncertainty relations in terms of operators.

$$\Delta A\ \Delta B \geq \tfrac{1}{2}\overline{AB - BA}\,, \tag{2.4.10}$$

where A and B are arbitrary Hermitic operators. This relation is very beautiful and suggestive. Maybe, because of its formal beauty many authors claim that the Robertson's formula is the most complete mathematical expression for the uncertainty relations. If A and B represent the operators Q and P, remembering that their commuter is

$$[Q,P] = i\hbar\,,$$

one gets directly, by simple substitution into (2.4.10), the relations of Kennard (2.4.8).

In spite of its formal attractiveness and elegance the Robertson's operator relation has nevertheless some inconveniences:

For instance, if the state function is an eigenfunction of one of the operators then ΔA or ΔB is null while their commuter can be different from zero. In order to avoid this inconvenience some authors restrict its validity and allege that Robertson's expression is only to be applied when the state function is not an eigenfunction of one of the operators.

Other deficiency of (2.4.10) as a good expression for the uncertainty relations results from the fact that there exists no quantum operator for time,

therefore it is impossible to derive, directly, from the operator expression of Robertson the time-energy uncertainty relation.

Nevertheless, as pointed out by Hilgevoord and Uffink, the most serious inconvenience of the standard Robertson uncertainty relation is its dependence on the standard deviation as a good measure for the quantum uncertainty. The quantum uncertainty is, as we have seen, represented by the general bulk of the density function.

In quantum mechanics the squared modulus of the wave function $|\psi|^2$ represents the distribution of the possible outcomes of a measurement. Therefore, as we shall see, only in the case when this distribution is a gaussian the standard deviation is a good measure for quantum uncertainty, in that case it coincides with its bulk. Let us, following Hilgevoord, consider a beam of particles with a known momentum which strikes perpendicularly a screen with an infinitely long slit of width *2a*. The position and momentum of the particle on the plane of the screen are q and p. Assuming the simple mathematical model for the single slit we have considered before, we get for the spatial part of the wave function

$$\psi(q) = \begin{cases} 1/\sqrt{2a}, & |q| \leq a, \\ 0, & |q| > a, \end{cases} \tag{2.4.11}$$

which is similar to the example used before to illustrate the Fourier transform for $q \equiv x$, $p \equiv k$, $a = L/2$ and $A_0 = 1/\sqrt{2a}$. Then the wave function in the momentum space is the Fourier transform of (2.4.11).

$$\varphi(p) = \frac{1}{\sqrt{2\pi}} \int_{-\infty}^{+\infty} \psi(q) e^{-ipq} dq, \tag{2.4.12}$$

which , as expected, gives

$$\varphi(p) = \sqrt{a/\pi}\ \mathrm{sinc}(ap). \tag{2.4.13}$$

Let us now calculate for this physical situation the standard deviation of the two conjugate variables q and p: For the variable q one has

$$\bar{q} = \int_{-\infty}^{+\infty} q\,|\psi|^2\,dq = \int_{-a}^{+a} q\,\frac{1}{2a}\,dq = 0\,, \tag{2.4.14}$$

and

$$\overline{q^2} = \int_{-\infty}^{+\infty} q^2\,|\psi|^2\,dq = \int_{-a}^{+a} q^2\,\frac{1}{2a}\,dq = \frac{1}{3}a^2\,, \tag{2.4.15}$$

that is

$$(\Delta q)^2 = \overline{q^2} - \bar{q}^2 = \frac{1}{3}a^2\,. \tag{2.4.16}$$

The calculation for the other conjugate variable gives:

$$\bar{p} = \int_{-\infty}^{+\infty} p\,|\psi|^2\,dq = \int_{-\infty}^{+\infty} p\left[\sqrt{\frac{a}{\pi}}\,\mathrm{sinc}(ap)\right]^2 dp = 0\,, \tag{2.4.17}$$

and

$$\overline{p^2} = \int_{-\infty}^{+\infty} p^2\,|\psi|^2\,dq = \int_{-\infty}^{+\infty} p^2\left[\sqrt{\frac{a}{\pi}}\,\mathrm{sinc}(ap)\right]^2 dp \to \text{diverges}\,, \tag{2.4.18}$$

therefore

$$(\Delta p)^2 = \overline{p^2} - \bar{p}^2 = \overline{p^2} \to \text{diverges}\,. \tag{2.4.19}$$

In such conditions the product of the uncertainties of the two conjugate variables diverges also

$$\Delta q\;\Delta p \to \text{diverges}\,.$$

Expression (2.4.18) could also be written

$$\overline{p^2} = \lim_{\ell \to \infty} \frac{\ell}{\pi a}\left[1 - \mathrm{sinc}(2a\ell)\right] \approx \lim_{\ell \to \infty} \frac{\ell}{\pi a} \tag{2.4.20}$$

and the product of the two uncertainties diverges

$$\Delta q\,\Delta p = \lim_{\ell \to \infty} \left(\frac{1}{3\pi} a\ell\right)^{\frac{1}{2}} \to \text{diverges}. \tag{2.4.21}$$

From this expression one sees that as the chosen point of the cutoff changes the value of the product also changes. Had we made the cutoff such that the main bulk of (2.4.13), which plot is shown in Fig.2.2 for $a = L/2$, stand between the first two zeros, $-\pi/a \le p \le +\pi/a$, the quantum uncertainty would be $\delta p = 2\pi/a$. One the other hand, taking in consideration that the equivalent uncertainty for the variable q is $\delta q = 2a$, their product would give

$$\delta q \delta p \approx 4\pi .$$

This expression, even if it reflects the spirit of Bohr's idea, is not very sound because it depends strongly on the arbitrary point where the cutoff is made. Had we chosen the second zero $-2\pi/a \le p \le +2\pi/a$, the uncertainty would then became

$$\delta q \delta p \approx 8\pi .$$

These facts indicate that the standard deviation, except in a few cases, such as, for instance, when the probability density is gaussian, is not, in general, a good measure for the bulk of the function. In this very special case the wave function has the form

$$\psi(x) = c_1 e^{-\frac{x^2}{2\delta_x{}^2}}, \tag{2.4.22}$$

and its Fourier transform

$$\varphi(k) = c_2 e^{-\frac{k^2}{2\delta_k{}^2}} \tag{2.4.23}$$

has precisely the same form. The two normalized functions are

$$\psi(x) = \frac{1}{\sqrt[4]{\pi}\sqrt{\delta_x}} e^{-\frac{x^2}{2\,\delta_x{}^2}}, \quad \varphi(k) = \frac{1}{\sqrt[4]{\pi}\sqrt{\delta_k}} e^{-\frac{k^2}{2\,\delta_k{}^2}},$$

and the probability density respectively

$$|\psi(x)|^2 = \frac{1}{\sqrt{\pi}\delta_x} e^{-\frac{x^2}{\delta_x{}^2}}, \quad |\varphi(k)|^2 = \frac{1}{\sqrt{\pi}\delta_k} e^{-\frac{k^2}{\delta_k{}^2}}.$$

Since the gaussians are centered in the point zero, the two standard deviations are given simply by the mean of the second moment because their means values are zero,

$$\overline{x^2} = \int_{-\infty}^{+\infty} x^2 |\psi(x)|^2 \, dx = \frac{1}{\sqrt{\pi}\delta_x} \int_{-\infty}^{+\infty} x^2 e^{-\frac{x^2}{\delta_x^2}} dx = \tfrac{1}{2}\delta_x^2 \qquad (2.4.24)$$

Which means that

$$\Delta x = \frac{1}{\sqrt{2}}\delta_x \qquad (2.4.25)$$

and by the same token, since the calculations are precisely the same

$$\Delta k = \frac{1}{\sqrt{2}}\delta_k, \qquad (2.4.26)$$

their product being

$$\Delta x \, \Delta k = \tfrac{1}{2}\delta_x \, \delta_k = \tfrac{1}{2}. \qquad (2.4.27)$$

This last expression confirms that in the particular case of a gaussian state function defined by formula (2.4.22) with the constants written in the typical form, the widths of the gaussians are related to the standard deviations by the usual expression

$$\delta\xi = \sqrt{2}\,\Delta\xi\,. \tag{2.4.28}$$

where ξ represents the generic variable. This formula could easily be deduced directly from the expressions relating the width of the wave function with the width of its squared modulus, which corresponds to the probability density function.

Formula (2.4.28) stands for the expression, written in most textbooks of quantum mechanics, relating the width, the general bulk, of the wave with the standard deviation. Nevertheless this expression only holds for the case of a gaussian wave function, and even so only for that particular choice of the constants in the denominator of the exponential argument. In the other cases it is not, in general, possible to establish a direct relationship between those two entities. When possible, the mathematical expression relating the general bulk of the wave with the standard deviation is usually much more complex than (2.4.28).

It seems now quite clear that the formula of Robertson for the uncertainty relations, and consequently the one of Kennard are not so general as usually claimed. The presented evidence indicates that these expressions must be used with some caution.

2.4.2 Meaning of the Uncertainty Relations

The success of the uncertainty relations was enormous! The scientific community soon understood their great importance and many works on the subject were published, not only on the physical domain but also in philosophy, epistemology and even in plain literature. These relations got indeed a sort of sacrosanct status a kind of mystical aura so that no one dared to challenge them. The success was so overwhelming that until recently no one had ever questioned its general validity. Not even among those scientists like Einstein, de Broglie and many others, which have always fought the so-called Copenhagen interpretation of quantum mechanics, we find a serious objection. The most they questioned was its meaning. In this general picture we can point out Dirac who in a later paper questioned these relations. Quoting his own words: *I think one can make a safe guess that the uncertainty relations in their present form will not survive in the physics of the future.* On the other hand it is also true that even if we can find a few

scientists that questioned their formal expression nevertheless none of them thought about a possible experimental violation of such relations.

It is known that some authors, less learned in quantum mechanics, claim violations of the uncertainty relations in situations that, according to the usual nonlocal paradigm, are perfectly irrelevant. These erroneous conclusions are mainly consequence of a grave misunderstanding of the conceptual structure of the orthodox quantum mechanics and consequently of the deep meaning of those relations.

The uncertainty relations are essentially connected with the measurement problem. As a matter of fact, as we shall see, it is possible, numerically, to overcome the limit imposed by those relations. As pointed out by Selleri and the author this has been recognized early by Heisenberg himself, and by Bohr. Even Popper wrote a lot on the meaning of the uncertainty relations in the thirties. Since then it is common lore in fundamental quantum mechanics. Still, this possibility of making measurements that in the past violated them doesn't, as we shall see, in any way challenge the true meaning of Heisenberg's uncertainty relations. This is a consequence of the fact that after the measurement, after the interaction, the product of the space and momentum uncertainties, $\Delta x \Delta p$, or of any other pair of conjugated observables, does indeed verify those relations.

In order to illustrate this problem let us see a concrete example of it. This example, one among many possibilities, is based on a work of Andrade e Silva.

Fig.2.10 is a sketch of an experiment that apparently violates the uncertainty relations, just before measurement takes place. An electron source emits electrons, one at a time, towards a monochromator. After leaving the monochromator the uncertainty in the momentum of the electron is Δp. Therefore, according to the Heisenberg uncertainty relations, its uncertainty in position must be Δx so that $\Delta x \, \Delta p \geq h$.

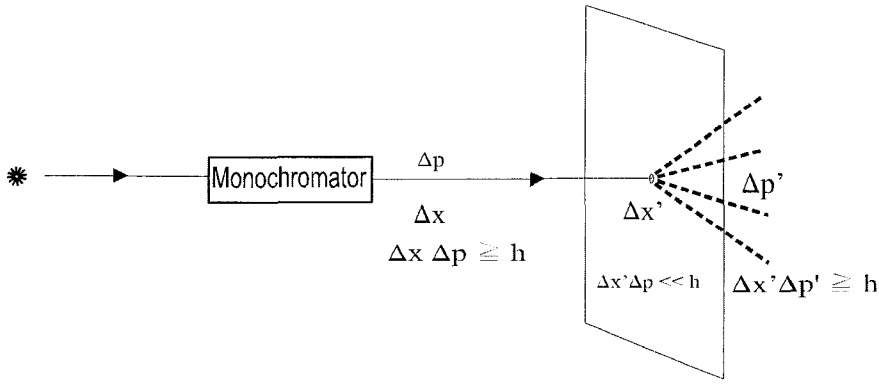

Fig.2.10 – Apparent violation of the uncertainty relations.

In its trip the electron goes through a screen with a hole. Behind that hole there is an electron transfer detector, that is, a detector that "sees" the electron without killing it. The detection is accomplished thanks to a small random momentum transfer from the electron to the detector. The hole and the detector are arranged in such a way that the uncertainty in position of the electron is $\Delta x'$. This uncertainty in position $\Delta x'$, as we can see, is completely independent of the uncertainty in momentum Δp. One can easily see that the uncertainty in momentum Δp depends only on the monochromator, the better the monochromating device the smaller Δp, while the uncertainty in position $\Delta x'$ depends only on the detecting device, that is, on the way the hole and the detector are arranged. The whole experimental setup can be arranged in such a way that the product of the two uncertainties, just before the interaction, is much less than the limit imposed by Heisenberg, $\Delta x' \Delta p << h$.

Still, during the interaction with the detector, the uncertainty in momentum of the electron spreads in such a way that the smaller the uncertainty in position $\Delta x'$ the greater the uncertainty in momentum $\Delta p'$. Therefore, at the end, after the measurement, after the interaction, the product of their uncertainties obeys Heisenberg's uncertainty relations $\Delta x' \Delta p' \geq h$.

This experiment clearly shows that the uncertainty relations only forbid the prediction of the uncertainties, such that their product is less than h after the measurement. This conclusion comes as a natural consequence from the quantum measurement process. Before the collapse of the wave function, due in general, but not always, to a physical interaction, as we have seen, all possibilities do exist only as potentialities. These possibilities are the probable final outcome of the measurement process. In this case, the measurement process is accomplished, when the electron is in fact "seen" at the detector. Therefore only after that moment the whole group of potentialities collapses into one. Out of a large bunch of potentialities the measurement process makes only one of them real. In these circumstances, before the measurement process we can perfectly have $\Delta x' \Delta p << h$, but this result is devoid of any real quantum physical meaning. Therefore, in this experiment, no harm is really done to the general validity of the Heisenberg uncertainty relations. Only after the interaction, after the measurement, we have a real physical situation corresponding to $\Delta x' \Delta p' \geq h$.

2.5 REFERENCES

On the principles and history of the orthodox theory:

N. Bohr, Nature, **14**, (1928)580.

N. Bohr, (1928) - *Como Lectures, Collected Works*, Vol. 6, North-Holland, Amsterdam, 1985.

W. Heisenberg, *The Physical Principles of Quantum Theory*, The University of Chicago Press, Chicago,1930.

J. Faye, *Niels Bohr: His Heritage and Legacy: An Anti-Realistic View of Quantum Mechanics*, Kluwer Academic Publishers, 1992.

D. Cassidy, *Uncertainty, the Life and the Science of Werner Heisenberg*, Freeman and Company, New York, 1992.

R.N. Moreira, Høffding and Bohr: Waves or Particles, *in Waves and Particles in Light and Matter*, ed. Alwyn van der Merwe and Augusto Garuccio, Plenum Press.

On the Fourier analysis:

H.S. Carslaw, *An Introduction to the theory of the Fourier's Series and Integrals*, Dover, New York, 1950.
M.G. Light Hill, *Fourier Analyses and Generalized Functions*, Cambridge University Press, Cambridge, 1950.

On operators and quantum measurement:

G. Temple, Nature,135(1935)957
F. London et E. Bauer, *La Theory de l'Observation en Mécanique Quantique*, Hermann, Paris, 1939.
W. Renninger, Zeit. F. Physik, 158(1960)147.
D. Bohm, *Quantum Theory*, Prentice-Hall, Englewood Cliffs. N.J. 1951.
L. de Broglie, *La Theorie de la Measure en Mécanique Ondulatoire*, Gauthier Villars, Paris,1957.

On other mathematical expression for the orthodox uncertainty relations:

M. Jammer, *The Philosophy of Quantum mechanics*, John Wiley and Sons, (New York, 1974)
J. Hilgevoord and J.B.M. Uffink, *In Microphysical Reality and Quantum Formalism*, Eds. A. van der Merwe et. al. Kluwer Academic press, Dordreckt, 1988.
P.M.A. Dirac, Scientific American, May, 208(1963)49.

On the meaning of the uncertainty relations:

K. Popper, *Quantum Theory and the Schism in Physics*, Hutchinson, London, 1972.
J. Andrade e Silva, *Peut-on Connaître Simultanément et avec Précision la Position e la Quantité de Mouvement d'une Particule?*, Portugalie Physica, 4(1966)257.
J.R. Croca and F. Selleri, Comm. Math. Theor. Physics, vol. 2, (1999)61.

CHAPTER 3

NEW GENERATION OF MICROSCOPES

3.1 INTRODUCTION

Until a few years ago the only way to look at the minute world was through the common Fourier microscopes. These microscopes, just like any other imaging system, have indeed a limit in its resolution power. Abbe, inspired by the work of Rayleigh, was able to demonstrate that the maximum possible resolution for any common Fourier microscope is of about half wavelength of the radiation being used in the observation. This resolution corresponds to the minimum possible distance separating two points such that can still be resolved as discrete entities. In this circumstances the greater the resolution of the imaging system the smaller can be the distance between those two points.

In the second half of the eighties this picture changed radically with the development of a new generation of microscopes with a resolution that does not depend intrinsically on the diffraction properties of the waves. In the common microscopes the minimum separation depends basically on the wave properties of the quantum entities while in the new microscopes the resolution does not essentially depend on it. This resolution, can, in principle, have any value, depending only on the practical physical limitation imposed on those systems.

The development of this new generation of microscopes led to new insights in the conceptualization of imaging systems. Now we are able to see that, in fact, the first devices working on the same principle, that is, non-Fourier observing systems did appear much earlier.

It is sufficient to recall with Pohl Lanz *(Optical stethoscopy; Image recording with resolution* $\lambda/20$*)* the familiar common stethoscope, used in medicine for diagnostic. This acoustic device is able to locate the human heart with great precision, thanks to the sound waves produced by the heartbeats. The doctor can locate the heart of the patient to within a precision

of about 10cm by moving the stethoscope over the patient's chest and by hearing the heartbeats. The sound frequency for this case can be assumed to be between 30Hz to 100Hz which corresponds to sound waves of a length of about 100 m. Had this observing system followed the resolution rule, of half wavelength $\lambda/2$, derived by Abbe for the common Fourier microscopes, then the physician would not be able to locate the heart in the patient's body because the theoretical maximum resolution of his observing system would be half wavelength, that is nearly, 50m! Still the real resolution of these observing instruments is of about 0.1m, which corresponds to a resolution of $\lambda/1000$.

This chapter begins with a study of the fundamental of the working principles of Fourier microscopes and with a derivation of Abbe's maximum theoretical resolution rule. These matters can be found in any good textbook of classical optics. Still they are presented here because by on one hand it is useful to gather the pertinent information on the resolution of the usual imaging devices, and for the other hand because of the important role they still play on the conceptual foundations of orthodox quantum theory.

3.2 THE COMMON FOURIER MICROSCOPES

The common microscopes are called Fourier microscopes for two main reasons:

First, because the resolving power of those microscopes is limited, in practice, by the diffraction phenomenon. The diffraction pattern of a circle, representing the real point source can, as is well known, be analytically described by its Fourier transform.

The second, and perhaps the most important reason, is related with the deep connections of those imaging devices with the Heisenberg's uncertainty relations which are, as we have seen, a direct consequence of the Fourier transforms.

The usual optical systems, dedicated to amplify images, like for instance the microscopes, have theoretical basic constraints in its augmenting power. At first sight this may look paradoxical. In fact, some readers, less familiar with physics, may be led to believe that the ability of a microscope to amplify an

image has no limits. The fundamental reasoning that leads to this conclusion is in reality very simple and naive:

Let us consider an object that we want to amplify. By using a certain microscope we obtain an amplification of, say, for example, one hundred times. This is easily achievable with any common microscope. Next we can use this image as a new seed object and amplify it with an identical microscope. In such circumstances we can amplify this second image object one hundred times more. This second image corresponds to an amplification equal to the product of the two amplifications, which means: ten thousand times. Following the same line of reasoning we would expect no limits in the amplifying power of the combined system of microscopes. However, and unfortunately, this is not true.

Every usual optical imaging system possesses in reality two kinds of limits in its power to amplify images:

One, the easiest to understand, is the result of the natural deterioration of the image in the successive amplifications. After a certain number of amplifications the image deteriorates in such a way that the final image is of no use. This natural degrading process is due to the imperfection of the lenses and other diverse causes and leads to a progressive loss of quality of the final image.

The second was discovered in the nineteenth century by the physicists. They discovered that there is a very important and basic cause that conduces to a limitation in the augmenting power of the optical systems.

This second fundamental cause of limitation they called resolution. The resolution of an imaging device is thus usually understood as the basic capability of the system to distinguish between two very near points. This concept is not, in general, very well defined and is somewhat rather artificial with the exception of a few situations; nevertheless it is a very useful concept to be used in practice. This optical systems characteristic, limiting the amplification power of the imaging systems, is much more fundamental, and is a consequence of the undulatory character of light. To understand this important, even if not very well defined, concept let us first discuss briefly the functioning of one the most common optical systems: the photographic camera.

In the following figure, Fig.3.1, we can see the scheme of the dark camera that embodies the essence of the photographic camera.

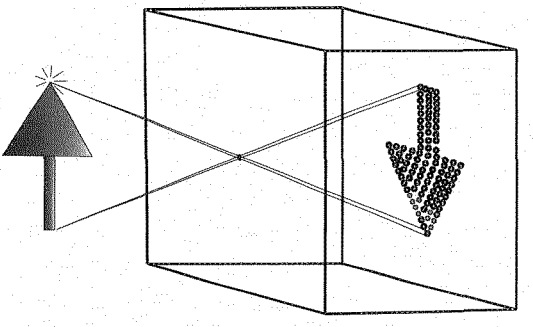

Fig.3.1 – Dark camera.

The light emitted from a point source in the object is sent in all directions but only a small fraction of it, a small cone, enters the pinhole and then goes to the screen generating a luminous spot corresponding to the image of the point on the screen.

From Fig.3.1 one gathers that the diameter of the entering hole defines the resolution of the final image. The smaller the diameter of the entrance point the higher the resolution. Geometrically, if the pinhole were a mathematical point, every point of the object would generate a single point in the image plane. In practice, because the physical hole is never a mathematical point, each point source in the object generates a circle in the imaging plane. This is what we can see in the sketch. Nevertheless the things are not as easy as they may seem. When the dimensions of the entrance circle decrease, we begin to observe the phenomenon of diffraction, and the dimensions of the image points increase instead of diminishing.

Abbe, a physicist of the last century, showed, based on the Rayleigh resolution thumb rule, that the maximum theoretical resolving power for these imaging systems is about half the wavelength of the light used in the device. The dependence of the imaging systems resolution on the wavelength explains the considerable investment currently being made to produce compact disks systems working with blue or violet light. This is perfectly understandable because the wavelength of violet light is about half the wavelength of red light. As a practical consequence the resolution of a reading system using violet light is about double of that of a reading system

using red light. In practice this means a four-fold increase in capacity in the usual storing devices. Just to have an idea of the practical and economical implications it is enough to recall that if on a CD written with red light it is possible to store a two-hour movie, on a CD using violet light we could have an eight-hour movie.

The next figure, Fig.3.2, illustrates this fundamental point. In this sketch, there is a screen with a circular hole and a faraway target screen where the image of the hole appears. Let us consider a beam of light, of a certain wavelength, impinging on the screen with the circular aperture. At the target placed far behind the screen we observe the image of the hole.

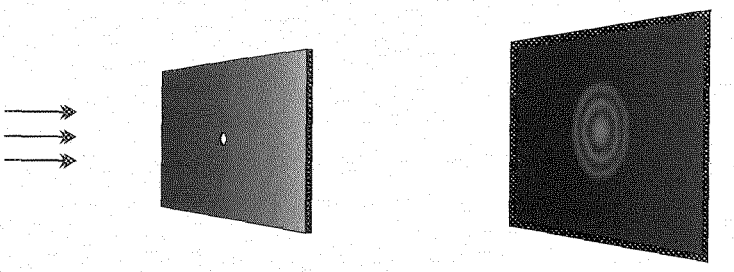

Fig.3.2 – Circular aperture and its far field image.

Due to the wave character of light, the image of the circular hole, instead of being very sharp, changes into a blurry diffraction pattern with a central primary maximum and a series of secondary maxima starting from the main one. In the picture only two secondary maximum are easily seen, the others, due to their small amplitude, are mixed up with the background. This intensity distribution is given by the known formula called the Fraunhofer diffraction pattern of the circular aperture,

$$I = I_0 \left[\frac{J_1(2\pi\rho)}{\rho} \right]^2, \quad \rho = \frac{a}{\lambda} \sin\theta = \frac{aq}{\lambda R} \tag{3.2.1}$$

where J_1 is the Bessel function of order one, a is the radius of the circular aperture, and θ is the observation angle, that is the angle between the perpendicular to the circle and the line from the center of the circle and the observation point at the screen, λ represents, as usual, the wavelength of the radiation, while R is the distance from the center of the circular aperture to

the considered point of radius q on the screen. For the sake of clarity the next figure, Fig.3.3, indicates the positions and roles of the variables

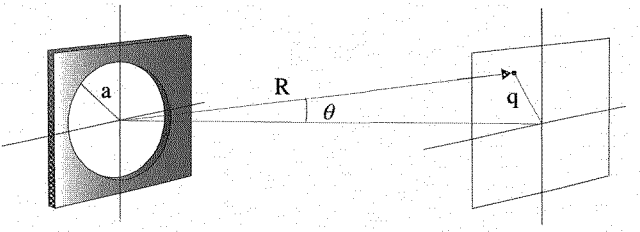

Fig.3.3 – Diffraction of a circular aperture.

The far field diffraction intensity pattern is, as is well known, the square of the modulus of the wave field at the screen. This field corresponds, mathematically, precisely to the Fourier transform of a circular aperture.

$$circ(a) \xrightarrow{Fourier} \frac{J_1(2\pi\rho)}{\rho}$$

Let us now consider the case of a screen with two circular holes sufficiently far from each other, so that the Fraunhofer approach could apply, as shown in the next figure, Fig.3.4. In this case we observe two different diffraction patterns corresponding to each one of circular holes with two primary maxima perfectly separated from each other. Assuming, as usual, that the light from each hole is not coherent, it is possible to calculate the final image as the overlapping of the Fourier transforms of the two slits each considered separately.

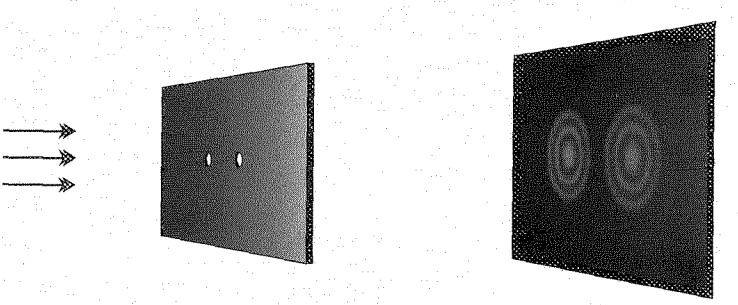

Fig.3.4 – Far field image of two well separated circular holes.

We may now ask, what will happen if the distance between the two circular holes in the screen decreases?

From what we have just seen the answer is quite simple. What we will observe on the target is the overlapping of the two different diffraction patterns where the two main maxima may merge into a single one. When the distance between the two holes is lesser than a certain value the two maxima are no more discernible. This represents the resolution limit due to the wave nature of light. The situation is represented in Fig.3.5

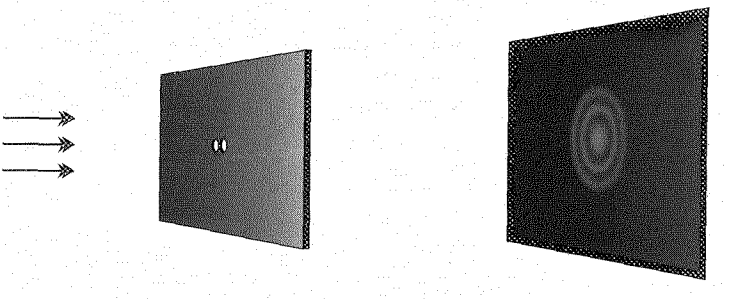

Fig.3.5 – Far field image of two near holes.

Abbe, using Rayleigh criterion, was able to show that this limit corresponds to about half a wavelength of the light crossing the screen. Thus, below this limit we can no longer distinguish the two holes in the final image.

The Rayleigh practical criterion, shown in the picture Fig.3.6, states that two point sources are resolved if the center of the first diffraction pattern falls on the first minimum of the other diffraction pattern. Graphically, one has

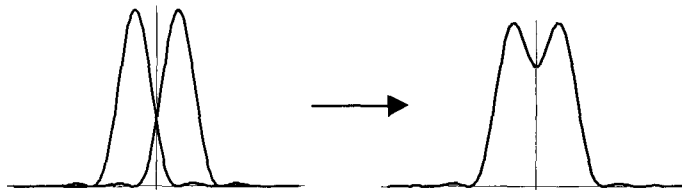

Fig.3.6 – Plot of Rayleigh criterion.

which clearly shows that the Rayleigh rule does not come from any basic first principles but results only from heuristic practical considerations.

For the basic optical microscope system sketched in Fig.3.7

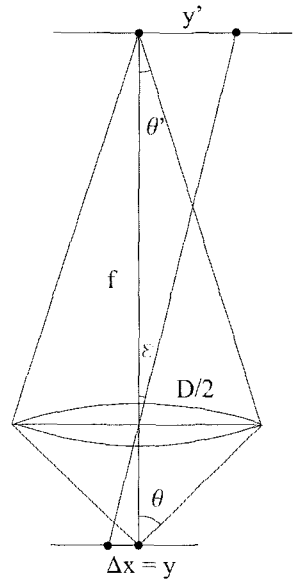

Fig.3.7 – Sketch of image formation in the common microscope.

this rule leads to the following relations:

$$y' = 1.22\frac{\lambda}{D} f$$
$$\varepsilon = 1.22\frac{\lambda}{D} \tag{3.2.2}$$

where λ is the wavelength of the light and the meaning of the other symbols can be inferred from Fig.3.7.

Recalling the sine condition, see Born and Wolf,

$$n\, y \sin\theta = n'\, y' \sin\theta', \tag{3.2.3}$$

stating the conditions under which a small region of the object plane in the neighborhood of the axis is imaged sharply, and by substitution of the value of y', taken from (3.2.2), one gets for the most common case when $n=n'=1$,

$$y \sin\theta = 1.22\frac{\lambda}{D} f\,\theta', \tag{3.2.4}$$

where we have made the small angle approximation $\sin\theta' \approx \theta'$. From Fig.3.7 we see that

$$\mathrm{tg}\theta' \approx \theta' = \frac{D/2}{f} \tag{3.2.5}$$

which by substitution in (3.2.4), and noting that $y = \Delta x$, leads to the known Abbe's formula

$$\Delta x \approx \frac{\lambda}{2\sin\theta}. \tag{3.2.6}$$

For a large diffusion angle it is reasonable to make

$$\Delta x \approx \frac{\lambda}{2}. \tag{3.2.7}$$

In this condition, as stated before, the resolution of a usual microscope is of the order of half wavelength.

The above derivation assumes that the light from each point source is not coherent. In the case when the light emitted by the two points sources keeps

a relatively reasonable stability in phase, i.e. when we are dealing with coherent sources, the cross section intensity distribution of the image at the screen is now the result of the overlapping of two correlated fields that can be written in normalized image coordinates

$$I(x)=\left|2\frac{J_1(\pi(x-0.6))}{\pi(x-0.6)}+2\frac{J_1(\pi(x+0.6))}{\pi(x+0.6)}\,e^{i\varphi}\right|^2 \tag{3.2.8}$$

which can be developed giving

$$\begin{aligned} I(x)=&\left(2\frac{J_1(\pi(x-0.6))}{\pi(x-0.6)}\right)^2+\left(2\frac{J_1(\pi(x+0.6))}{\pi(x+0.6)}\right)^2+\\ &2\left(2\frac{J_1(\pi(x-0.6))}{\pi(x-0.6)}\right)\left(2\frac{J_1(\pi(x+0.6))}{\pi(x+0.6)}\right)\cos\varphi. \end{aligned} \tag{3.2.9}$$

The plot of this intensity distribution can be seen in Fig.3.8, for three values of the phase difference, $\varphi=0$, $\varphi=\pi/2$, $\varphi=\pi$.

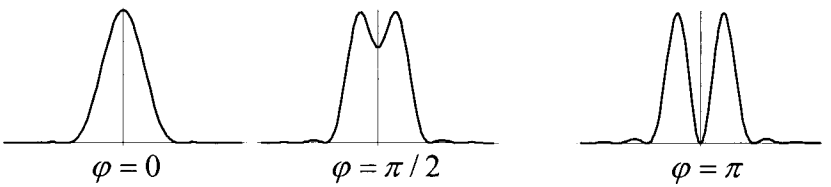

Fig.3.8 – Plot of the intensity distribution for two coherent point sources for three values of the phase difference.

For a null phase difference the two points are not resolved, when $\varphi=\pi/2$, the situation is similar to incoherent imaging since it corresponds to the cancellation of the interferometric cross term, finally for a phase difference $\varphi=\pi$, the two image points are completely separated. Therefore for coherent imaging the Rayleigh practical criterion leads to a dead end. No sound conclusion can be drawn from this case since the resolution of the two points depends in a very significative way on the relative phase difference.

Even within those Fourier imaging systems it is possible, in principle, to go beyond the classical diffraction limit. The reader interested in this fascinating theme should consult to the work of Goodman *Introduction to Fourier Optics*.

3.3 TUNNELING SUPER-RESOLUTION MICROSCOPE

The tunnel effect is related with the ability shown by the quantum particles to go through a region where predominates a repulsive potential higher than the kinetic energy of the particles. This strange effect is a direct consequence of the undulatory nature of the quantum entities and is in a certain way equivalent to the classical optical phenomenon known as frustrated total reflection. This property of quantum systems was used, in 1928, by Gamow to explain the alpha decay. The basics of the problem are a classic textbook example of the applications of quantum mechanics.

The effect can be observed when a mono-kinetic beam, with E < V, hits a square barrier as depicted in Fig.3.9.

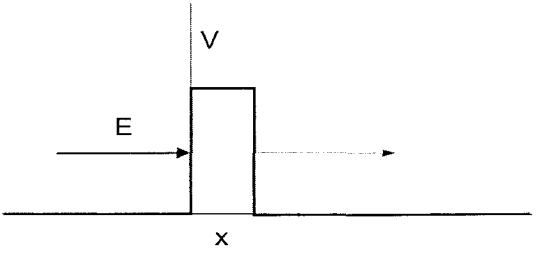

Fig.3.9 – Square potential with V > E.

The next step is to find the solutions for the Schrödinger equation in the three different regions, that is: before the barrier, inside, and after it. After this it is necessary to connect the solutions and its first derivatives at the two limiting points. After some algebra one gets for the transmission coefficient through the barrier

$$T = 8/\left\{\frac{V^2}{E(V-E)}\left[\cosh\left(\frac{2}{\hbar}\sqrt{2m(V-E)}\,x\right)-1\right]+8\right\} \qquad (3.3.1)$$

which for a thick barrier, large x, gives

$$T \cong 16\frac{E(V-E)}{V^2}e^{-\frac{2}{\hbar}\sqrt{2m(V-E)}\,x}. \tag{3.3.2}$$

or in a more simplified formula

$$T \propto e^{-\mu x}, \tag{3.3.3}$$

where μ is the transmission parameter, given in relation (3.3.2) and x is the thickness of the barrier.

In the early eighties two IBM researchers Gerd Binning and Heinrich Roher developed a concrete operational imaging device based in this principle. They named the new device scanning tunneling electron microscope. Later, in 1986, they received the Nobel Prize for this discovery.

The scanning tunneling electron microscope is made of a probe, a tiny tungsten needle with its tip ground so finely that it may consist of only a single atom. This probe scans with great precision the specimen with the help of piezoelectric controls. The tip is maneuvered to within a nanometer or two of the of the conducting specimen surface. When a small tension is applied to the tip electrons, due to tunnel effect, cross the gap generating a minute current. The intensity of such current depends exponentially, according to expression (3.3.3), on the distance between the tip and the specimen. As the probe scans the sample, line after line, the intensity of the current changes according to the distance between the tip and the surface. These variations in current intensity feed a computer and after an adequate imaging treatment this information is converted into an enlarged image of the surface of the sample. A sketch of the scanning tunneling electron microscope can be seen in Fig.3.10.

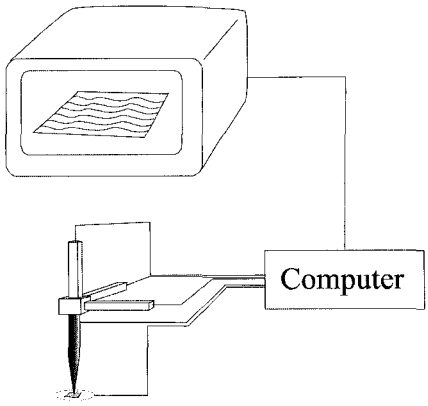

Fig.3.10 – Scanning tunneling electron microscope.

The images obtained with this new super-resolution microscope can separate points 0.2 nanometer apart.

Afterwards those ideas for new imaging systems were extended to other domains and gave birth to whole generations of super-resolution microscopes. The first development was designed to overcome one of the major limitations of the scanning tunneling electron microscope the restriction to imaging only conductor samples able to generate an electric current. This effort gave origin to the atomic force microscope. Where, in place of a tungsten tip of the first microscope, the scanning device now moves an atomic sharp diamond mounted on strip of metal. Instead of a minute current, the tip "feels" the Van der Waals forces between the tip and the electron clouds of the sample. The minute changes in the elastic metal strip feed, in this case, the system processing the information.

3.3.1 Measurements of First and Second Kind

It is worthwhile to call your attention to this new type of measurements and compare the processes for obtaining the final enlarged images with those underlaying the usual imaging devices.

In common Fourier imaging systems the information emanating from the object in form of a wave front enters the optical device. Let us consider the simplest of them all, the single magnifying glass. This optical imaging system upon receiving the light from the object, one way or another, gives

origin, depending on the situation, to a real or virtual image that can eventually be registered into a physical support.

In this and other similar cases the information is treated directly by the imaging system without direct intervention of the observer.

The imaging device works like an analog system built specifically for that kind of work. Had the form of the composing lenses been other, instead of a reasonable image of the object one would obtain an image with little or no resemblance with the original object. In this sense the final image is a consequence of the workmanship of the imaging device. It was precisely for this reason that when Galilei showed the first enlarged images of the Moon and other celestial bodies, obtained with the help of his telescope most people, including some learned men did not believe them. They thought that the images they saw generated by the telescope were hoaxes created by the observing device. In this sense they could not distinguish the images coming from the telescope with the images generated by other optical devices like, for instance, the kaleidoscope. In order to accept the observed images by its face value it was first necessary to develop a whole theory of the imaging devices, which, as we know Galilei did not have. Without a truth validation criteria the astronomical images obtained with the telescope had, in reality, no meaning at all. This happens due to the obvious reason that these images cannot be compared with the original objects, since the heavenly bodies are faraway. It was necessary to modify the whole Aristotelic paradigm so that they could be accepted by their face value.

Since in these situations and similar others the final image is obtained in a so relatively straightforward and direct way we may call them observations, or measurements of the first kind.

The working of the new generation super-resolution microscopes is much more complex. In these imaging devices the final image is obtained only after a very hard labor. The information collected from the specimen by the sensing probe is sent to an "intelligent" system, a computer that processes it according to a program. In some cases the code for the calculating process may attain a high level of complexity so that it may take some significative time to obtain the final image. The code of the program must take into account all the physics underlying the diverse type of interactions occurring during the operation of observation, the working of the scanning mechanism, the systematic and random possible errors and weigh up all relevant factors so that at the end, after the necessary smoothing and coloration, a reasonable rendered image of the specimen appears on the display. On the other hand, it is worth to recall that in order to get the

enlarged final image, these systems need to have associated an overall feedback system, between the processing device and all the other parts of the imaging apparatus including the specimen to be observed. In such condition the "intelligent" system, the computer, establishes, following an iterative process, the optimal interaction process between the specimen, to be analyzed, and the apparatus in order to obtain the best possible final image.

In most imaging health technologies the overall process for obtaining the final image is much the same as in the new generation of microscopes. For instance in nuclear magnetic resonance, or in computerized axial tomography, the program that processes the information arriving at the sensors works much like an expert system allowing the choice of diverse options and may even suggest the best possibilities.

The very complex software of these new imaging systems processes the information collected by the sensing probes, and takes in consideration the overall behavior of the system. The whole working of these systems gave origin to a highly intricate observational process. This measurement process is much more complex than the straightforward process performed by the usual Fourier systems. In these Fourier systems of the first kind the measurement is done directly. Therefore it is natural to call these more complex measurements, made with these non-Fourier apparatus, measurements of the second kind. As stressed before, in these measurements of the second kind the measuring apparatus behaves as having some kind of inner rudimentary intelligence, so that the final image depends strongly on the program.

3.4 APERTURELESS OPTICAL MICROSCOPE

The ideas of the scanning tunneling electron microscope were extended to the optical domain and gave origin to a whole panoply of imaging devices able to explore the optical properties of the samples. The first of these optical imaging devices was developed by Pohl et al. in 1984 with a resolution of about ten times the usual Fourier microscopes, that is $\lambda/20$. Today the resolution of the most common scanning optical microscopes is of about 10 nm, which for a $\lambda = 633$nm corresponds to a resolution of more than $\lambda/50$. Although the determination of the true resolution of these devices constitutes a very arduous problem, some authors claim the possibility of attaining, with special illuminating systems, spatial resolutions of the order of 1nm which, for the same wavelength, gives a ratio of about $\lambda/500$.

After the demonstration of the feasibility by Pohl and al. of the scanning optical microscope, this field grew up rapidly, so the interested reader can find in the abundant literature written on the subject a wealth of information on all aspects of these very interesting imaging devices. Just like the case of the common Fourier microscopes, here we refer only to the basics of the super-resolution optical microscope, which shall be needed in order to compare with the usual microscope.

Since these imaging devices perform measurements of the second kind they are composed by the hardware part plus the "intelligent" system. The "intelligent" system receives and processes the information while controlling the required feedback mechanism. As we have stressed, the code for processing the information can be very complex in some of these imaging apparatus. The usual hardware, of these imaging devices is essentially composed of three basic parts:

1 – A small sensing probe collecting the light emitted from the sample. In some of these microscopes, with a resolution of the order of 10nm, the probe, the light sensor, is made of an optical fiber etched to a very sharp needle with a very small sensing area, smaller than that of a human hair. The capturing area of the sensing probe is critical for the final resolution of the apparatus because it depends strongly on the size of that area.

2 – The illuminating system. In some types of super-resolution optical microscopes, with a resolution within reach of 1nm, the critical factor is the illuminating system while the collecting area of the light sensor is not so important. In such optical imaging devices the light source is the tip of a very sharp needle. The resolution in such case depends basically on the size of this illuminating point source.

3 – The scanning device. The scanning system, common to all these super-resolution microscopes, is in general made of a cantilever with piezoelectric crystal arms. The application of an adequate voltage allows the scanning of the entire sample, line by line. Most commonly the scanning system is connected to the sensor probe that gathers the light from the sample. In some other microscopes it is the illuminating device, the illuminating point source, which is connected to the scanning system.

In these optical imaging systems the light gathered by the sensor is converted into an electric current. This current constitutes the information that feeds the processing system and is proportional to the intensity of the light locally diffused by the sample. This information allows the creation of a map of light intensity distribution of the sample. In order to further increase the resolution, the feedback mechanism controls the optimal distance between the specimen and the collecting probe or the tiny emitting source of the sample. In any case after a convenient treatment of the received information, taking in account the removal of most of the noise, the smoothing, and the due coloring, a final rendered enlarged image of the sample appears at the display. Some of these final images, obtained with these optical instruments, are really beautiful. They indeed look like works of art!

A sketch of one type of these super-resolution microscopes, with a resolution of about $\lambda/50$, is shown in Fig.3.11.

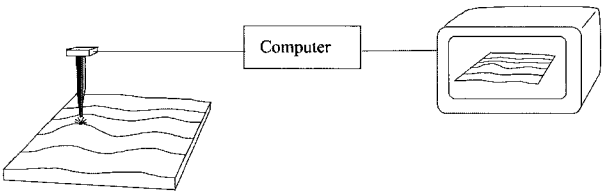

Fig.3.11 – Scanning super-resolution optical microscope.

In order to simplify the drawing the scanning device, which in this case is connected to the light sensor probe, is not shown. Also the illuminating system, which in this type of optical microscope is not critical for the final resolution, is not represented.

In this specific type of microscope the resolution depends basically on the area of the photon-sensing probe, on the distance from the tip to the sample to be observed and of course on the minimum possible step for the scanning system.

3.5 REFERENCES

On common microscopes:

M. Born and E. Wolf, *Principles of Optics*, Pergamon Press, New York, 1983.
E. Hecht and A. Zajac, *Optics*, Addison-Wesley, Reading, Mass. 1974.
J.D. Gaskil, *Linear Systems, Fourier Transforms and Optics*, John Wiley and Sons, New York, 1978.
J.W. Goodman, *Introduction to Fourier Optics*, MacGraw-Hill, New York, 1996.

On super-resolution microscopes:

G. Gamow, Zeit. f. Physik, 51(1928)204.
G. Binning and H. Roher, Reviews of Modern Physics, 59(1987)615.
D.W. Pohl, W. Denk, and M. Lanz, *Optical stethoscopy image recording with resolution* $\lambda/20$, Appl. Phys. Lett. Vol. 44, no 7 1984, pag. 651.
H. Heiselmann, D.W. Pohl, Appl. Phys. A, 59(1994)89.
F. Zenhausern, M.P. O'Boyle and H.K. Wickramasinghe, Appl. Phys. Lett. 65(1994)1623.
B.Hecht, H. Bielefeld, Y. Inouye, D.W. Pohl and L. Novotny,J. Appl. Phys. 81(1997)2492.

CHAPTER 4

BEYOND HEISENBERG'S UNCERTAINTY RELATIONS

4.1 INTRODUCTION

When Niels Bohr, in his now famous Como lecture, gave the interpretation of the mathematical inequalities, derived by Heisenberg, as a particular case of his more general principle of complementarity, in a certain way, he proposed the limits for the human possibilities of knowledge. In this system Reality no longer behaves classically in the sense that it is not possible to access, at the same time, the dual complementary attributes of Nature like, for instance, the undulatory aspect of quantum beings and the corpuscular character. The same statement is, of course, valid for any other two complementary properties. So, in this conceptual framework, it is never possible to know, for instance, the position of a particle and its velocity with better precision than the one allowed by Heisenberg relations. This happens because, in fact, in this paradigm, there are no real particles before the measurement, and for that reason it makes no sense to talk about real position and real velocity of an entity that does not have true existence. Under such circumstances, in this system of thought, Heisenberg's relations are to be seen as indeterminacy relations. This conclusion is contrary to the causal interpretation that sees the same expressions as uncertainty relations. In this frame of thinking the meaning of uncertainty relations follows directly from the usual causal reasoning. They state that the true position and the true momentum of a particle do exist even before any measurement process. What really happens is that due to the imperfections and the necessary interaction with the measuring apparatus it is usually impossible to simultaneously measure these two conjugate quantities without error.

In the orthodox approach for quantum mechanics, the reality, that is, the photons, the electrons, any microparticle, and consequently all material

entities, since they all are made of microparticles, do not exist truly before the measurement. What in reality exists is a whole set of potentialities, with certain probabilities, that the act of measurement may eventually make real. Summarizing, our lack of knowledge results not from the imprecision of our measuring interacting apparatus but from the most basic fact that before the measurement the micro entities do not really exist. In the last instance they are created out from an infinite number of possibilities by the measurement operation that includes, as we have seen in the indirect measurements, as essential ingredient, the observer.

Prior to the Copenhagen interpretation of quantum physics it was generally understood that the physical entities and therefore their properties, like position and velocity, for instance, existed by themselves independently of the measuring operation. To put it bluntly, the Moon and the other planets, even the unknown ones do exist independently of being observed or not. Their existence does not depend on the measurement process and therefore on the observer. In such circumstances it would be possible, in principle, to increase progressively our knowledge of Nature by devising better and better models for explanation and for prediction of the new experimental evidence. These ideas imply that, in this causal paradigm, Heisenberg's relations are assumed only as factual uncertainty relations. At this point it is convenient to draw the attention to the well-known, but some times forgotten fact, that even in plain classical physics any measurement implies an inherent interaction between the apparatus and the object upon which the measurement is made. The difference between the two conceptions for measurement is that in a causal interpretation, the reality exists previous to any measurement, even if the interaction may, in some cases, change drastically what is being measured. By progressive reduction of the basic experimental measuring tool it would be possible, in principle, to make measurements where this unavoidable interaction would be so small that for all practical effects it would be of no consequence. Accepting this causal viewpoint for all physics, including quantum physics, it would be expected that the limit for a measurement would be given the by the smaller available physical entity that in the present situation corresponds to the quantum of light. If further development of science proved that this strange entity we call photon had an inner deep structure, then the limits for measurement would be increased and, in that case, would be of subquantum order.

In order to develop the basics for a research program which goal is the elaboration of a causal local measurement theory for quantum physics it is

convenient to introduce a new mathematical tool developed in the last years. As was indicated before, the usual interpretation of quantum theory is deeply rooted on the nonlocal Fourier analysis. The consequences of this basic fact lead mainly, from the interpretative point of view, to the nonlocal problems and consequently to the so-called quantum paradoxes. These quantum paradoxes, in the borhean paradigm, are not paradoxes at all but a mere consequence of trying to interpret nonlocal and nontemporal situations in terms of local causal epistemology. These facts seem to indicate that if instead of using Fourier nonlocal analysis as the basic mathematical tool for describing the micro entities one uses a kind of local analysis it would be possible to overcome the nonlocal implications of usual quantum mechanics. It is very satisfactory to acknowledge that today we are in much better position than at earlier times when Einstein, de Broglie and many others tried to explain the quantum phenomena in a local causal way but with the recourse of the nonlocal and nontemporal mathematical tools. Now, thanks to the recent development of a finite local analysis, also called wavelet local analysis, the way to develop a causal local quantum theory looks much facilitated.

4.2 WAVELET LOCAL ANALYSIS

Wavelet local analysis was developed in the early eighties. Contrary to what would be expected this important mathematical breakthrough was accomplished not in the field of mathematics, nor in the domain of physical mathematics but in geophysics. Jean Morlet, a geophysicist working in oil prospection devised this mathematical tool for denoising the very sharp seismic signals. The seismic impulses, produced by explosions, soil hammering, or any other means are collected by the sensor probes and later are used to devise earth's structure, allowing eventually the detection of oil deposits. Since these seismic impulses result from a very complex interaction with hundreds of layers with different materials and properties the seismic signal is very complex and carries a lot of noise. To analyze these rapid varying signals nonlocal Fourier analysis proved to be not well suited. Under these circumstances, Morlet, instead of using infinite waves, thought about some kind of localized, both in space and time, wavelets that could help to extract the information from the seismic data. Later, these early attempts were developed and formalized by Grossmann, Meyer, and many others until the wavelet local analysis was made into a powerful

mathematical tool, competing side by side with Fourier nonlocal analysis. Today, there is a whole universe of scientific literature dealing with the all-different aspects of wavelets. This field is developing at a so fast rate that even the very definition of wavelet that at the beginning seemed fairly settled, is today an uncertain ground. These facts lead some authors to say that the precise mathematical definition of wavelet is a kind of scholastic question without any useful meaning. For reasons that will be made clear, in this work, the basic property we retain here for the concept of wavelet is its localization or finiteness contrary to the Fourier sines and cosines that are infinite both in space and time. This option comes naturally from the aims of this work which is centered mainly on the physical implications while the mathematics are seen here as tools to help to understand Nature.

In order to understand the conceptual and practical importance and grasp the deep significance of this new local analysis by wavelets it will be useful to make a short comparison with nonlocal Fourier analysis.

As we have seen previously, Fourier analysis must be considered nonlocal or global because its basic elements, its constituting blocks, are monochromatic harmonic plane waves infinite both in space and time. This construction implies the nonlocal or global nature of Fourier analysis.

The nonlocal or global character of Fourier analysis can be easily understood with the following example.

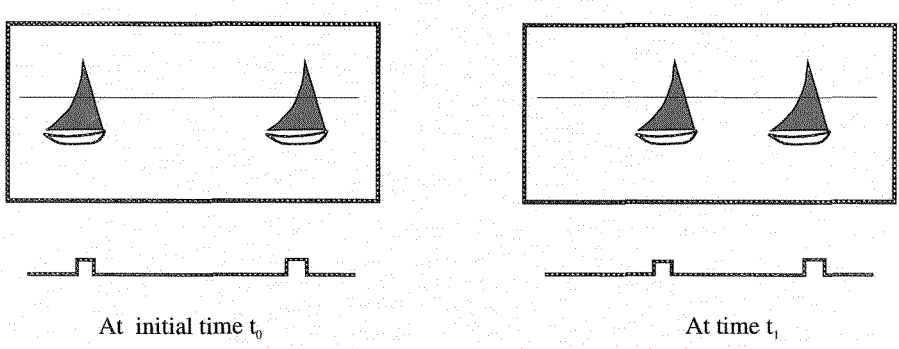

Fig.4.1 – Digitalized images to Fourier analyze.

Suppose that it is necessary to record, line by line, for instance, in a CD disk, the first image, of two ships sailing in the sea, as sketched in Fig.4.1. In order to simplify the problem let us consider only the line indicated in Fig.4.1. The plot of the picture intensity along that line is represented below in the same figure. In order to Fourier represent this variation in intensity it

is necessary to find the amplitudes, frequencies and phases of the infinite monochromatic harmonic plane waves. The sum of all these waves reproduces the initial function. This immensity of harmonic plane waves interferes negatively in all points of space except in those two regions where the interference is constructive. Mathematically, as we know, this is represented by the Fourier integral.

$$f(x) = \int_{-\infty}^{+\infty} [A(k)\cos kx + B(k)\sin kx]dk$$

Generally, the analytic work of finding the coefficients $A(k)$ and $B(k)$, that allows the synthesis of the initial function $f(x)$, is automatically done with the help of fast computers. The treatment of the other intensity lines, not shown, is precisely the same.

Let us now suppose that, for instance, the first ship moves to the right, while the other remains in the same position. This situation is represented in the second image of Fig.4.1. Next we ask how this motion of the first ship is to be Fourier represented? Just like in the example presented in the second chapter, in this type of analysis, both the first and the second ship are made of the same infinite harmonic plane waves. In these circumstances a modification in the position of the first ship implies naturally a modification in the amplitude, frequency and phase of all the waves, so that their interference is constructive only in the new position. This means that in this process of nonlocal Fourier analysis and reconstruction, even if the two ships may seem separate entities they are in reality treated as a unique entity. So, a modification in the position of one implies a simultaneous modification of the other, no matter how distant they are one from the other. This mathematical consequence of dealing with infinite both in time and space plane waves, has not only deep implications in the notion of nonlocality in physics but also has serious practical technical drawbacks, namely when, as is the case, one wants to register video images. In general, as is very well known, from video image to video image there are only slight variations. Nevertheless, in this type of nonlocal or global analysis, a minor modification on one region of the image implies the necessity of analyzing and rebuilding the whole image. Even with the help of the now available powerful computers this work consumes much time and needs a lot of space to register the enormous amounts of coefficients produced.

If, instead of the nonlocal Fourier analysis, one uses local wavelet analysis, the modification of the position of one ship as nothing to do with

the other, naturally assuming that the two objects are sufficiently apart. In this case, the group of wavelets that sums up to recreate one object is completely independent from the wavelets corresponding to the reconstruction of the other ship. This is precisely the reason why this type of analysis is called local analysis by finite waves.

The difference between the two types of analysis is shown graphically in Fig.4.2.

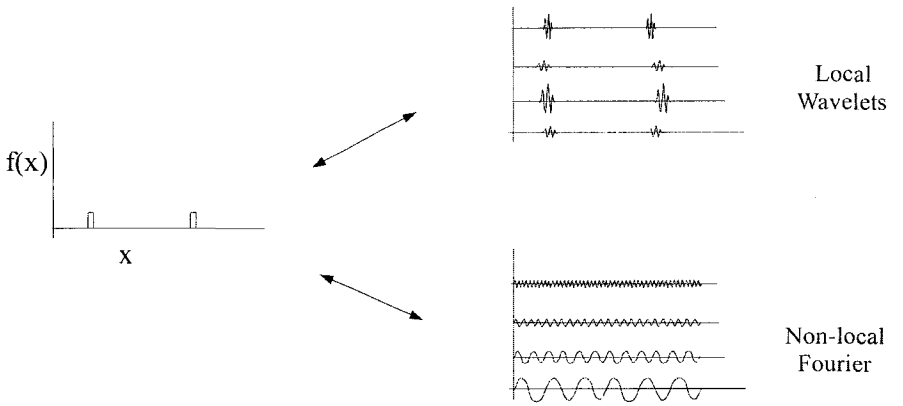

Fig.4.2 – Comparison between local wavelet analysis and Fourier nonlocal analysis.

Another important advantage of local wavelet analysis is related with the fact that in order to represent a given signal one is free to use different types of basic wavelets, contrary to Fourier nonlocal analysis where the building blocks are always harmonic functions, sines and cosines. In these circumstances, a good choice of the basic wavelet can further increase the rate of compression and the quality of the reconstruction and the denoising capability.

The reader interested in this fascinating field of wavelets should have a look at the works referenced at the end of this chapter. Here we refer only briefly to the essentials.

In order to do this analysis it is necessary first to choose the basic wavelet. This basic wavelet is chosen taking in consideration basically the form of the signal function and, of course, the nature of the problem one wants to track. This point differs from Fourier analysis where the basic elements, harmonic plane waves, were fixed once and for all.

$$f(x) \xrightarrow{\text{Choice of the basic wavelet}} \psi \xrightarrow{\text{analysis}} g(a,b) \xrightarrow{\text{syntesis}} f(x)$$

The coefficient function g, in this case, corresponding to the most common set of wavelets, is function of two variables $g(a,b)$, while in the usual nonlocal Fourier it is only function of one variable. It must be said in passing that for certain classes of wavelets the coefficient function may be a function of more than two variables, for instance in the analysis by wavelet packets, or even of one variable when the size of the wavelets is fixed and no translations are done. There are also cases where the analyzing wavelet has one form and the reconstruction wavelet another. These wavelets are called biorthogonal.

Just like in Fourier analysis any well-behaved function can be represented by a discrete or continuous sum of wavelets. These wavelets, in the most common case, are no more than expansions and translations of the basic or mother wavelet. Analytically this situation can be represented by

$$f(x) = \iint_D g(a,b)\,\psi\left(\frac{x-b}{a}\right) da\,db\,, \tag{4.2.1}$$

which is generally called synthesis of the function $f(x)$. Symmetrically the analysis, that is, the determination of the coefficient function $g(a,b)$ can be represented

$$g(a,b) = \frac{1}{c}\frac{1}{|a|a^2}\int_{-\infty}^{+\infty} f(x)\,\psi^*\left(\frac{x-b}{a}\right)dx\,, \tag{4.2.2}$$

where c is a constant defined by the expression

$$c = \int_{-\infty}^{+\infty} \frac{|\hat{\psi}(k)|^2}{k}\,dk\,, \tag{4.2.3}$$

and $\hat{\psi}(k)$ is the Fourier transform of $\psi(x)$.

The above representation emphasizes the reconstruction aspect leading to a simpler expression for $f(x)$, in a certain sense analogous to that of the Fourier transforms, while the expression for $g(a,b)$ is relatively more

complex. Nevertheless in the wavelet literature certain authors favoring the analysis point of view represent $g(a,b)$ by a more straight formula being led consequently to a much less clear expression for $f(x)$. Yet, in reality nothing changes, the situation is essentially the same, it is only a cosmetic operation.

These functions, representing finite waves, in order to be acceptable, as wavelets, must verify certain mathematical restrictions, namely:

$$\int_{-\infty}^{+\infty} |\psi(x)|\, dx < \infty \tag{4.2.4}$$

and

$$c = \int_{-\infty}^{+\infty} \frac{|\hat{\psi}(k)|^2}{k}\, dk < \infty \tag{4.2.5}$$

that corresponds to the definition of constant c, expression (4.2.3), which is also called admissible condition.

Just for the sake of illustration let us mention two much used continuous wavelets: The one called Mexican hat with the form

$$\psi(x) = (1 - x^2)\, e^{-\frac{1}{2}x^2}, \tag{4.2.6}$$

which plot can be represented, Fig.4.3,

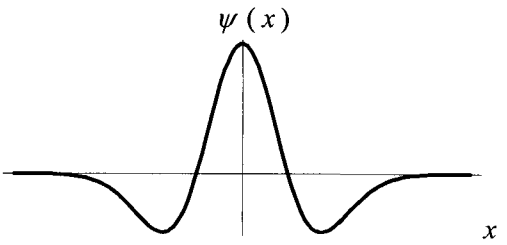

Fig.4.3 - Plot representation of the wavelet Mexican hat.

and the Morlet or gaussian wavelet,

$$\psi(x) = e^{-\frac{x^2}{2} + ikx} . \tag{4.2.7}$$

This wavelet does not verify the admissible condition (4.2.5) nevertheless for a
$k > 4.5$ this condition is practically fulfilled.

4.3 SOME ELEMENTS OF THE CAUSAL THEORY OF DE BROGLIE

As is known, de Broglie never accepted quite well the usual interpretation of quantum mechanics given by Niels Bohr and followers even if for many years he taught it. He felt obliged to accept Bohr's interpretation because the way to build a solid causal quantum theory was blocked by van Neumann's theorem. Only after the work of David Bohm who, in a very important paper published in 1952, demonstrated the limitations and exposed the limitative implicit physical assumptions of the regrettably famous theorem of von Neumann was the way free to build a consistent causal quantum theory. This theorem, like many others of the type called no-go theorems, try to impose absolute barriers on the future development of human knowledge of Nature. This happens in spite of the fact that the natural development of science, has always shown that the impossibility statements and theorems were wrong. Wrong in the sense that they are not so general as their authors claim and therefore do not fully describe the external objective reality. It seems like a curse that man has always tried to develop impossibility theorems. Even if from the mathematical point of view these theorems are correct, nevertheless, in order to be of any physical significance they must be applied to the real world. Still, to apply them to the real physical situations it is necessary to make assumptions. If these assumptions, never stated by the authors, are limitative, as they must inevitably be since they are human constructions, the theorem fails to apply to reality. It's a sad fate that in spite of the historical evidence against the applicability of such impossibility theorems man always keeps trying to develop such theorems in order to impose limits, boundaries on our possibility of knowing. The years that followed the overcoming of von Neumann impossibility theorem were of great productivity for de Broglie. He, with the help of his collaborators, was

able to develop a consistent causal quantum theory. De Broglie named it meaningfully theory of the double solution.

His starting point, his basic assumption, is that it is necessary to retain the concept that there is an objective physical reality independent of the observer. Just as in classical physics, the causal quantum theory describes the real physical processes in the framework of space and time. So, in this picture, a quantum particle is understood as a real objective physical entity. Nevertheless in order to cope with its undulatory and corpuscular properties the model describing the behavior of a quantum particle must have a certain degree of complexity. This because we are not dealing with a single corpuscular classical description nor with an exclusively undulatory process, but with a phenomenon that simultaneously has properties of both. We are faced with the challenge of building a causal local model that could exhibit, at the same time, the apparently contradictory properties of quantum particles.

The possibility that, in the known double slit experiment, what we call a quantum particle go through the two slits at the same time, since it must give origin to an interference pattern, and at the same time through one slit or the other because we are dealing with one single particle seems, in a first approach, very difficult to understand. The assumption that the quantum particle goes through one slit or the other can easily be checked with two common detectors placed in front of each of the slits. It can easily be seen that it never happens that the two detectors are activated at the same time. It would mean, in this case, that the quantum particle, the neutron, for instance, had to be splitted into two. This is impossible since we have never seen half neutron. What really happens is that sometimes the detector placed in front of one of the slits that is triggered, and other times it is the second detector that is activated.

The question now arises how to devise a causal model able to conciliate these apparently contradictory properties exhibited by quantum particles in this experiment? Passing simultaneously by the two slits and precisely at the same time passing through one or the other slit.

In order to solve this riddle we have to accept, like de Broglie, that what is called a quantum particle is, in reality, a far more complex entity than the simple classical particle we are used to. We are faced with the conclusion that the simplistic model of a ball of essentially local nature cannot represent the quantum particle. A quantum particle has to be, at the same time, a wave, an extended entity, and a particle so that it could pass and not pass, at the same time, by the two slits. A moment reflection allows us to devise a

classical macroscopic model having at the same time corpuscular and undulatory properties. Naturally one must be aware that any classical macroscopic model we could eventually formulate, however perfect and complete cannot in any case represent the true quantum particle. This macroscopic model is above all, a tool to help us to understand in a straightforward way what could eventually be that baffling quantum entity.

Let us consider a hurricane, a macroscopic phenomenon of big dimensions that, as is well known, is made of a large mass of air in motion occupying a large region of space. Somewhere, inside it, there is a small region, the kernel or, as is usually called, the eye of the typhoon, possessing a colossal amount of energy. Most of the energy of the cyclone is concentrated in its nucleus, and the extended part, what we call here the wave, has a relatively lesser energy. Let us now consider an observer, at high altitude, placed in such a way that is outside the influence of the typhoon. Furthermore, due to the sensing devices he has, the observer is unable to see directly the hurricane. He can only detect it by its effect on the ground. If in its path the tempest goes in the direction of an urban center, the observer would have no possibility of detecting it if only the extended part of the typhoon crossed the city, while the eye remained outside. Since the extended part of the tempest, the wave, has a relatively small energy, the buildings in its path would remain, for the observer, perfectly unaltered. The worse that could happen to them would be to have some glasses broken or some other minor disturbances that the observer is unable to detect from his viewpoint. Nevertheless, if the eye of the typhoon went through the buildings, they will be shattered and the observer would see a path of destruction. He therefore would conclude that a hurricane has gone through that city. It can now be easily understood that it is perfectly possible to conceive a comprehensible model having at the same time the two apparently contradictory properties of quantum particles of being extended and localized. What we need for that is creative imagination!

The causal model, for the quantum particle, devised by de Broglie can now be fairly understood. A quantum particle is indeed a very complex real entity made of an extended part, the wave, plus a singularity. The wave has a very small amount of energy while the singularity carries practically the whole energy of the quantum particle. The wave consequently is responsible for the interferometric properties of the particle while the singularity gives origin to the common quadratic detection.

The causal model of de Broglie for the quantum particle can mathematically be represented by an extended yet finite wave with a singularity such that:

$$\phi = \theta + \xi \tag{4.3.1}$$

Here θ represents the extended part, the wave of the quantum particle, responsible for the interference properties, and ξ stands for the singularity with almost all the energy of the particle. A trivial quadratic detection process results from the interaction of this singularity ξ with the detector. In order to put in evidence the extended wave θ, with almost no energy, a common quadratic detector is not enough; it will be necessary, as we shall see in the following chapter, to use more sophisticated means. The full wave ϕ, describing the quantum particle, cannot, of course, be normalized at will, like the usual function ψ solution to the known Schrödinger linear equation. This real finite wave is solution to a more general nonlinear Schrödinger equation.

It is well known that de Broglie never presented any form for the nonlinear master equation describing quantum reality. Nevertheless his Theory of Double Solution is a linear approximation to this more general nonlinear theory. In this theory the extended wave θ, solution to a nonlinear master equation, is approximated by the real wave υ that represents also a real physical solution to the familiar Schrödinger wave equation. A major inconveniency of this first approach is that in the case of a free particle this real wave υ is a monochromatic plane wave which size is infinite either in space and time.

Since the ordinary probability wave ψ normalized at will and representing the information we possess on the particle is also solution to the same linear Schrödinger equation, they must be somehow connected. The ψ wave, which is a mere representation of probabilities, and therefore must be built on the information we got on the state of the particle is everywhere proportional to the real wave υ, such that

$$\psi = C\upsilon \tag{4.3.2}$$

where C is the proportionality constant. In this natural way the mystery of the objective and subjective nature of the wave, solution to the linear Schrödinger equation, is completely cleared out. Now we understand why de Broglie named his theory double solution. The two solutions to the

Schrödinger equation have different meanings: one υ objective, responsible for the physical phenomena such as interference, quantization of energy; the other the subjective probability wave ψ that can be normalized at will.

In the case of particles without spin and in the non-relativistic approximation the Schrödinger equation comes

$$-\frac{\hbar^2}{2m}\nabla^2\upsilon + U\upsilon = i\hbar\frac{\partial\upsilon}{\partial t}. \tag{4.3.3}$$

This complex equation indicates that the wave υ can also be represented by two real functions connected by two real equations. Writing υ in the general form

$$\upsilon = ae^{\frac{i}{\hbar}\varphi} \tag{4.3.4}$$

with real amplitude a and phase φ. By substitution and separation of the real from the imaginary parts one gets after some easy calculations

$$\begin{cases} \dfrac{1}{2m}(\nabla\varphi)^2 + U - \dfrac{\hbar^2}{2m}\dfrac{\nabla^2 a}{a} = \dfrac{\partial\varphi}{\partial t} \\ \dfrac{1}{m}\nabla(a^2\nabla\varphi) - \dfrac{\partial a^2}{\partial t} = 0 \end{cases} \tag{4.3.5}$$

If in the first formula one considers $\hbar$ equal to zero, that is one assumes the quantum contribution negligible, and making $\varphi = S$, the equation becomes

$$\frac{1}{m}(\nabla S)^2 + U = \frac{\partial S}{\partial t} \tag{4.3.6}$$

the classical Hamilton Jacobi equation for the action S. The term with the Planck constant

$$Q = -\frac{\hbar^2}{2m}\frac{\nabla^2 a}{a} \tag{4.3.7}$$

is usually called the quantum potential.

By analogy with the classical formula

$$\frac{\partial S}{\partial t} = E \quad \text{and} \quad -\nabla\varphi = p \tag{4.3.8}$$

we get

$$\upsilon = \frac{p}{m} = -\frac{1}{m}\nabla\varphi \tag{4.3.9}$$

which corresponds to the "guidage", the guiding, a formula that gives the velocity of the particle as a function of the local variation of the phase of the wave.

The second expression that can be written in the form

$$\frac{\partial \rho}{\partial t} + \mathrm{div}(\rho\upsilon) = 0 \tag{4.3.10}$$

where we have made $\rho \propto a^2$, represents the continuity equation of hydrodynamics.

De Broglie and collaborators developed further the theory, always in the linear approximation, as can be seen in the related literature published on the subject, to include thermodynamics, systems of particles and extended it to include relativity and spin. The theory was perfected in such a way that in the great majority of cases it stands side by side with the usual Copenhagen interpretation. In another variant, the nonlocal causal theory of Bohm, the predictions are precisely the same as the standard theory. Still, the most important characteristic of a physical theory, besides its internal coherence and beauty, is the ability of dealing, predicting and integrating new phenomena. In this way new realms for understanding Nature are opened. It is here, precisely at this point, that the bohmian causal and nonlocal version fails. The predictions of this causal nonlocal theory are essentially the same as the Copenhagen theory. On the contrary, the aims of de Broglie's causal local theory, being essentially a nonlinear theory, point clearly to a new experimental realm in quantum world. In such circumstances a whole

panoply of crucial experiments, able to decide on the validity of the two theories was developed. It is true nevertheless that, unfortunately, for reasons incomprehensible to any true natural philosopher, some theoretical researchers do give preference to theories that cannot be put to the verdict of experiment. In this way it is possible to do almost anything and sometimes, more often than one would suppose, such theories confound themselves with bad science fiction.

4.4 A NONLINEAR SCHRÖDINGER EQUATION

As we have seen, even if de Broglie never proposed a nonlinear master equation for quantum physics he always thought that quantum mechanics must be intrinsically a nonlinear theory. This idea was shared by many other authors namely Einstein and, of course, de Broglie followers. Among those we may refer Vigier, Mackinnon and Gueret, which proposed equations and soliton like solutions to the nonlinear Schrödinger equation. There are two main reasons why finding a nonlinear equation describing quantum phenomena turns out to be a very tough problem:

One difficulty is mathematical and springs from the fact that in a nonlinear approach the superposition principle, a cardinal rule in quantum mechanics, does not hold any more.

This basic quantum principle is a consequence of Schrödinger equation linearity. As is well known if

$$\psi_1,\ \psi_2,\ \psi_3,\cdots,\ \psi_n,$$

are solutions to the linear equation, namely of the Schrödinger equation, then their sum is also a solution

$$\psi = \psi_1 + \psi_2 + \psi_3 + \cdots + \psi_n .$$

This mathematical expression renders evidently the superposition principle as a consequence of the linearity of the equation. If the same set of functions were solutions to a nonlinear equation then the same additive rule in general does not hold and consequently one has to give up the important superposition principle. Even the composition rule for solutions to the nonlinear equations

$$\psi = \psi(\psi_1, \quad \psi_2, \quad \psi_3, \cdots, \quad \psi_n)$$

is, generally, not known. The mathematical problem is so complex that there are no known general rules for the composition of the solutions. I would like to refer that efforts for finding a composition rule for the nonlinear Schrödinger equation, that shall be discussed later, have been made at the school of Lisbon. In fact Rica da Silva has arrived at promising results that may lead to a partial solution to the problem.

The second problem arises from the fact that the usual Schrödinger linear equation is indeed a very good equation able to provide solutions to quantum problems with an astounding precision.

From these and other reasons any attempt to propose a nonlinear master Schrödinger equation, describing quantum evidence, must, of course, lead, for all practical situations at the mean statistical level, into the usual linear Schrödinger equation. Next a heuristic derivation of a nonlinear master Schrödinger equation is presented. Nevertheless it must be kept in mind that this is only an approximation, a trial of a decisive solution to the problem. Among other inconveniences of the model it misses the necessary stochastic nature of the guidage principle, the interaction among singularities, and does not explicitly take into account the subquantum fluctuations.

4.4.1 Derivation of the Nonlinear Master Schrödinger Equation

In the derivation of the nonlinear equation for quantum physics a heuristic approach is followed. The word derivation was chosen instead of deduction because the way of arriving at the final equation is not entirely deductive. On the same foot stands the usual Schrödinger linear equation that cannot be deduced from first principles, and so needs to be postulated. Starting from heuristic assumptions and following a more creative way, as an alternative to an entirely more direct approach, it is possible to arrive at a nonlinear equation equal to the common Schrödinger equation plus a nonlinear term called quantum potential. In science, this method of arriving at a final result by intuitive, inductive, apparently unrelated jumps is much more common than is usually thought, even if most authors fail to acknowledge the creative process conducing to the final result. Once we deeply feel that the final solution to the problem ought to have a certain generic form then we proceed in steps not always wholly logically deductive to arrive at it. The only

restriction one puts is that the whole inductive process be correct in every step and furthermore have an overall coherence.

The basic assumption, the basic principle, we start from is that a true model for describing quantum phenomena needs to include both the corpuscular or local and the undulatory or extended properties. This basic necessity is a consequence of the fact that experimental evidence teaches us, as we have seen, that quantum systems share simultaneously corpuscular and undulatory properties. Therefore it seems quite natural to assume that the basic equation describing quantum phenomena needs to incorporate into a single whole these two fundamental aspects of the classical physics. These two classical properties are described by two real equations: one for the classical well localized particles, that originating from Newton mechanics has led to the Hamilton Jacobi equation, and the other, the fluid equation of continuity, to account for the extended properties. These equations, as is well known, are no more than conservative or balance equations. The first one is essentially for particles the second one for fluids.

Now the next step is to assume that these two classical balance equations still hold in a synergetic way at the quantum level. Since we want to generate one single equation from two real equations it is convenient to melt them into a single imaginary equation.

In such conditions we have the two basic classical balance equations

$$\begin{cases} T+V=E \\ \nabla J+\dfrac{\partial \rho}{\partial t}=0 \end{cases} \tag{4.4.1}$$

where the symbols have the usual meaning.

Writing the solution of these two equations in the general form

$$\psi(\vec{r},t)=a(\vec{r},t)e^{-\frac{i}{\hbar}\varphi(\vec{r},t)}$$

as we have done before, and recalling the preceding relations

$$\nabla\varphi = p; \quad \upsilon = \frac{\nabla\varphi}{m}; \quad J = \rho\upsilon; \quad \rho = a^2; \quad J = a^2\frac{\nabla\varphi}{m}$$

$$T = \frac{1}{2}m\upsilon^2 = \frac{1}{2m}(\nabla\varphi)^2; \quad E = -\frac{\partial\varphi}{\partial t} = -\varphi_t$$

and by substitution into (4.4.1) we have the usual Hamilton-Jacobi together with the equation of continuity

$$\begin{cases} \dfrac{1}{2m}(\nabla\varphi)^2 + V = -\varphi_t \\ \dfrac{1}{m}\nabla(a^2\nabla\varphi) = -\dfrac{\partial a^2}{\partial t} \end{cases} \tag{4.4.2}$$

or, for the one-dimensional case

$$\begin{cases} \dfrac{1}{2m}\varphi_x^2 + V = -\varphi_t \\ \dfrac{1}{m}\partial_x(a^2\varphi_x) = -\partial_t a^2 \end{cases} \tag{4.4.3}$$

with $\partial_\xi = \partial/\partial\xi$, by developing the last equation one has

$$\begin{cases} \dfrac{1}{2m}\varphi_x^2 + V = -\varphi_t \\ \dfrac{1}{2m}(2a_x\varphi_x + a\varphi_{xx}) = -a_t \end{cases} \tag{4.4.4}$$

Now by multiplying the first of these equations by a, and the second by (-1) we get

$$\begin{cases} \dfrac{1}{2m} a\varphi_x^2 + Va = -a\varphi_t \\ -\dfrac{1}{2m}(2a_x\varphi_x + a\varphi_{xx}) = a_t \end{cases} \tag{4.4.5}$$

By adding and subtracting the same quantity $(\hbar^2 a_{xx}/2m)$ to the first equation and multiplying the second by $(i\hbar)$ they become

$$\begin{cases} -\dfrac{\hbar^2}{2m} a_{xx} + \dfrac{1}{2m} a\varphi_x^2 + \dfrac{\hbar^2}{2m} a_{xx} + Va = -a\varphi_t \\ -\dfrac{i\hbar}{2m}(2a_x\varphi_x + a\varphi_{xx}) = i\hbar\, a_t \end{cases} \tag{4.4.6}$$

In order to obtain a single equation we add the two equations, and after arranging the terms we get

$$-\frac{\hbar^2}{2m}\left[a_{xx} - \frac{1}{\hbar^2} a\varphi_x^2 + \frac{i}{\hbar}(2a_x\varphi_x + a\varphi_{xx})\right] + \frac{\hbar^2}{2m} a_{xx} + Va = i\hbar\,(a_t + \frac{i}{\hbar} a\varphi_t)\,, \tag{4.4.7}$$

multiplying and dividing by a the second term in a_{xx} and finally multiplying both members of the expression by a phase factor $e^{\frac{i}{\hbar}\varphi}$ one arrives at

$$-\frac{\hbar^2}{2m}\left[a_{xx} - \frac{1}{\hbar^2} a\varphi_x^2 + \frac{i}{\hbar}(2a_x\varphi_x + a\varphi_{xx})\right] e^{\frac{i}{\hbar}\varphi} + \frac{\hbar^2}{2m}\frac{a_{xx}}{a} a e^{\frac{i}{\hbar}\varphi} + Va\, e^{\frac{i}{\hbar}\varphi} = i\hbar(a_t + \frac{i}{\hbar} a\varphi_t) e^{\frac{i}{\hbar}\varphi} \tag{4.4.8}$$

Recalling that

$$\psi = a e^{\frac{i}{\hbar}\varphi}$$

$$\psi_t = (a_t + \frac{i}{\hbar} a\varphi_t) e^{\frac{i}{\hbar}\varphi}$$

$$\psi_{xx} = \left[a_{xx} - \frac{1}{\hbar^2} a\varphi_x^2 + \frac{i}{\hbar}(2a_x\varphi_x + a\varphi_{xx}) \right] e^{\frac{i}{\hbar}\varphi}$$

we get by substitution into (4.4.8)

$$-\frac{\hbar^2}{2m}\psi_{xx} + \frac{\hbar^2}{2m}\frac{a_{xx}}{a}\psi + V\psi = i\hbar\psi_t\,, \tag{4.4.9}$$

that stands for the proposed nonlinear Schrödinger master equation. For the three dimensional case it reads

$$-\frac{\hbar^2}{2m}\nabla^2\psi + \frac{\hbar^2}{2m}\frac{\nabla^2(\psi\psi^*)^{\frac{1}{2}}}{(\psi\psi^*)^{\frac{1}{2}}}\psi + V\psi = i\hbar\frac{\partial\psi}{\partial t}\,. \tag{4.4.10}$$

Nonlinear equations of this type were presented initially by Guerra, Pusterla and Smolin. Also Gueret and Vigier following a causal approach inspired in de Broglie double solution theory arrived at a similar equation, when they were looking for an equation having as a solution a soliton like function. Their equation has the form

$$-\frac{\hbar^2}{2m}\nabla^2\psi + \gamma\frac{\hbar^2}{2m}\frac{\nabla^2(\psi\psi^*)^{\frac{1}{2}}}{(\psi\psi^*)^{\frac{1}{2}}}\psi + V\psi = i\hbar\frac{\partial\psi}{\partial t}\,, \tag{4.4.11}$$

where the difference between the two equations lies in the parameter γ. In the first case this parameter, affecting the quantum potential, is equal to one while in the Vigier and Gueret model the magnitude of the parameter is practically negligible. They assumed this hypothesis so that the nonlinear equation could approach easily the linear Schrödinger equation.

The presented approach has the advantage of stemming from solid sound epistemological principles. The nonlinear equation comes as a result of the basic causal assumption that the same fundamental balance or conservative equations still hold both at the classical and quantum descriptions of the world. The difference between the two cases being that in the classical case the corpuscular and extended undulatory properties are treated separately as two independent realities. In the quantum description these two apparently distinct properties are integrated in a whole single complex entity. This is a consequence of the basic fact that Nature is a whole, and that our models, our theories, correspond only to levels, to scales of description. Generally, in physics, the most basic equations are balance equations that should be valid in the diverse scales of description of Nature. In this case we have two levels of description of the reality, the classical and the quantum description, where the same conservative equations apply.

Since the derivation of the nonlinear Schrödinger master equation presented before was based on the two fundamental equations of classical physics it seems reasonable to accept that the value of parameter γ need to be one.

It is convenient to recall, that taking as starting point the nonlinear master equation, and following an inverse process, it is possible to arrive, directly and without more or less subtle complicated tricks, at the two basic equations of classical physics. This process is in all similar to the one shown in the paragraph devoted to de Broglie's double solution theory starting from the linear Schrödinger equation.

Starting from the nonlinear Schrödinger equation

$$-\frac{\hbar^2}{2m}\nabla^2\psi+\frac{\hbar^2}{2m}\frac{\nabla^2(\psi\psi^*)^{\frac{1}{2}}}{(\psi\psi^*)^{\frac{1}{2}}}\psi+V\psi=i\hbar\frac{\partial\psi}{\partial t},$$

writing again the solution in the generic form

$$\psi(\vec{r},t)=a(\vec{r},t)e^{-\frac{i}{\hbar}\varphi(\vec{r},t)},$$

and by substituting and separating the real part from the imaginary we get nice and clear the two basic conservation equations:

$$\begin{cases} \dfrac{1}{2m}(\nabla\varphi)^2 + V = -\varphi_t, \\ \dfrac{1}{m}\nabla(a^2\nabla\varphi) = -\dfrac{\partial a^2}{\partial t}. \end{cases}$$

Once the nonlinear equation accepted as the fundamental equation for the quantum realm, in order to arrive at classical physics it is only necessary to keep in mind that at the non-quantum level description of physics the undulatory and the corpuscular properties are to be treated as separate independent realities.

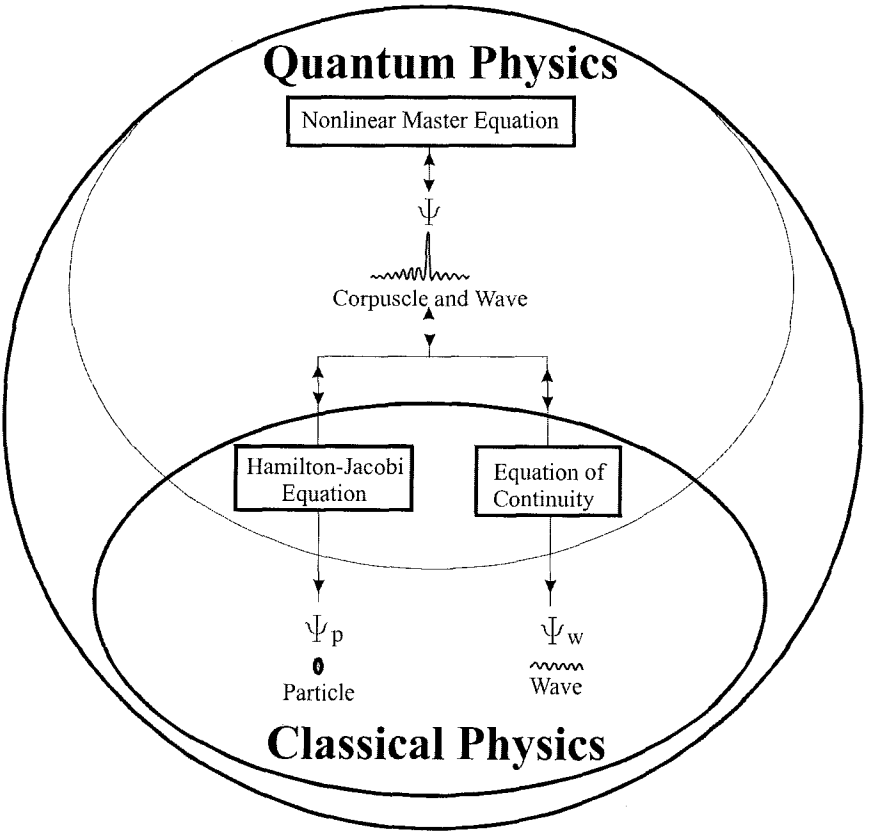

Fig.4.4 – Global synthesis for Classical and Quantum Physics.

Summarizing, the essential difference between classical physics and quantum physics is: In the former description, the corpuscular local properties and the extended undulatory properties had to be treated as independent properties, while in the later, at the quantum realm, they must be considered together as a whole.

In the figure, Fig.4.4, a sketch representing this synthesis is shown.
In order to summarize these ideas it is convenient to keep in mind that Nature is extremely complex, therefore in order to understand the observable reality we have to proceed by levels or scales of understanding. Before the discovery of quantum phenomena we had classical physics. Classical physics described very well on one side the behavior of corpuscles, localized entities, and on the other the extended, or continuous entities like fields, as separated conceptual beings. When the experimental developments, at the beginning of the XXth century, led to the quantum realm researchers were faced with physical systems that had strange properties. The experiments shown, without any margin of doubt, that quantum particles had, at the same time, corpuscular and extended undulatory properties. The problem theoretical physicists of that time had before them was to conciliate, into a coherent harmonic model, these two apparently contradictory properties of quantum beings, of being localized and, at the same time, extended. We know that Heisenberg derived his matrix mechanics mainly based in the corpuscular properties while Schrödinger obtained the wave equation leading to the wave mechanics, inspired in the undulatory properties of quantum entities. The synthesis of these two apparently contradictory properties into a coherent whole was, as we know, the work of Niels Bohr. He was capable of presenting a consistent unitary paradigm, the orthodox quantum mechanics, able to deal with the quantum evidence. We also know that the price to pay for this beautiful synthesis was very high. The price of this synthesis was the abandon of causality.

The basic equation of quantum theory, for the non-relativistic approach and for particles without spin, is the Schrödinger equation. In fact the equation is one of the basic postulates of the theory. This equation is a wave equation, which is an equation describing continuous extended phenomena so, like other continuous equations, uses as basic mathematical formalism the nonlocal or global Fourier analysis. Therefore, when it is necessary to treat local corpuscular properties of quantum entities this equation dedicated to treat essentially extended phenomena is no longer so useful. In such circumstances some mathematical artifices are to be used in order to recover a kind of pseudo locality.

On the other hand we also know that a great number of the founding fathers of quantum mechanics like Einstein, de Broglie, Schrödinger, Planck and many others never fully accepted the epistemological proposal of the orthodox Copenhagen School for quantum physics. It is also true that some of them like for instance de Broglie were able to present reasonable and very fecund causal alternatives. Nevertheless they were never able to present a consistent general local causal epistemological picture describing both quantum and classical phenomena. One of the reasons of this failure stemmed from the fact that they were not able to get rid of the omnipresent nonlocal Fourier analysis by one hand and by the other they never developed any quantum nonlinear equation.

Now, thanks to the development of local wavelet analysis we are able to go beyond Fourier nonlocal analysis opening the way to a nonlinear master equation describing simultaneously the dual properties of wave and corpuscle of quantum beings. This situation provides us with the necessary theoretical and experimental tools for improvement of our understanding of nature. In such circumstances it is no surprise that such a general synthesis could now be done and a new more general causal paradigm for quantum physics could be presented.

In the proposed causal approach, the master equation describing quantum phenomena integrates into a single coherent whole the local and extended properties of quantum beings. Naturally, as we shall see, the more convenient mathematical tool to use in this approach is not nonlocal Fourier analysis, but local wavelet analysis. This analysis, when needed, can even in certain circumstances approach the extended nonlocal Fourier analysis. One other important advantage of this more general synthesis of physics is that if one wants to change the level of description going from the quantum scale to the macroscopic scale, then the master equation splits into two: one for corpuscles and other for extended phenomena, which are then treated as separate realities. In this way a beautiful global synthesis unifying classical and quantum physics is achieved.

4.4.2 Some Particular Solutions to the Nonlinear Schrödinger Equation

Now that we have built, from first conceptual principles, the master nonlinear Schrödinger equation it is convenient to seek the general form of some particular solutions to this equation. Instead of using the merged single

nonlinear equation it will be more useful to use the equation splitted into Hamilton-Jacobi and the continuity equations while keeping in mind that the solution must verify both equations,

$$\begin{cases} \dfrac{1}{2m}\varphi_x^2 + V = -\varphi_t \\ \dfrac{1}{m}\partial_x(a^2\varphi_x) = -\partial_t a^2 \end{cases} \tag{4.4.12}$$

or

$$\begin{cases} \dfrac{1}{2m}\varphi_x^2 + V = -\varphi_t \\ \dfrac{1}{2m}(2a_x\varphi_x + a\varphi_{xx}) = -a_t \end{cases} \tag{4.4.13}$$

A particular solution to the first equation is

$$\varphi = px - Et - \varepsilon \tag{4.4.14}$$

with

$$\varphi_x = p; \quad \varphi_{xx} = 0; \quad \varphi_t = -E \tag{4.4.15}$$

Then the last equation of (4.4.13) becomes

$$\frac{p}{m}a_x + a_t = 0 \tag{4.4.16}$$

or,

$$\frac{\partial a}{\partial x} + \frac{1}{\upsilon}\frac{\partial a}{\partial t} = 0 \tag{4.4.17}$$

which is a linear equation. This result is very interesting, because if one restricts oneself to that particular form (4.4.14) for the phase, then the composition rule for the solutions becomes additive and consequently the superposition principle is recovered.

This linear equation for the amplitude accepts a constant, as a particular solution

$$a \neq a(x,t); \quad a = c^{te} \tag{4.4.18}$$

which means that the monochromatic plane wave

$$\psi = c^{te} e^{\frac{i}{\hbar}(px - Et - \varepsilon)} \tag{4.4.19}$$

is solution to the nonlinear Schrödinger equation.

The general solution to the equation (4.4.17) can be written in the form

$$a = a(x - \upsilon t - \varepsilon_0) \tag{4.4.20}$$

Then, for this case, as a general solution to the nonlinear Schrödinger equation we have

$$\psi = a(x - \frac{p}{m}t - \varepsilon_0) e^{\frac{i}{\hbar}(px - Et - \varepsilon)}. \tag{4.4.21}$$

4.4.3 A Mathematical Model for the Quantum Particle

Now that we are in possession of the nonlinear equation describing, in a first approach, quantum evidence, it is relatively easy to build a mathematical model for the particle. This mathematical model describing the particle must follow as closely as possible the early ideas of de Broglie. Recalling his formula for the particle

$$\phi = \xi + \theta$$

Where θ represents the extended part of the quantum particle and ξ the localized wave, that is: a kind of singularity that keeps its identity throughout the interactive process. This singularity, with a very small spatial dimension, localized on the theta wave, has almost all the energy of the particle. The

theta wave, sometimes called empty wave, carrying wave, or guiding wave, carries practically no energy at all and is responsible for the interferometric properties of the particle. This wave, practically devoid of energy, guides the singularity through a nonlinear interacting process preferentially to regions where the amplitude is higher. This nonlinear process is such that the two waves beat always in phase. In such conditions a first approach for a function representing the quantum particle, solution to the nonlinear equation, can be written, for free space, as a function of the Morlet wavelet type. The carrying extended wave, practically without energy, solution to the nonlinear Schrödinger equation can then be written

$$\theta = a\, e^{-\frac{1}{\hbar^2}\frac{(px-2Et-\varepsilon')^2}{2\sigma^2}} .e^{+\frac{i}{\hbar}(px-Et)} \tag{4.4.22}$$

In the expression σ representing, for the case of a single particle in the free space where the classic potential is null, $V = 0$, and in the fundamental state of lesser energy, the region of the space where the particle can exhibit interferometric properties. As shall be shown later it is possible to establish a relation between the wavelength of the particle and its width. Generally, as a consequence of the fact that in a common source there are lots of secondary sources, and that even the "empty" space, the subquantum medium, is full of waves, the final guiding wave is usually the result of the superposition of all present waves. For common sources with lots of secondary practically coherent sources with a random gaussian distribution of width σ_ε it is possible to write

$$\theta = \int_{-\infty}^{+\infty} e^{-\frac{\varepsilon'^2}{2\sigma_\varepsilon^2}} e^{-\frac{1}{\hbar^2}\frac{(px-2Et-\varepsilon')^2}{2\sigma^2}+\frac{i}{\hbar}(px-Et)}\, d\varepsilon' \tag{4.4.23}$$

that by integration gives

$$\theta = \sqrt{\frac{2\pi}{\frac{1}{\sigma_\varepsilon^2}+\frac{1}{\hbar^2\sigma^2}}}\, e^{-\frac{(px-2Et)^2}{2(\sigma_\varepsilon^2+\hbar^2\sigma^2)}} e^{\frac{i}{\hbar}(px-Et)}, \qquad (4.4.24)$$

which, as expected, is also solution to the nonlinear Schrödinger equation. On the other hand by adding uniformly coherent θ waves, just as is approximately done in a laser cavity, it is possible to obtain waves, in principle, as large as one wishes, as shown in the picture

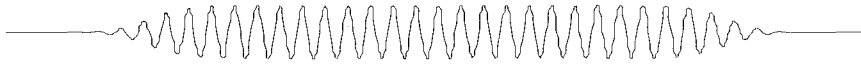

Fig.4.5 – Composite guiding wave θ.

In spite of its eventually enormous size, the energy of this carrying wave is always much less than the energy of the singularity and therefore fails to trigger the common quadratic detectors.

In a similar way it is possible to represent the extremely localized singular wave ξ, that transports practically al the energy of the particle

$$\xi = Ae^{-\frac{1}{\hbar^2}\frac{(px-2Et-\varepsilon_0')^2}{2\sigma_0^2}} e^{\frac{i}{\hbar}(px-Et)} \qquad (4.4.25)$$

where σ_0 is very small and is related with the size of the particle responsible for the usual quadratic detection process. The translation parameter ε_0' is such that the singularity is always inside the transporting wave. We must stress that it is just a first tentative model because in a better one, to be later developed, this parameter must be seen as an aleatory variable proportional to the intensity of the wave θ. This last statement is no more than the guiding principle. This assumption maintains its validity even in the case when the porter wave θ is a composite wave resulting from the sum of other waves of the same type. When more than one singularity share the same guiding wave it is necessary to take in consideration the nature of

the quantum particle, for instance, if it is a boson or a fermion. In such case a supplementary interaction between singularities must be taken into account. For the case of photons, bosonic particles, this type of interaction leads them to be together, the bunching effect, while the electrons, fermions, tend to be apart from each other. In any case in this first approach, which corresponds to statistical the case of many particles, these interactions are not taken in consideration.

Now, and in this first approximation, the complete model for the quantum particle assumes the form

$$\phi = \left[A e^{-\frac{1}{\hbar^2}(px-2Et-\varepsilon_0')^2/2\sigma_0^2} + a e^{-\frac{1}{\hbar^2}(px-2Et-\varepsilon')^2/2\sigma^2} \right] e^{\frac{i}{\hbar}(px-Et)}, \tag{4.4.26}$$

Recalling that

$$p = \hbar k, \quad E = \hbar\omega,$$

we get by substitution

$$\phi = \left[A e^{-\frac{(kx-2\omega t-\varepsilon_0)^2}{2\sigma_0^2}} + a e^{-\frac{(kx-2\omega t-\varepsilon)^2}{2\sigma^2}} \right] e^{i(kx-\omega t)}, \tag{4.4.27}$$

giving for each component

$$\begin{cases} \xi = A e^{-\frac{(kx-2\omega t-\varepsilon_0)^2}{2\sigma_0^2}} . e^{i(kx-\omega t)} \\ \theta = a e^{-\frac{(kx-2\omega t-\varepsilon)^2}{2\sigma^2}} . e^{i(kx-\omega t)} \end{cases} \tag{4.4.28}$$

The energy of the real quantum particle can be expressed, just like in the case of a physical wave, by

$$E = \hbar\omega = \int_{-\infty}^{+\infty} |\phi|^2 \, dx \,. \tag{4.4.29}$$

Since it is assumed that practically all the energy of the particle is concentrated in the singularity it is reasonable to make

$$\int_{-\infty}^{+\infty} |\xi|^2 \, dx = \int_{-\infty}^{+\infty} |\phi|^2 \, dx = E = \hbar\omega \tag{4.4.30}$$

or

$$\hbar\omega = A^2 \int_{-\infty}^{+\infty} e^{-\frac{(kx-2\omega t-\varepsilon_0)^2}{\sigma_0^2}} dx = \sqrt{\pi} A^2 \sigma_0 \tag{4.4.31}$$

which means that

$$A = \sqrt{\frac{\hbar\omega}{\sqrt{\pi}\sigma_0}} = \sqrt{\frac{E}{\sqrt{\pi}\sigma_0}} \,. \tag{4.4.32}$$

Writing the constant of the guiding wave as a fraction to the one of the singularity

$$a = \alpha A, \quad 0 < \alpha <<< 1 \tag{4.4.33}$$

the expression for the quantum particle, solution to the nonlinear Schrödinger equation, can then be fully written

$$\phi = \sqrt{\frac{E}{\sqrt{\pi}\sigma_0}} \left[e^{-\frac{1}{\hbar^2}(px-2Et-\varepsilon_0')^2/2\sigma_0^2} + \alpha e^{-\frac{1}{\hbar^2}(px-2Et-\varepsilon')^2/2\sigma^2} \right] e^{\frac{i}{\hbar}(px-Et)} \,. \tag{4.4.34}$$

or, which amounts to the same

$$\phi = \sqrt{\frac{\hbar\omega}{\sqrt{\pi}\sigma_0}}\left[e^{-\frac{(kx-2\omega t-\varepsilon_0)^2}{2\sigma_0^2}} + \alpha\, e^{-\frac{(kx-2\omega t-\varepsilon)^2}{2\sigma^2}} \right] e^{i(kx-\omega t)} . \tag{4.4.35}$$

the real part of which can be represented graphically, see Fig.4.6.

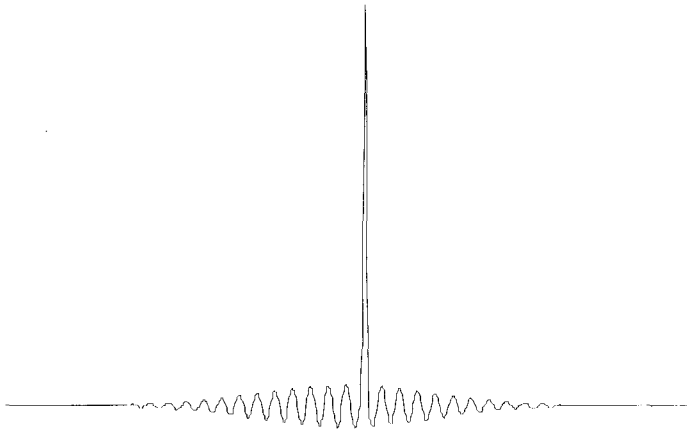

Fig.4.6 – Graphical representation of the causal particle of de Broglie.

4.4.4 An Example of the Application of the Model

Let us now see how this model works in the case of a very simple example like that of a flux of particles, with the same energy, running into a square potential. It is convenient to recall that the causal model sees the orthodox quantum approach as a kind of statistical approximation of a deeper level of reality, named by de Broglie as subquantum medium. This statistical approximation that in the present case corresponds to the stationary case deals with so many particles that the final amplitude of the guiding composite wave remains, in the experimental apparatus, practically constant.

On the other hand and since we are considering a very large number of particles it means that we have a very large number of singularities merged in an almost continuous carrying wave. In such case for a reasonable description of the occurrence it is convenient to consider only the composite porter θ wave resulting from the uniform composition of the single waves

$$\theta = \int_{-\infty}^{+\infty} g(\varepsilon') a e^{-\frac{1}{\hbar^2}\frac{(px-2Et-\varepsilon')^2}{2\sigma^2}+\frac{i}{\hbar}(px-Et)} d\varepsilon'. \qquad (4.4.36)$$

For a constant $g(\varepsilon)$, implying that the weight of each particle is equal, and that they are uniformly spaced, the integral gives

$$\theta = \sqrt{2\pi}\sigma a e^{\frac{i}{\hbar}(px-Et)}, \qquad (4.4.37)$$

or,

$$\theta = A e^{\frac{i}{\hbar}(px-Et)}, \quad A = \sqrt{2\pi}\sigma a \qquad (4.4.38)$$

As expected, the uniform sum of the single carrying waves produced a wave of constant amplitude, a monochromatic plane wave. This fact implies that the nonlinear master Schrödinger equation transforms itself into the common linear equation, since the nonlinear term, for constant amplitude, becomes null. In such case it is possible to write the solution in the usual stationary way, that is writing the solution in a form of the product of two functions one for the spatial part, another for time

$$\theta(x,t) = \psi(x) f(t) = A e^{\frac{i}{\hbar}px} e^{-\frac{i}{\hbar}Et} \qquad (4.4.39)$$

with

$$\begin{cases} \psi(x) = A e^{\frac{i}{\hbar} px} \\ f(t) = e^{-\frac{i}{\hbar} Et} \end{cases} \tag{4.4.40}$$

From this point on the calculating process is precisely the same in the two approaches.

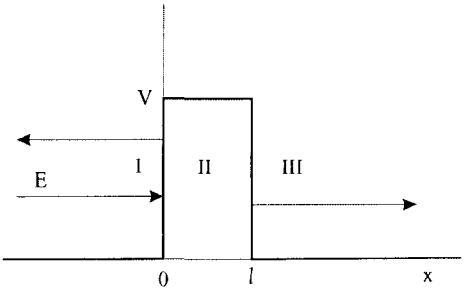

Fig.4.7 – Square potential.

Recalling that $p = \sqrt{2m(E-V)}$ the solutions in the three regions can be written

$$\begin{cases} \psi_I(x) = A e^{\frac{i}{\hbar}\sqrt{2mE}\, x} + B e^{-\frac{i}{\hbar}\sqrt{2mE}\, x} \\ \psi_{II}(x) = C e^{\frac{i}{\hbar}\sqrt{2m(E-V)}\, x} + D e^{-\frac{i}{\hbar}\sqrt{2m(E-V)}\, x} \\ \psi_{III}(x) = F e^{\frac{i}{\hbar}\sqrt{2mE}\, x} \end{cases}$$

where no incoming wave from region III is supposed to exist. Applying the continuity condition in the boundaries to the function and to its first derivative we get the relations

$$\begin{cases} \psi_I(0) = \psi_{II}(0) \\ \psi'_I(0) = \psi'_{II}(0) \end{cases} \qquad \begin{cases} \psi_{II}(\ell) = \psi_{III}(\ell) \\ \psi'_{II}(\ell) = \psi'_{III}(\ell) \end{cases}$$

that allow the determination of the transmission and reflection coefficients.

4.5 LOCAL PARADIGM IN PLACE OF THE NONLOCAL FOURIER PARADIGM

It is amazing to see how long some early philosophical ideas last in science. At the golden Greek age, Plato, in order to conciliate the apparent mutability, motion, with the necessity of permanency of heavens proposed the idea that the sphere was indeed the most perfect body. One important reason for this assumption comes directly from the fact that the sphere has the known property of maintaining its form even when in motion. That is, remains equal to itself even in motion. With the sphere the Holy Grail is found, giving the insight of what could be a still motion. In sequence of these ideas Plato assumed that the motions of the heavenly bodies ought to be necessarily circular motions. For the stars, there was no problem since, with the precision of the observations of those times, their motions looked indeed as perfect circles, but for the planets, which name means vagabond star, the problem was not so easy. Observations showed that the motion of the planets is very far from the perfect circle. For some planets like for instance Mars its movement is very complex, sometimes going on one direction and other times on the inverse, retrograde motion. The scientific project Plato left for his successors was to show, to prove, that the strange motions of the planets were in reality illusions of our senses. It would be possible to explain these intricate movements as a judicious combination of perfect circular uniform motions. We know that this scientific project was taken and was developed by the ancient astronomers until it culminated with the magnificent work of Ptolemy *The Almagest*. The word Almagest means in Arabic the Great Book. In this work the motions of the planets are explained as a combination of perfect circular motions. These ideas lasted for so long that even the revolutionary Copernicus kept the paradigm of circularity in the orbits of the planets. He changed the center of the Cosmos, putting the Sun at the center instead of the Earth, but still kept the combination of cycles and epicycles to obtain the apparent orbit of the planets. It was Kepler who stroke the first

blow to the circular paradigm. Based in Tycho Brahe observations on the heavenly positions of Mars Kepler assumed rightly that the orbits of the planets are indeed ellipses. To us, that are some centuries apart from those times, it seems amazing to verify that the idea of circular uniform motion being the perfect motion had been so appealing to so many people. After all, it seems that, in a more general perspective, the elliptic motion must look a more perfect motion since it includes the circular motion as a particular case. For a less attentive observer it would appear that with the development of classical mechanics the circular paradigm, the idea that the most fundamental, the most perfect motion was the timeless circular uniform motion, would vanish completely from science. Nothing more wrong and farther from the truth! As we shall see, those ideas of perfection and permanency and eternity are at the very foundations of the epistemology of orthodox quantum mechanics.

In order to study the diffusion of heat Joseph Fourier showed that any function well behaved could be represented by an infinite sum of sines and cosines. That is, any function could be described as a sum of harmonic plane waves that are infinite both in time and space. At this point one must recall that a harmonic plane wave is no more than the projection on a straight line of a point of a circle, performing endlessly, like a planet in Plato paradigm, a uniform circular motion. As the circle turns endlessly the point describes the infinite uniform harmonic motion whose mathematical representation is the sines or cosines. This mathematical method for representing a function, called Fourier analysis, was applied to many domains of physics, namely to the study of the extended oscillating or periodic phenomena. Nevertheless it was the orthodox quantum theory, developed by Niels Bohr and his school that really put emphasis on Fourier mathematical method of composition of functions. From a mere mathematical process among others, without physical meaning, of representation of functions it was promoted to the ontological status of paradigm. For this fact the orthodox quantum paradigm would also be named Platonic or Fourier paradigm.

The basic idea behind Fourier paradigm is that if one has a finite pulse produced, for instance, by a piano chord, or by the tube of an organ, then the finite pulse is in reality the result of a sum of monochromatic harmonic plane waves, infinite in time and space. Still, the piano sound is a physical vibration of the air, which was started at one instant of time and will finish a short time later. Just like any human physical action it has unavoidably a beginning and an end. Furthermore, this sound, produced by the tuned musical instrument, seems to have a very well defined frequency.

Nevertheless, in the Fourier paradigm it is assumed that this finite sound wave is composed intrinsically by an infinitude of so called pure frequencies, each corresponding to an harmonic plane wave. Just like in Plato paradigm for heavens where the non-circular orbits of the planets were no more than an illusion of our senses since in reality these strange motions were composed of perfect eternal circular motions, now the finitude of the short pulses is also a fantasy, an illusion of our senses.

The pure frequencies of the Fourier paradigm are the monochromatic harmonic plane waves produced by a uniform perfect motion. Since these waves are infinite both in time and space it means that the piano, or the organ, started playing them from the infinite beginning of times and will be playing them forever. The fact that the real physical musical instrument was built at a certain time and will eventually disappear sometime later has no importance. Their finitude is a kind of fantasy of our senses. It implies that the perfect sounds, the monochromatic harmonic plane waves, should exist even before the piano was built, and will last forever even when the material musical instrument no longer exists. These assumptions deeply rooted in the Fourier paradigm imply in reality the return to Plato paradigm, which led to the Ptolemaic model for the heavens, where the heavenly bodies existed forever playing endlessly the eternal and ethereal harmonic music of the spheres.

Concluding, in the Fourier paradigm it is stated the impossibility of producing finite pulses with a well-defined frequency. Only the infinite harmonic plane waves do have a well-defined frequency. A finite signal is always composed of many frequencies, each corresponding to a harmonic plane wave, that sum up to produce the pulse.

In orthodox quantum mechanics, as we have seen, a fairly localized particle is built from the sum of harmonic waves. Since each of these infinite pure waves has a well-defined energy or frequency it means, in this description, that the quantum particle does not have a well-defined energy. Since no real particle can have more than one energy it follows, as a single corollary, that quantum particles before measurement do not have real existence.

If one rejects the Fourier paradigm for describing Reality and accepts that the infinite, in space and time, harmonic plane waves are only mathematical abstract entities devoid of intrinsic physical meaning then it is logically possible to assume that it is viable to have a finite sign with a well-defined frequency.

When the hammer strikes a diapason a wave of a fairly well-defined frequency is produced. Therefore it seems quite reasonable to represent this sound by a finite wave of a well-defined frequency. For what physical reason has one to say that this finite wave, of a well-defined frequency, is composed of an infinitude of harmonic plane waves that have no real physical existence? We are so immersed in the Fourier paradigm that when one has a finite pulse one tries immediately to decompose it into the so-called pure frequencies of the harmonic plane waves to obtain the power spectrum. We forget the fact that in Nature no one has ever seen a device able to produce the infinite harmonic plane waves.

The recent development of wavelet analysis allows us mathematically to represent the diapason sound by a finite wave of a well-defined frequency. It is true that prior to wavelet local analysis, we had to describe mathematically these finite physical waves, as a sum of infinite waves whether we give them a basic epistemological ontological status or not. Now, since we have a mathematical tool that allows us to avoid the physical nonsense of Fourier analysis one is free to reject the old paradigm. By replacing the old nonlocal Fourier paradigm by the local causal paradigm it is then possible to accept that a finite pulse could have a well-defined frequency.

The denial of the Fourier paradigm in quantum physics is equivalent to the abandon of the old Plato scientific proposal for a more general one just as was done before in astronomy by Kepler. Naturally, as expected, in the new causal local paradigm there is no room for the Copenhagen interpretation of quantum physics

4.6 DERIVATION OF A MORE GENERAL SET OF UNCERTAINTY RELATIONS

In orthodox quantum mechanics a particle is represented by a sum of infinite, both in time and space harmonic plane waves. The two extreme cases, as we have seen before, are the following: when the particle is represented by only one wave and in this case its energy is perfectly determined and consequently, according to Fourier analysis, the position is completely unknown. In this case the particle can be somewhere between minus infinity and plus infinity, meaning that it is omnipresent in all space and time. In the second case the particle is it perfectly localized and we need an infinite number of harmonic plane waves to sum up in order to give a precisely defined position, which analytically corresponds to a Dirac delta function. As a consequence of the representation of the particle by an infinite number of waves, each corresponding to a single precise frequency, nothing is known on its energy. By the Fourier interdependency between the two conjugate observables, in this case position and momentum, the more the position is determined the less one knows on its velocity. The Heisenberg's relations are no more than the statement of this basic method for the representation of the particle. This situation is quite similar to the following case. Suppose that one puts only red balls in a bag and later tries to study the probability distribution of the color of the balls picked from the bag. Under these circumstances, after picking the balls, one by one, from the bag, one arrives at the sound conclusion that the probability of picking a red ball is one. This inference is, of course, a direct and necessary consequence of the way we had previously chosen to prepare the distribution of the elements and of the rules of the game. In reality the final conclusion is not a true inference resulting from a complex reasoning but a simple statement, expressed in other words, of what we had previously done. In such conditions the Heisenberg's uncertainty relations are no more than a necessary consequence of the chosen process for describing a quantum particle. As a consequence they are devoid of any deep ontological physical meaning. These facts open the way for other possible forms of the uncertainty relations as a direct consequence of other choices for the quantum particle description.

In the framework of de Broglie causal theory we have chosen other way to describe the quantum particle, and therefore the uncertainty relations derived from this approach are expected to be different. In this local causal paradigm we have chosen to describe a quantum particle not by infinite

harmonic plane waves but by finite waves of a well-defined frequency. This finite wave of a well-defined energy is, in a first approach, the composite gaussian Morlet wavelet solution to the nonlinear master Schrödinger equation. On the other hand since we are only interested in the collective mean statistical approximation only the porter or guiding θ wave is here of any interest to us. The spatial mother wavelet can thus be represented

$$f_0(x) = e^{-\frac{x^2}{2\sigma^2}+ikx} \tag{4.6.1}$$

the real part of which is shown in Fig.4.8

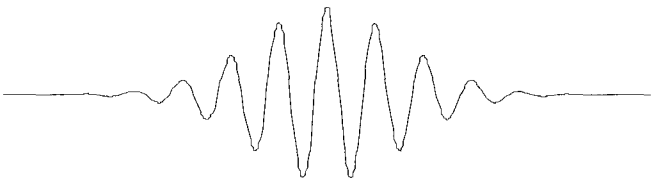

Fig.4.8 – Real part of the gaussian or Morlet wavelet.

In principle there were other open possibilities to represent the undulatory part of the quantum particle using other basic wavelets submitted, of course, to the condition of being solutions to the master nonlinear equation. We chose among the others, in principle, immense possibilities the Morlet gaussian wavelet for of the following reasons:

The first one is based on the simplicity and beauty criteria. In fact the Morlet gaussian wavelet is one of the simplest forms of the analytically expressible wavelets. The formal mathematical simplicity of this wavelet allows us to do most calculations thoroughly without approximations that necessarily shadow the end results. This is indeed a very interesting property for the basic wavelet. I am sure most agree on this point. Everybody knows that sometimes the end result of a complex calculation depends much more on the approximations and assumptions made during the whole calculating process than on the fundamental theory involved.

One other important point of the Morlet gaussian wavelet results from the non-minor fact that when the width of the basic wavelet σ is large

enough the finite wave transforms itself into the kernel of Fourier analysis. It means that, in this case, the gaussian wavelet approaches the harmonic plane wave and with it Fourier nonlocal analysis. In this sense the utilization of the gaussian Morlet wavelet contains, as a particular case, the habitual Fourier analysis.

In such conditions and taking in consideration the assumptions done in this approach the most general form for the spatial extended part of the quantum particle can be written

$$\psi(x) = \iiint_D g(k,\sigma,b,e)\, e^{-\frac{(x-b)^2}{2\sigma^2}+ik(x-e)}\, dk\, d\sigma\, db\, de, \qquad (4.6.2)$$

where we made the time equal to zero in the solution to the nonlinear equation, and the four independent parameters are accordingly: two scaling parameters, the spatial frequency of the wave k, and the size, width, of the gaussian σ; the two translating parameters are the one of the gaussian b, and e which corresponds to the initial phase of the oscillating wave. D represents generically the domain of the integrating variables.

Since this expression is too general, in order to arrive at some expression directly integrable and physically significative it is necessary to make some simplifications. The most immediate simplification of this expression consists in making the translating parameters equal and the size of the gaussian constant

$$e = b, \quad \sigma = \text{const.} \qquad (4.6.3)$$

for this approximation (4.6.2) becomes

$$\psi(x) = \iint_D g(k,b)\, e^{-\frac{(x-b)^2}{2\sigma^2}+ik(x-b)}\, dk\, db\,. \qquad (4.6.4)$$

To proceed with the calculation it is necessary to have the form of the coefficient function $g(k,b)$. One possibility that much simplifies the calculation is to do:

$$g(k,b) = g(k)\,\delta(b)\,. \tag{4.6.5}$$

By substitution in (4.6.3), one has

$$\psi(x) = \int_D g(k) \int_{-\infty}^{+\infty} \delta(b)\, e^{-\frac{(x-b)^2}{2\sigma^2} + ik(x-b)}\, db\, dk\,, \tag{4.6.6}$$

which gives

$$\psi(x) = \int_D g(k)\, e^{-\frac{x^2}{2\sigma^2} - ikx}\, dk\,. \tag{4.6.7}$$

Now assuming that the spatial frequencies are gaussian distributed around k_0,

$$g(k) = A e^{-\frac{(k-k_0)^2}{2\sigma_k^2}}\,, \tag{4.6.8}$$

where A is a proportionality constant and the width σ_k is also constant. In this conditions expression (4.6.7) becomes

$$\psi(x) = \int_{-\infty}^{+\infty} A e^{-\frac{(k-k_0)^2}{2\sigma_k^2}}\, e^{-\frac{x^2}{2\sigma^2} - ikx}\, dk\,, \tag{4.6.9}$$

which gives,

$$\psi(x) = \sqrt{2\pi}\, A \sigma_k\, e^{-\frac{x^2}{2/(\sigma_k^2 + 1/\sigma^2)} - ik_0 x}$$

or

$$\psi(x) = \sqrt{2\pi}\, A \sigma_k\, e^{-\frac{x^2}{2\sigma_x^2} - ik_0 x}\,, \tag{4.6.10}$$

where

$$\sigma_x^2 = \frac{1}{\sigma_k^2 + \frac{1}{\sigma^2}}. \tag{4.6.11}$$

Other possible approximation is to assume that the initial phase e is constant and equal to zero and the translation parameter b is gaussian distributed, while the width of the gaussians are still kept constant

$$g(k,b) = g(k)\, e^{-\frac{b^2}{2\sigma_b^2}}, \quad e = 0, \quad \sigma = \text{const}, \quad \sigma_b = \text{const}, \tag{4.6.12}$$

by substitution in (4.6.2) one gets

$$\psi(x) = \int_D g(k) \int_{-\infty}^{+\infty} e^{-\frac{b^2}{2\sigma_b^2}}\, e^{-\frac{(x-b)^2}{2\sigma^2}+ikx}\, db\, dk, \tag{4.6.13}$$

which gives

$$\psi(x) = \sqrt{2\pi}\left(\frac{1}{\sigma^2+\sigma_b^2}\right)^{-\frac{1}{2}} \int_D g(k)\, e^{-\frac{x^2}{2(\sigma^2+\sigma_b^2)}+ikx}\, dk. \tag{4.6.14}$$

Assuming, as before (4.6.8), that the distribution of the spatial frequency is also gaussian the integral (4.6.14) becomes

$$\psi(x) = 2\pi A\left(\frac{1}{\sigma^2+\sigma_b^2}\right)^{-\frac{1}{2}} \sigma_k\, e^{-\frac{x^2}{2/(\sigma_k^2+\frac{1}{\sigma^2+\sigma_b^2})}+ik_0x}, \qquad (4.6.15)$$

or

$$\psi(x) \propto e^{-\frac{x^2}{2\sigma_x^2}+ik_0x} \qquad (4.6.16)$$

with the width of the extended part of the particle given now by

$$\sigma_x^2 = \frac{1}{\sigma_k^2+\frac{1}{\sigma^2+\sigma_b^2}}, \qquad (4.6.17)$$

which contains the expression (4.6.11) as a particular case when the width of translation parameter distribution σ_b goes to zero.

Another, less simplistic, approach to the general expression (4.6.2), more meaningful from the mathematical point of view, which allows the reconstruction of the function $f(x)$, representing the extended undulatory part of the quantum particle of de Broglie, in terms of the common wavelets with usual properties is the one relating the width of the gaussian with the dilatation parameter *k*. This simplification of the general formula makes a lot of sense from the physical point of view. In the two previous models, which correspond to the first two approximations, the width of the particle is constant independently of the spatial frequency, which certainly corresponds to a very rough approximate model. These approaches imply that, in practice, for certain values of the spatial frequency, that is for large values of the wavelength $\lambda >> \sigma$, the oscillatory component of the extended part of the particle would practically be inexistent. A more accurate model describing the extended spatial part of the quantum particle must assume that the width of the particle is a natural function of the wavelength. In this case the mother gaussian Morlet wavelet undergoes an affine transformation

$$f_0(x) = e^{-\frac{1}{2}\frac{x^2}{\sigma^2}+ikx} \xrightarrow{\text{affine transformation}} e^{-\frac{\beta_1^2}{2}\left(\frac{x-b}{\beta_1\sigma}\right)^2+i\beta_2\left(\frac{x-b}{\beta_2/k}\right)} \equiv f_0\left(\frac{x-b}{a}\right), \tag{4.6.18}$$

where

$$a = \beta_1\sigma = \beta_2 / k, \tag{4.6.19}$$

that is

$$\sigma = \frac{\beta_2}{\beta_1}/k = \frac{\beta_2}{2\pi\,\beta_1}\lambda, \tag{4.6.20}$$

or

$$\sigma = M\,\lambda, \tag{4.6.21}$$

with the universal constant *M,* relating the size of the extended part of the free independent single particle with the wavelength, given by

$$M = \frac{\beta_2}{2\pi\,\beta_1}. \tag{4.6.22}$$

Later, in the next chapter, this concept of a free independent extended single particle will be developed and furthermore a feasible experimental process for determination of the constant *M* shall be presented.

With these assumptions in mind the representation of the undulatory extended spatial part of the particle can be written in the form

$$\psi(x) = \iint_D g(k,b)\, e^{-\beta^2k^2(x-b)^2+ik(x-b)}dk\,db, \tag{4.6.23}$$

where

$$\beta = \frac{\beta_1}{\sqrt{2}\beta_2} = \frac{1}{2\pi\sqrt{2}\,M}. \tag{4.6.24}$$

For calculation simplicity reasons let us assume that $g(k,b)$ is here also given by formula (4.6.5), and then (4.6.23) transforms into

$$\psi(x) = \int_D g(k)\, e^{-\beta^2 k^2 x^2 - ikx} dk \ , \tag{4.6.25}$$

which for $g(k)$ with gaussian form (4.6.8) becomes

$$\psi(x) = \int_{-\infty}^{+\infty} A e^{-\frac{(k-k_0)^2}{2\sigma_k^2}} e^{-\beta^2 k^2 x^2 - ikx} dk \ , \tag{4.6.26}$$

which by integration gives

$$\psi(x) = \sqrt{2\pi}\, A \frac{\sigma_k}{\sqrt{2\sigma_k^2\beta^2 x^2 + 1}} e^{-\frac{x^2}{2\sigma_x^2} - i\frac{k_0}{2\sigma_k^2\beta^2 x^2 + 1}x} \ , \tag{4.6.27}$$

with

$$\sigma_x^2 = \frac{2\sigma_k^2\beta^2 x^2 + 1}{\sigma_k^2 + 2\beta^2 k_0^2} \ . \tag{4.6.28}$$

In order to study the behavior of this formula it is convenient to plot the real part of expression (4.6.27), as a function of x and also of the parameter σ_k, for some fixed reasonable values of the constants,

$$\beta = \frac{1}{2\pi\sqrt{2}\, M} \leq 10^{-3}, \quad k_0 \approx 10 \ , \tag{4.6.29}$$

which corresponds to the assumption that the constant M holds the approximate value M = 100, meaning that the extended part of the particle contains roughly more than one hundred oscillations.

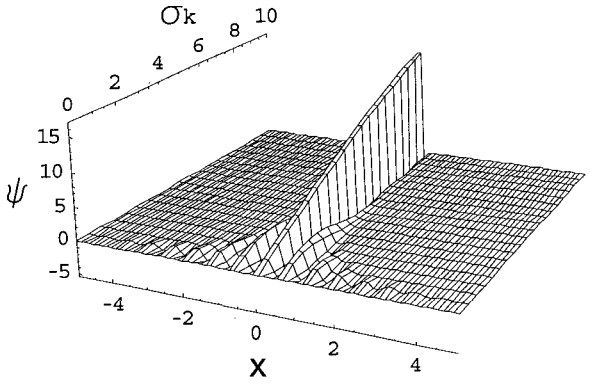

Fig 4.9 – Plot of the real part of the expression (4.6.27).

From the plot Fig.4.9 it is clearly seen that the bulk of the function $\psi(x)$ is roughly contained in the domain $-2 \le x \le +2$. Outside this domain, for any value of parameter σ_k, the function is practically zero. In such conditions the expression for the width of the function (4.6.28) can be approximated fairly by

$$\sigma_x^2 \approx \frac{1}{\sigma_k^2 + 2\beta^2 k_0^2}, \tag{4.6.30}$$

since it is reasonable to make

$$2\sigma_k^2 \beta^2 x^2 << 1. \tag{4.6.31}$$

The rightness of this approximation can be inferred from the plot, Fig.4.10, that shows the difference between the two widths {(4.6.28) – (4.6.30)}, which reads

$$\text{widths difference} = \frac{2\sigma_k^2 \beta^2 x^2}{\sigma_k^2 + 2\beta^2 k_0^2}, \quad -2 \le x \le +2, \tag{4.6.32}$$

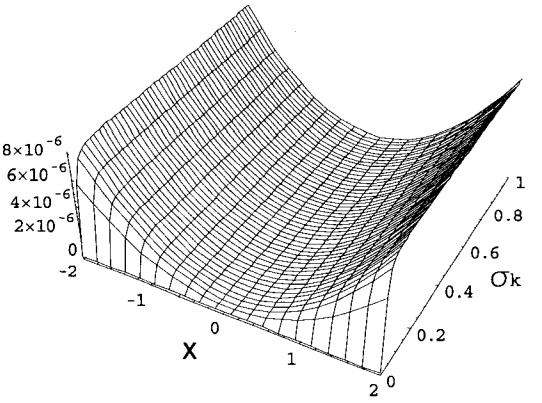

Fig.4.10 – Plot of the difference between the width of the function and the approximate width.

In any case, the maximum difference, for the domain of variation of x, is of the order of β, which for this situation, was chosen to be of about 10^{-6}. This value corresponds roughly to the limit of the difference when $\sigma_k \to \infty$, which is $2\beta^2 x^2$, that for the extreme values of x leads to $8\beta^2$. For this approximation expression (4.6.27) becomes

$$\psi(x) = \sqrt{2\pi}\, A\sigma_k\, e^{-\frac{x^2}{2\sigma_x^2} + ik_0 x}, \tag{4.6.33}$$

which apart from the constants is equal to formulas (4.6.10) and (4.6.15).

From the above representation of the undulatory part of the quantum particle in terms of finite wavelets one gathers that the general expression relating the final width of the particle with the width of the frequencies distribution of the composing wavelets has the form

$$\sigma_x^2 = \frac{1}{\sigma_k^2 + \gamma^2}, \tag{4.6.34}$$

with the constant γ given by

$$\gamma = \sqrt{2}\beta k_0 = 1/\sigma_0 , \tag{4.6.35}$$

where it was assumed that the variation of the translation parameter b is practically zero. Remembering the value of constant β given by the expression (4.6.24) and by substitution one gets

$$\gamma = \frac{k_0}{2\pi M} , \tag{4.6.36}$$

which shows that this constant depends on the mean spatial frequency k_0 of the building wavelets and on the universal constant M.

Substituting in (4.6.34)

$$\sigma_x^2 = \frac{1}{\sigma_k^2 + \frac{k_0^2}{4\pi^2 M^2}} , \tag{4.6.37}$$

taking in consideration the usual quantum basic equalities, and identifying here the widths of the gaussians with the quantum uncertainties, one gets for the uncertainty relations

$$\Delta x^2 = \frac{h^2}{\Delta p_x^2 + \frac{h^2}{4\pi^2}\frac{k_0^2}{M^2}} , \tag{4.6.38}$$

which in terms of the width $\sigma_0 = 1/\gamma$ of the central wavelet

$$\Delta x^2 = \frac{h^2}{\Delta p_x^2 + \frac{h^2}{\sigma_0^2}} , \tag{4.6.39}$$

where, as in Bohr's derivation, we used $k = 1/\lambda$. For the usual definition of $k = 2\pi/\lambda$, it is only necessary to change in the two formulas, (4.6.38) and (4.6.39), h for $\hbar = h/2\pi$.

A quick look at expression (4.6.39), representing the new formula for the uncertainty relations, deduced from finite waves, indicates that it contains the usual Heisenberg relations

$$\Delta x \Delta p = h \tag{4.6.40}$$

as a particular case when the mean width of the wavelet increases indefinitely $\sigma_0 \to \infty$ when the local process transforms into the Fourier nonlocal analysis. This conclusion is particularly clear in the plot Fig.4.11, where the two relations are seen for one particular value of the width of the mother wavelet.

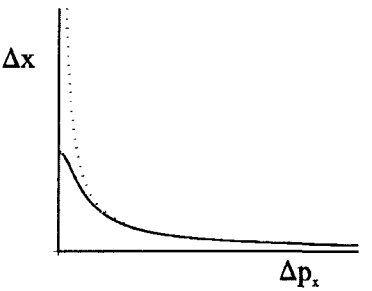

Fig.4.11 – Plot of the uncertainties: Solid line new relations, for one particular value of the wavelet width; doted line usual relations.

The plot shows the convergence of the new relations with Heisenberg usual relations. It can be seen from the plot that only in a small region near the origin the two relations are different.

The Heisenberg's uncertainty relations as given by (4.6.40) correspond to the ideal case of gaussian distributions of minimum uncertainty. In most cases the equality turns into the usual inequalities $\Delta x \Delta p \geq h$, which defines a measurement space, the Heisenberg space, shown in Fig.4.12.

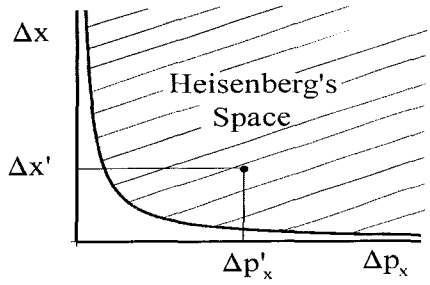

Fig.4.12 – Plot of the Heisenberg's measurement space.

The Heisenberg's space defines the available region where, in quantum mechanics, it is possible to make measurements. Outside this region, according to the usual quantum paradigm, it is impossible to predict the value of any measurement. Orthodox quantum mechanics states that for any measurements of two conjugated observables, whose operators do not commute, like, in this case, position and momentum, the uncertainties must be such that the point $P(\Delta x', \Delta p_x')$ must lie in the dashed region of the space, only in the ideal case of a gaussian distribution can the point be in the boundary line. In no circumstance can the point be in the non-dashed area, because this would correspond to $\Delta x \Delta p < h$. This impossibility, as was stressed before, results not from the fact that the measurement apparatus is inherently imperfect and therefore modifies in an unpredictable way what is being measured, but because prior to the measurement operation the orthodox quantum system does not really possess that property. We must recall that in this model describing Nature, the measurement process creates the physical properties of a quantum system out of a bunch of potentialities.

The new more general uncertainty relation (4.6.39) was derived in a causal framework, assuming that the physical properties of a quantum system are observer-independent and what is more, they exist before the measurement process. Naturally, due to the physical interaction during the measurement process the quantum system may not remain in the same state. In last instance the precision of the measurement depends on the relative size between the measurement apparatus and the system upon which the measurement is being done. Since in the derivation of the new uncertainty relation it was assumed that quantum systems are to be described by local finite wavelets the measurement space resulting from this general relation must depend on the size of the basic wavelet used. As the width of the

analyzing wavelet changes, the measurement scale also changes. This can be seen in the following plot, Fig.4.13

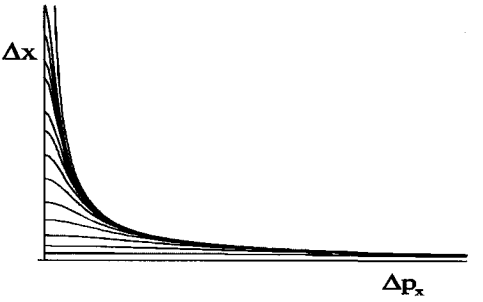

Fig.4.13 – Wavelet measurement space.

From the picture one sees that as the mean width of the basic wavelet σ_0 changes all the previously not allowed measurement space becomes accessible. As the scale of the basic wavelet changes all forbidden space is scanned. The smaller σ_0 the greater is the precision of the position measurement, that is, smaller is the uncertainty Δx, for any value of the error in the momentum. Given that the new uncertainty relation contains the habitual relations as a particular case it implies that the measurement space available to the general uncertainty relations is the whole space, as shown in Fig 4.14. In this causal local interpretation the precision of any measurement depends only on smallest available interacting basic device.

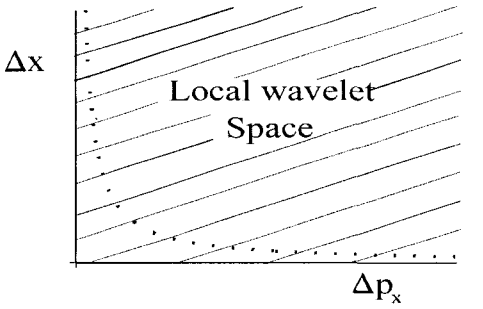

Fig.4.14 – Available measurement space for the causal uncertainty relations.

The above results are rather satisfactory because in this new causal paradigm the precision of the quantum measurement process depends only on the measurement standard. We are, in principle, free to choose the size of the mother wavelet σ_0 in order to increase or reduce the uncertainty of the measurement. In the Copenhagen paradigm this standard cannot be changed at will since it is composed of harmonic plane waves that, as we well know, are infinite.

In the previous derivation of the new uncertainty relation we were concerned only with space and momentum. The same process can be used, step by step, to derive the relation concerning energy and time. It is sufficient to change the variables

$$x \to t$$
$$k \to \omega$$

make the usual quantum transformations and we get the general local time energy uncertainty relation

$$\Delta t^2 = \frac{h^2}{\Delta \omega^2 + \frac{h^2}{\sigma_0{}^2}}. \tag{4.6.41}$$

or

$$\Delta t^2 = \frac{h^2}{\Delta E^2 + \frac{h^2}{\sigma_0{}^2}} \tag{4.6.42}$$

All the above discussion on the two orthodox Heisenberg's relations and the more general uncertainty relations concerning space and momentum are naturally applied to the time energy relation, with the due adaptations.

4.7 EXPERIMENTS TO TEST THE GENERAL VALIDITY OF THE USUAL UNCERTAINTY RELATIONS

We have seen that starting from the local causal conceptual framework of de Broglie and using finite wavelets, solutions to the nonlinear Schrödinger equation, to represent the quantum particle it was possible to derive a more general form for the uncertainty relations. These new more general uncertainty relations contain Heisenberg's relations as a particular case. The problem we now face is to know the meaning of theses new uncertainty relations.

Are they mere mathematical manipulations more or less cleverly done, or in reality they have a deep physical meaning implying necessarily that orthodox quantum mechanics is a limited human approach for the reading of nature? If that is the case there is every reason for a replacement of the non-causal and nonlocal orthodox quantum paradigm by a more general causal quantum paradigm!

Since, fortunately, Physics is a natural experimental science the answer to that important question is to be given by experiments.

The theoretical conclusions, drawn from de Broglie causal model and the nonlinear approach allow the anticipation that, in certain very special cases, the common Heisenberg uncertainty relations are not so general as claimed. For this reason the hunting for experimental conditions allowing the clarification of the problem began some time ago.

Even if some early experiments were proposed by Scheer and his group, in this work I shall only discuss experiments that are, in principle, conclusive. One of these is the photon ring experiment, and the second one is based on the endless spreading of matter wave packets even in the free "empty" space.

4.7.1 Photon Ring Experiment

In its essence the idea behind this experiment was presented by the author, for the first time, in 1990 at the International Congress Quantum Measurements in Optics, at Cortina d'Apezzo, Italy.

The central idea is quite simple and results directly from the following considerations: Consider, for instance that a continuous light beam feeds a physical optical medium, an optical crystal, or a special optical fiber, where the beam is bent in such a way that it follows a closed path converging to a limiting circle, as shown in the picture.

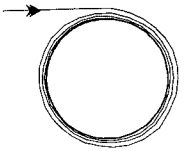

Fig.4.15 – The incident beam converges to a closed orbit in an appropriated optical medium.

The beam is passively trapped in the medium that behaves like a kind of optical cavity. The problem how to built such a device has been solved at the Department of Physics of the University of Lisbon, where we found diverse geometries for passively trapping the photons and furthermore an exit gate for discharging was developed. The device was given the name of photonic condenser in analogy with the equivalent device developed early in the eighteenth century for electrons.

There happens to be many different possibilities to produce such a "light condenser". Here we present only a sketch of the device, a ring made of an optical fiber having a relatively large section as shown in Fig.4.16. The light entering the ring cannot leave it except as an amplified short pulse when the gate G touches the ring at the exit region.

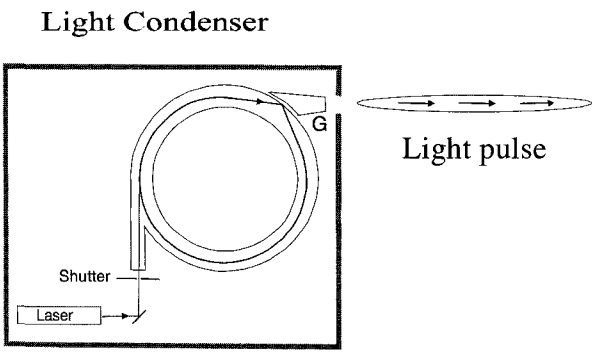

Fig.4.16 – Outline of a new kind of pulsed light source with the optical ring condenser.

Under these circumstances the overall device works like a kind of pulsed light source.

Consider then the experimental setup sketched out in Fig.4.16. The feeding beam of light, from the laser source, with frequency dispersion $\Delta\nu_0$ enters the light condenser where the light is trapped. After a certain time, necessary to reach equilibrium in the cavity, the shutter is closed blocking completely the incoming light from the laser. After this, the gate contacts with the light condenser, thus breaking the condition of total internal reflection. As a direct consequence, a finite pulse of light is released. This chain of events generates a puzzling question:

For these pulses of light what shall be the expected values for frequency bandwidth $\Delta\nu$ and for its duration Δt ?

The time duration of the pulse Δt depends on the specific geometry of the ring and on the working time of the gate. In any case it seems clear that Δt depends merely on the characteristics of the light condenser.

The value of the frequency bandwidth $\Delta\nu$ of the exit pulse does not seem to depend on the properties of the light condenser. This is a consequence of the fact that we are always working at low intensities therefore no nonlinear effects are expected to occur within the apparatus. Since the light condenser always behaves as a passive medium, no change in color of the incident light is to be expected. This assumption can evidently be tested experimentally. Therefore, since the device works in the linear regime, it looks that no change in the frequency bandwidth is to be expected. In such conditions one has every reason to make $\Delta\nu \cong \Delta\nu_0$.

If the above conclusions are correct, we may be in a situation of trouble with the orthodox uncertainty relations. When the frequency dispersion $\Delta\nu_0$, of the laser pump beam is large no problem is expected to arise. But, the difficulty arises if the pump laser has a high frequency stability with a very short bandwidth $\Delta\nu_0$. In this case, of a very short frequency bandwidth, and for certain geometries of the light condenser, it would also be possible to have a short Δt. This last conclusion is a consequence of the fact that, in this concrete special device, the two variables, the frequency bandwidth of the output light pulse $\Delta\nu$, and its duration Δt are independent quantities. Therefore, since they are independent variables it is possible to choose real physical situations where $\Delta\nu\Delta t \cong \Delta\nu_0\Delta t << 1$. This conclusion, which can

be tested in laboratory, is totally in contradiction with the orthodox uncertainty relations of Heisenberg, which predict the opposite.

4.7.2 Limitless Expansion of Matter Wave Packets

Every student of quantum mechanics knows that matter wave packets even in the absence of a field exhibit an endless dispersion. This limitless spreading of matter wave packets has always been a source of a certain discomfort among the scientific community. It is also true that in orthodox quantum theory nobody says that the particle, whichever the quantum particle, in this paradigm could be, increases its size without limits. The continuous increase of the size of the matter wave packets, as they travel in free space, is a consequence of the fact that they are, according to nonlocal Fourier analysis, made of many waves, with different frequencies. Since the different matter waves, which build the packets, travel with different velocities, it follows that the packet spreads indefinitely with time.

The mathematical expression for this spreading can be found in almost every textbook of quantum mechanics and has the form

$$\Delta x(t) = \Delta x_0 \sqrt{1 + \frac{\hbar^2 t^2}{m^2 (\Delta x_0)^4}}, \tag{4.7.1}$$

that, in practice, can be approximated to a linear function of time

$$\Delta x(t) \approx \frac{\hbar}{m \Delta x_0} t . \tag{4.7.2}$$

Assuming that this relation holds true in all cases then some bizarre conclusions can be drawn from it. For instance, an electron ejected by the Sun, represented by a wave packet of about the size of an atom, $\Delta x_0 \approx 10^{-10} m$, would exhibit a dimension greater than the Earth's diameter itself when approaching the Earth!

On the other hand it would be expected, in a first approach, that if two coherent extended wave packets were superimposed there should be interference, total or partial according to the degree of overlapping.

Nevertheless it is known from experiments performed with electrons and neutrons that the spreading of matter wave packets has no influence on the interference properties of the packets. Accordingly, see Rauch, for all practical situations in matter interferometric experiments everything happens as if there were no actual dispersion of the wave packets. This experimental result seems surprisingly in contradiction with the endless spreading of matter wave packets. Although strange in the orthodox framework this result had been originally predicted by de Broglie himself.

In order to fully appreciate the significance of the problem let us investigate the following situation. Consider the case of two coherent matter wave packets that at the initial time have a size of about $\Delta x_0 \approx 10^{-10} m$, and furthermore that they are separated by $10^{-10} m$.In such scenario they do not overlap, and consequently there shall be no interference between then. These two distinct matter wave packets keep expanding endlessly as the time passes according to the above expression (4.7.2) in such a way that their size reaches eventually a magnitude of about one kilometer. At this instant of time the overlapping of the two wave trains is practically complete. In a distance of one kilometer only a small piece of $10^{-10} m$, does not superimpose, with the ratio of superposition continuing to increase as the time passes. Nevertheless even if the overlapping of the packets is almost complete no interference is to be observed. Still, some authors like Comsa, in the framework of the orthodox theory, were able to engender a justification for this lack of interference. Nevertheless due to the various assumptions made in the explanation, we are led to believe that if experiments had shown an interference pattern, the followers of the orthodox paradigm would have demonstrated, with the same very theory that there must be interference. By the habitual process of introducing ad-hoc parameters and supplementary hypotheses one can go very far. Indeed, by this process, unfortunately followed by many researchers, it is always possible, a posteriori, to fit almost any experimental result.

If one accepts the local causal model for the quantum particle, developed above, the explanation for the absence of interference comes naturally. The limitless spreading of matter packets is a consequence of the fact that in the initial burst, coming from the source, each individual localized quantum particle travels at a different velocity. Therefore as the time increases, the distance among them also increases, see Fig.4.17.

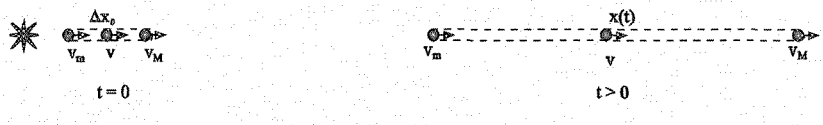

Fig.4.17 – At time $t=0$, the particles with different velocities are localized in the pulse of small size Δx_0. Later, at time $t > 0$, they will be spread continuously.

In this situation two matter packets of macroscopic size overlapping almost completely except in a small region, of angstrom order, do not interfere because the small wavelets, corresponding to each particle, do not superimpose with each other, as can be seen in the picture

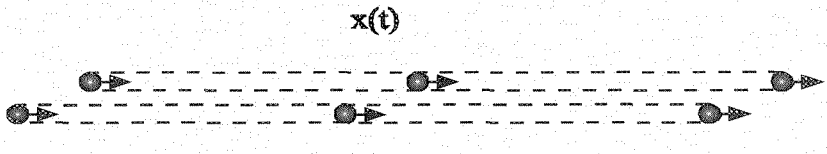

Fig.4.18 – In the mixing region of the interferometer the extended pulses of particles overlap almost completely. Due to the constant minute non-overlapping the small real wavelets, representing the extended part of the quantum particles, do not superimpose. In such circumstances no interference is to be expected.

These wavelets transporting the singularity once produced by the source keep their size. This statement is perfectly comprehensible because the different theta waves composing the final wavelet packet propagate with the same velocity therefore the initial shape of the wave resulting from the composition with many single wavelets keeps its form. It must be understood that the final size of the wavelet packet can be larger or smaller than the size of the free single individual theta waves. We have seen, when discussing the example of a penetration of a square potential, that the size of the final wavelet, resulting from the composition of many finite waves, could tend to infinity, approaching the monochromatic plane wave.

In this causal framework the spreading of matter wave packets has no true meaning for the individual particles. This spreading represents only a mathematical mean statistical description of the time increasing separation between particles with different velocities. A possible way to test the general validity of the usual uncertainty relations comes directly from this causal interpretation of the infinite spreading of matter wave packets.

Let us now consider the experimental situation in which an electron source emits, at a reference known time t_0, electrons in such a way that their uncertainty in position is $\Delta x_0 \approx 10^{-8} m$. According to Heisenberg uncertainty relations this dispersion in position corresponds to a minimum possible dispersion $\Delta v_0 \cong 10^4 m/s$ for the velocity so that $\Delta x_0 \Delta v_0 \approx \hbar / 2m$. As time passes, say a millisecond later, the initial wave packet due to spreading will have increased its size. The value of this increase can be obtained with the help of formula (4.7.2) which, at one millisecond gives for the spread wave packet a size of about $\Delta x = 10 m$. Suppose that with the help of a special cutter one cuts from each expanded electron wave packet a small piece $\delta x_0 \approx 10^{-8} m$ long, as shown in Fig.4.19.

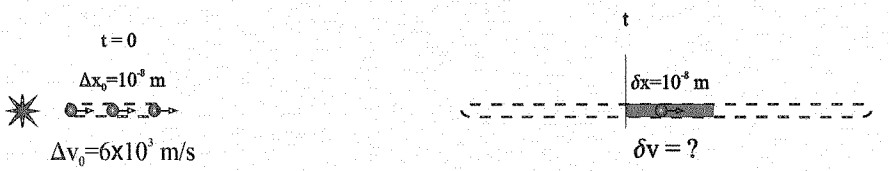

Fig.4.19 – At the initial time the uncertainty in position for the electron pulse is $\Delta x_0 \approx 10^{-8} m$. A certain time t later, a piece of size $\delta x_0 \approx 10^{-8} m$ is chopped from the extended pulse of actual length $\Delta x = 10 m$.

This cut can be done in many ways like for instance by a knife made of an electrostatic field. The knife, allowing for the necessary delay, is triggered by the electrons emission from the source. In practice this knife may consist of a monolayer of gold atoms deposited on slab of silica. Later the electrons forming the slice enter an electron detector. The overall sketch of the experiment is shown in Fig.4.20, where the electron detector needs to have a good energy resolution.

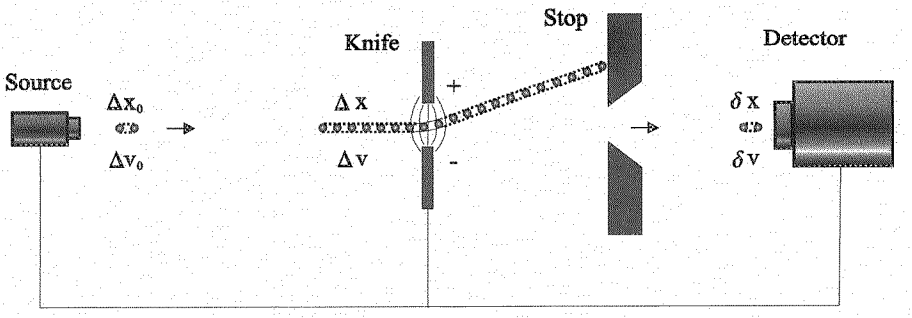

Fig.4.20 – Set up to test the general validity of the Heisenberg uncertainty relations based on the spreading of matter wave packets.

The question to be put now is the following. What are the predictions for the velocity dispersion δv of the electrons from the slices, of actual size $\delta x = \Delta x_0$, cut from the expanded wave packet?

For this question there are two possible answers: one given by the orthodox quantum mechanics based on the Fourier nonlocal paradigm and the other coming from the causal local approach following as close as possible the initial ideas of de Broglie.

(a) Orthodox theory

In this model describing quantum phenomena the uncertainty relations of Heisenberg ought to hold true in all and every experimental circumstance. Therefore the product of the two uncertainties must be such that at least $\delta x \delta v = \hbar / 2m$, which corresponds to the ideal case of minimal dispersion. Within the orthodox framework of nonlocal Fourier analysis this conclusion is perfectly natural. When the cut is performed in the extended wave packet, one necessarily interacts with all the Fourier components of the packet. Therefore according to Fourier nonlocal relations the shorter the slice δx the larger the δv. On the other hand since the experimental conditions were set such that $\delta x = \Delta x_0$, that implies that $\Delta x_0 \, \delta v = \hbar / 2m$. Also at the initial time $\Delta x_0 \Delta v_0 \approx \hbar / 2m$ and therefore the final conclusion to be drawn from this approach is that the energy dispersion of the electrons from the small slices must be greater or equal to the initial dispersion of the pulse of particles $\delta v \geq \Delta v_0$.

(b) Causal approach

In this approach the real quantum particle is to be described by a finite localized wavelet and consequently the spreading of matter "wave packets" has no intrinsic meaning. Nonlocal Fourier analysis, having in this causal local model no ontological significance, represents only a statistical description of the average separation among pulse particles having different velocities. Therefore in this experiment nothing is really sliced. What the knife really accomplishes is a selection of a small subensemble from the large ensemble of particles having different velocities. Under these conditions from the initial ensemble of electrons that now are fairly well separated a smaller range of particles is then picked. Naturally, this, small subgroup of electrons, from the larger group needs to have a smaller range of velocities. These electrons of this small group of particles are the only that enter the detector. All the other electrons are stopped at the absorber.

Therefore, according to the stated hypothesis if a single electron at the initial time can be localized in the pulse of length $\Delta x_0 = 10^{-8} m$, chosen for instance to be the experimental coherence length, then one millisecond later $t = 10^{-3}$ s, its size will be practically the same since for these electron wavelet packets with the same frequency there is no significative dispersion with time. So the physical meaning of the large size of the whole packet is related with the fact that the initial pulse of particles may have electrons with many velocities. These electrons have a velocity range given by the difference between the fastest and the slowest, $\Delta v_0 \approx v_M - v_m$. Therefore, as time passes the distance between these particles with different velocities increases without limit. This subensemble of particles from the initial pulse can have in principle any number of electrons depending on how the source is made. The size of the packet in this natural intuitive model corresponds roughly to the distance between the fastest and the slowest particle. The velocity dispersion of the electrons of the initial ensemble must be constant with time since there are no interactions to increase or reduce the velocity of the particles. Therefore we have every reason to make $\Delta v = \Delta v_0$. In this sense when the "cut" is made with the knife what really takes place is a selection of a small subensemble of particles from the large group. This subensemble of electrons needs, in this natural approach, to have a smaller range of velocities. The ratio between the size of the slice cut $\delta x = \Delta x_0 = 10^{-8} m$ and

the size of the expanded electron wave packet, $\Delta x = 10\,m$, one millisecond after the initial time is

$$\rho = \frac{\delta x}{\Delta x} = 10^{-9}. \tag{4.7.3}$$

On the other hand the ratio for the velocity range is precisely the same

$$\begin{cases} \Delta x = \ell_M - \ell_m = v_M t - v_m t = \Delta v.t, \\ \delta x = \ell'_M - \ell'_m = v'_M t - v'_m t = \delta v.t, \end{cases} \tag{4.7.4}$$

where ℓ_M and ℓ_m are the distances traveled by the fastest and slowest particle of the pulse; δv being the range of velocities of the electrons from the slice of length δx. In such conditions it is possible to write

$$\rho = \frac{\delta v}{\Delta v}, \tag{4.7.5}$$

or

$$\delta v = \rho \Delta v = 10^{-9} \Delta v, \tag{4.7.6}$$

which means, for the chosen parameters

$$\delta x = 10^{-9} \Delta v = 10^{-9} \Delta v_0, \tag{4.7.7}$$

where we made $\Delta v = \Delta v_0$. The justification for the equality results, as we have previously seen, from the fact that there is no interaction and consequently the particles cannot increase or decrease their individual velocities.

Recalling that the source was built to have a minimal dispersion

$$\Delta x_0 \Delta v_0 = \hbar / 2m, \tag{4.7.8}$$

and that the experiment was set to have $\delta x = \Delta x_0$ and $\delta v = 10^{-9} \Delta v_0$, its product is

$$\delta x \delta v = \Delta x_0 \times 10^{-9} \Delta v_0$$

which by substitution gives

$$\delta x \delta v = 10^{-9} \frac{\hbar}{2m}. \tag{4.7.9}$$

This result shows that if the assumed hypotheses are correct then the orthodox uncertainty relations of Heisenberg-Bohr also cannot describe this experiment.

Summarizing, the predictions for the expected velocity dispersion of the electrons seen by the detector are:

Orthodox nonlocal approach

$$\delta v \geq \Delta v_0$$

Causal local approach

$$\delta v <<< \Delta v_0 .$$

These different predictions are shown in Fig.4.21.

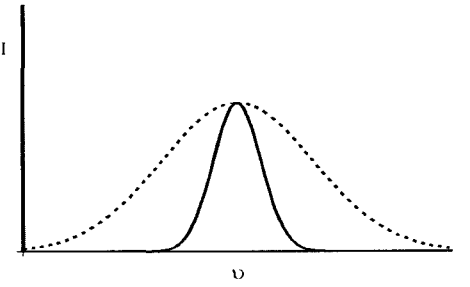

Fig.4.21 – Prediction of the two approaches: Orthodox theory dashed line; Causal theory solid line.

As a concluding remark, we have to say that if the measured dispersion for the velocity δv of the electrons, from the small subensemble, is less than the dispersion of the total ensemble Δv_0 then we have to conclude that the orthodox uncertainty relations are not appropriate to describe this experiment. In this situation the above experiment would be precisely a special case where the orthodox non-causal uncertainty relations do not apply!

4.8 AN EXAMPLE OF A CONCRETE MEASUREMENT THAT GOES BEYOND HEISENBERG'S UNCERTAINTY RELATIONS

We have just presented two feasible proposals of experiments that can test the limits of the usual orthodox nonlocal uncertainty relations. Now we are going to discuss a concrete physical experimental situation where the limitations of the uncertainty relations of Heisenberg have already been shown. The problem of the applicability or inapplicability to real experiments of the uncertainty relations of Heisenberg is very important because this principle lies at the very heart of orthodox quantum theory. Furthermore, since the Copenhagen approach is the one accepted by most in the scientific community, even if they do not fully understand their deep meaning, the problem of the limits of validity of the uncertainty relations of Heisenberg-Bohr deserves a full discussion. The statement that the so-called uncertainty principle can be violated is more than enough to rise a feeling of strong opposition among conservative people. Still the word violation does not fully account for what is involved. In reality the word violation does not render what really happens. Nobody says that classical mechanics is violated because there are phenomena not described by it like, for instance, in the domain of large velocities, approaching the one of light, or at the quantum level. The word violation is not sufficient to give complete account of the fact that if classical mechanics does not describe the natural phenomena at the quantum level it is because the theory, being developed in a certain experimental environment, has, just like any human construction, necessarily its limits of applicability. A good theory is not violated. It would imply its general validity in whole actual and future physical situations. This is clearly impossible. On the same foot is orthodox quantum mechanics, which is in fact a very good theory able to predict the natural phenomena with a very

great precision. Therefore the uncertainty relations of Heisenberg-Bohr, being a direct consequence of the usual quantum theory are not simply violated. What happens is that the empirical evidence and the conceptual tools have changed since they were developed. Therefore it seems quite natural to expect that the limits of their validity soon or later would come out. What is being proposed is more basic, is a change from the orthodox nonlocal and non-causal paradigm, developed by the Copenhagen School, to a more general causal local paradigm. The non-applicability of the orthodox uncertainty relations to every, present and future, physical situation is a mere consequence of the fact that the Copenhagen paradigm has indeed reached its limits of validity. It is not a single local violation of the established paradigm that eventually could be surmounted, it is much more, it implies a change of the whole quantum orthodox paradigm. The more general uncertainty relations being a consequence of a new more general causal paradigm would then be able to deal with the new experimental evidence.

In order to present a sound clear demonstration of the limitations of the orthodox uncertainty relation to all open minded learned people we shall analyze the paradigmatic example of the so-called Heisenberg's microscope experiment with two optical microscopes: one, the usual Fourier microscope, the other, of new generation microscope developed by Pohl and his group. This classic experiment has the advantage of being treated in most textbooks of quantum mechanics and therefore is familiar to all who have followed quantum mechanical courses.

Essentially the experiment consists in having a microscopic particle on the observation region of the microscope. Upon the incidence of a quantum of light on the small particle transferring to it an indeterminate amount of energy the photon is diffused entering eventually the microscope. After a suitable treatment of the incoming information an, in general, enlarged image of the particle appears in the display device. Our problem is to predict, before the actual measurement takes place, the uncertainty in momentum for the microscopic particle, due to the unavoidable interaction with the quantum of light, and at the same time compute the error, the uncertainty, in the determination of the position of the particle.

We shall begin to predict the maximum possible uncertainty for the momentum of a small particle M after the interaction with the incident photon. The prediction of this uncertainty can be done in many ways. Each author of quantum textbooks, that studies the Heisenberg microscope, as expected, tries to present the most original possible calculation for the uncertainty. Therefore, as can be seen in the quantum textbooks dealing with

this problem, they take in consideration more or less parameters, weigh the diverse factors, but in the end the conclusions of all authors are the same. No matter the method they followed all them arrive at the same final result. This is a consequence of the fact that all authors are eager to arrive at the expression initially obtained by Heisenberg and Bohr, that is the orthodox uncertainty relation for position and momentum. Since the theoretical error in the determination of the position of the small particle is given by the resolution of the microscope that, as we know, is the same for all common Fourier microscopes it follows necessarily that in order to arrive at the orthodox uncertainty relation, which is the product of the two uncertainties, the uncertainty for the momentum must have, in practice, a fixed value.

In any case, just for the sake of exemplification, it is convenient to derive here the formula for the uncertainty in momentum. In order to do that, and without pretension of being original, here we follow, almost step by step, the demonstration de Broglie gave in his book *Les Incertitudes d'Heisenberg et l'Interprétation Probabiliste de la Mécanique Ondulatoire.*

Fig.4.22 shows the region of detection of the two types of microscopes. In the derivation one considers the case of horizontal incidence. The calculations could, evidently, be done for any other photon angle of incidence, as can be seen in the literature.

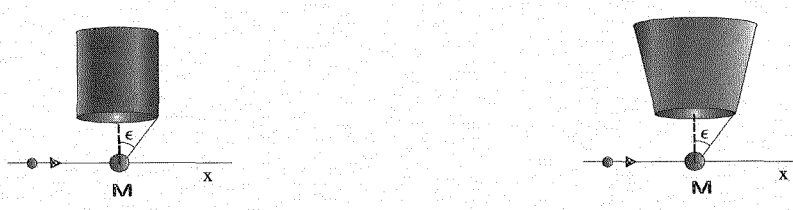

Usual Fourier microscope Super-resolution microscope

Fig.4.22 – Region of detection of the microscopes.

There is an important point we must keep in mind. The calculations for the uncertainty in the momentum are the same for the two microscopes as can be inferred from the picture. This conclusion results from the fact that the physical situation in the two cases is precisely the same. The horizontally incoming photon strikes the microparticle M to be observed and after having transferred to it an uncertain amount of momentum is later diffused. The

future eventual capture of the diffused quantum of light by the microscope has nothing to do with the amount of momentum that has been transferred from the photon to the microparticle.
In the following calculations, it is assumed that before the interaction with the quantum of light, the particle to be observed M is at rest. Furthermore, it is understood that during the interaction photon-microparticle there is conservation of linear momentum.

In such circumstances before the interaction the total momentum of the two particles, photon and microparticle, is equal to the momentum of the incident photon.

$$\vec{p}' \rightarrow |\vec{p}'| = p' = p'_x = h/\lambda\,. \tag{4.8.1}$$

After the interaction between the quantum of light and the microparticle we must have along the x-axis

$$p'_x = p''_x + p_x\,, \tag{4.8.2}$$

with the component of the linear momentum p_x of the particle M being

$$p_x = p'_x - p''_x = p' - p'' \sin\varepsilon \cong \frac{h}{\lambda}(1 - \sin\varepsilon) \tag{4.8.3}$$

Therefore, the value of the momentum of particle M along the x-axis lies between the two extreme values

$$\frac{h}{\lambda}(1 - \sin\varepsilon) \le p_x \le \frac{h}{\lambda}(1 + \sin\varepsilon) \tag{4.8.4}$$

consequently the overall uncertainty in the momentum of the microparticle along the x-axis is given by

$$\delta p_x = 2\frac{h}{\lambda}\sin\varepsilon \tag{4.8.5}$$

which has a maximum for a diffusion angle of $\pi/2$. Therefore the maximum possible uncertainty in the momentum of the microparticle M due to the interaction with the incident photon is given by the expression

$$\delta p_x = 2\frac{h}{\lambda}. \tag{4.8.6}$$

This value, as expected, relates to the maximum possible momentum transferred from the photon to the microparticle. It implies a complete photon momentum transfer to the right and to the left. Naturally some values of the diffusion angle obviously have a very low or even zero probability.

As we have already seen, this formula for the uncertainty in the momentum of the microparticle M after the necessary interaction so that the measurement, the observation, could take place, is precisely the same for both microscopes. On the other hand at this particular step of the measurement process, in order to predict the error of the two conjugated observables position and momentum, it is necessary to keep in mind that the interacting photon behaves like a corpuscle.

Having predicted the maximum possible error in the measurement of the linear momentum we now proceed with the determination of the maximum possible error in the measurement of the position. This value, which corresponds to the uncertainty in the position, after the interaction, for the common Fourier microscopes is given by its theoretical resolution. The resolution of a common Fourier microscope is, as we have seen, the intrinsic capacity of the apparatus to separate two points. Abbe, based on Rayleigh criteria, obtained for the imaging systems the maximum theoretical resolution of

$$\delta x = \frac{\lambda}{2} \tag{4.8.7}$$

This is a theoretical value obtained in ideal conditions, which means that the actual resolution of the real Fourier microscopes is, in general, worse.

Now, since we have predicted the two values (4.8.6) and (4.8.7) for the uncertainties in a concrete measurement, the next step is to make their product, which gives

$$\delta x \delta p_x = h, \tag{4.8.8}$$

which, as expected, is the current mathematical form for Heisenberg's uncertainty relations. The above result corresponds to the theoretical ideal case and consequently they lie precisely in the boundary of Heisenberg's uncertainty measurement space. In a real measurement, made with these common Fourier microscopes, in which the experimental realistic resolution is always worse, the equality turns into the habitual inequality

$$\delta x \delta p_x \geq h.$$

These values lying well inside Heisenberg's measurement space.

Now let us see what happens with the super-resolution optical microscope. As we have seen previously for these super resolution microscopes, there is actually no mathematical formula, derived from first principles, to calculate its resolution limit. Still, the practical experimental resolution must certainly be smaller than the theoretical limit. For super resolution microscopes, of the type under consideration, we know that experiments have shown resolutions of the order of

$$\delta x = \frac{\lambda}{50}, \tag{4.8.9}$$

or even better.

Then the product of the uncertainties in momentum (4.8.6) and in the position (4.8.9) for a measurement done with the super-resolution microscope is given by

$$\delta x \delta p_x = \frac{1}{25} h. \tag{4.8.10}$$

This result is in clear discrepancy with the orthodox uncertainty relations of Heisenberg by a significant factor of 1/25. Even with this moderate chosen resolution we have found an important deviation from the orthodox behavior. Had we used a better actual experimental resolution for the super-resolution microscope the discrepancy would be even greater. Clearly this

result lies outside Heisenberg's measurement space, nevertheless it still belongs to the more general wavelet measurement space.

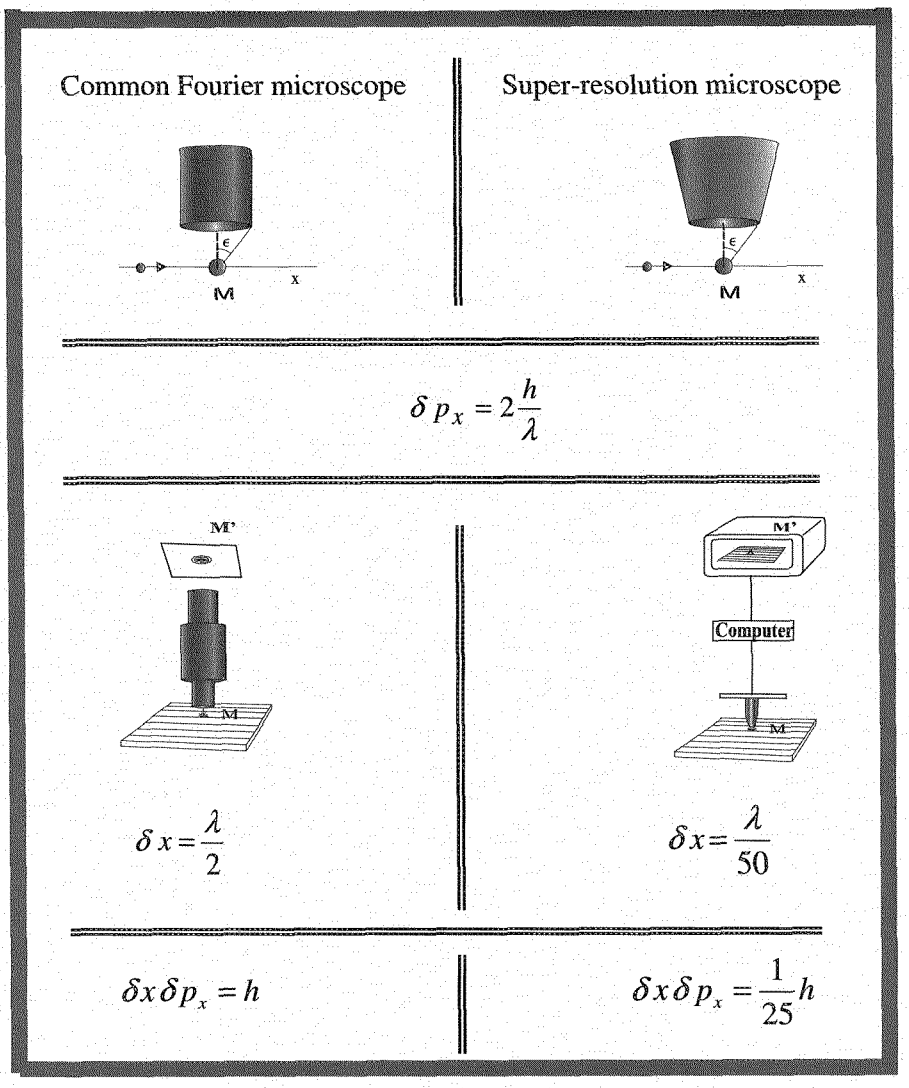

Fig. 4.23 – Predictions for the two kinds of microscopes.

For the sake of further clarification these results are summarized in Fig.4.23, where the measurement predictions for the two types of microscopes are shown side by side.

Since these super-resolution microscopes are new, some people, less familiar with them, may raise the question whether these devices work at a single photon regime. We know that, generally, in practice both microscopes work with a large number of photons. There are various reasons for that, namely that it is not easy to make single photon sources and even more critical from the experimental point of view, one hundred per cent detection of diffused photons is, in laboratory practice, unattainable. Nevertheless there is no in principle theoretical reasons why either the common Fourier or the super-resolution microscopes could not work at single photon regime.

In order to clarify a little more this problem let us consider the optical super resolution microscope working with a single photon. It is assumed, for the sake of conceptual consistency, that the illuminating source delivers only one single photon that always hits the microparticle which position is to be measured, the detecting optical device has one hundred per cent efficiency and furthermore during the experiment there is no photon noise, nor any other experimental nuisances that may shadow the measurement. In other words, we are working in experimental ideal circumstances that we also well know that are impossible to meet in any real concrete experiment.

Thus the conceptual simplified experiment runs like this: The single photon emitted by the source strikes the microparticle, transferring to it a certain amount of linear momentum and afterwards is diffused. This diffused photon, by the small particle, enters the optical sensing device, which happens to be precisely at the seeing cone of detection. The electric pulse, generated at the sensing device, feeds the computer. Next, the computer knowing the position of the light-collecting detector produces on the display a non-null intensity pixel, which corresponds to the position of the microparticle. The dimension of this pixel depends on the overall resolution of the apparatus. The size of this non-null region corresponds, of course, to the error in the determination of the position of the microparticle. Elsewhere on the display, making the background, null pixels are seen.

If it happens that the photon does not hit the microparticle target no photon is diffused and no measurement is done. On the other hand if the sensing optical device is not positioned in the detection range no diffused photon is collected, therefore no electric pulse feeds the computer and on the display a null intensity pixel is laid. In such conditions no measurement is done, which is against our initial assumptions.

The working process of the common microscope displays a nice dual role, so that this is a paradigmatic experiment in which Nature exhibits its dual character. Indeed, in the eyes of Bohr, the conceptual microscope experiment of Heisenberg-Bohr is a clear manifestation of the applicability of the Principle of Complementarity. First, when the incident photon interacts with the microparticle, transferring a certain amount of momentum, and is later diffused. In this process the quantum of light behaves like a corpuscle. After being diffused the photon enters the microscope crossing the diverse lenses of the optical device until an enlarged image of the small particle appears on the display. In this process throughout the microscope the photon manifests its undulatory nature. Summarizing, sometimes the photon behaves live a corpuscle other times like a wave. Therefore it is no surprise that this experiment cannot be described by the orthodox uncertainty relations that are a physical consequence of the complementarity principle.

Looking at the same experiment done with the super-resolution microscope one sees that the incident photon during the whole measurement process behaves always like a corpuscle. When it strikes the microparticle and is diffused, just like the common microscope, it behaves like a corpuscle. Also, when it is collected by the optical sensing device, producing an electric pulse that feeds the computer, it still keeps behaving as a corpuscle. In this conditions, since the complementarity principle does not apply it is no surprise that the uncertainty relations of Heisenberg-Bohr do not describe this new type of measurement. The entire measurement process is done in the generalized wavelet measurement space and consequently needs to be described by the more general uncertainty relations.

As concluding remarks we would like to add that it was shown, following a process analogous to the one followed by Niels Bohr and since then followed by most authors of quantum textbooks, that the orthodox uncertainty relations of Heisenberg-Bohr, after all, are not so general as most in the scientific community believe.

4.9 REFERENCES

On wavelets:

A. Grossmann and J. Morlet, SIAM *J. Math. Anal.* **3**, (1989) 723.
C.K Chui, *An Introduction to Wavelets*, Academic Press, N.Y. 1992.
P. Kumar, Rev. Geophysics, 35(1997)385.

B.B. Hubbard, *The Word According to Wavelets*, A. K. Peters Wellesley, Massachusetts, 1998.

On de Broglie causal theory:

J. von Neumann, *Mathematical Foundations of Quantum Mechanics*, Princeton University Press (N.J.)1955.
D. Bohm, Phys. Rev. 85(1952)186.
L. de Broglie, The Current Interpretation of Wave Mechanics: A Critical Study, Elsevier, Amsterdam, 1969.
L. de Broglie, Les Incertitudes d'Heisenberg et l'Interprétation Probabiliste de la Mécanique Ondulatoire, Gauthier-Villars, Paris, 1988.
L. de Broglie and J.L. Andrade e Silva, *La Réinterprétation de la Mécanique Ondulatoire*, Gauthier-Villards, Paris, 1971.

Nonlinear contributions:

F. Guerra and M. Pusterla, Lett. Nuovo Cimento, 34(1982)351.
Ph. Gueret and J.P. Vigier, *Lett. Nuovo Cimento*, **38,** 125(1983).
L. Smolin, Phys. Lett. A 113(1986)408.
J.P. Vigier, *Phys. Lett. A,* **135**, (1989) 99.
J.P. Vigier, Found. Phys. 21(1991)125.
A.R. Silva, J.S. Ramos, J.R. Croca and R.N. Moreira, J.R. Croca, , in *Causality and Locality in Modern Physics and Astronomy*, eds. S. Jeffers et al. Kluwer Academic Publishers, 1998.

On causal models for the quantum particle:

J.P. Vigier, Found. Phys. 21(1991)125.
J.R. Croca, *Physics Essays*, **1**, 71(1990).
J.R. Croca, *In Modern Nonlinear Optics*, Vol.119, Eds. M.W. Evans, John Wiley and Sons, N.Y. 2002.

Some works related with the general uncertainty relations:

J.R. Croca, in *Fundamental Problems in Quantum Physics*, Eds. M.Ferrero and A. van der Merwe, Kluwer Academic Publishers, 1995.
J.R. Croca, Apeiron, 6, Nr.3-4, (1999)151.

On Plato paradigm:

A. Koré, *From the Closed World to the Infinite Universe*, John Hopkins Press, Baltimore, 1957.
T. S. Kuhn, *The Copernican Revolution*, Harvard University Press, Cambridge, 1977.

On experiments related with the uncertainty relations:

D. Bohm, *Quantum Theory*, Prentice-Hall, New York, 1955.
H. Rauch, 2nd ISQM – Meeting, Tokyo, Sept. 1986.
G. Möllenstedt and G. Wohland, in Electron Microscopy, eds. P. Bredero and G. Boom, Leiden, 1980, Vol.I.
H. Keiser, S.A. Werner and E.A. George, Phys. Rev. Lett. 50(1986)560;
G. Comsa, Phys. Rev. Lett. 51(1983)1105;
A.G. Klein, G. Opat and W.A. Hamilton, Phys. Rev. Lett. 50(1983)563.

Beyond the orthodox Heisenberg's uncertainty relations:

J.R. Croca, *Experimental Violation of Heisenberg's Uncertainty Relations*, talk at the 5th UK Conference on the *Conceptual and Philosophical Problems in Physics*, at Oxford, Sept. 1996.
J.R. Croca, Hadronic Journal **22**, 29-39 (1999).
J.R. Croca, and F. Selleri, Comm. Math. Theor. Physics, vol. 2, pp.61-69(1999).

Works related with the proposal of experiments to test the orthodox uncertainty relations:

D. Bohm, *Quantum Theory*, Prentice-Hall, New York, 1955.
J. Scheer and M. Schmidt, *Phys. Lett. A,* **115**, 322(1986).
T. Götch, T. Coch, G. Luning, J. Scheer and M. Schmidt, in *Problems in Quantum Physics*, Gdansk, eds. L. Kostro, A. Posiewnik, J. Pykacz and M. Zukowski, World Scientific, 1987.
J.R. Croca, *Physics Essays*, **1**, 71(1990).
J.R. Croca, in *FundaMental Problems in Quantum Physics*, Eds. M.Ferrero and A. van der Merwe, Kluwer Academic Publishers, 1995.

CHAPTER 5

THE MEANING OF THE WAVE FUNCTION

5.1 INTRODUCTION

The fundamental evolution equation for orthodox quantum physics is the Schrödinger equation, which, as is well known, is a wave equation. This means that the solution to this equation must, in one way or another, represent a wave. On the other hand we also know that these quantum waves, solution to the wave equation, may describe quantum particles like the electrons, neutrons, protons, atoms and other similar massive particles. Also these quantum waves, like the vulgar macroscopic waves, can be reflected, diffracted and so on by physical devices. The problem we have before us is to know what is the "true" meaning of these quantum waves solutions to the Schrödinger equation.

According to the orthodox interpretation of quantum formalism, these waves are mere probability waves therefore devoid of any physical meaning. Being only probability entities these waves can evidently be normalized at will without any problem.

The causal local school of de Broglie, on the contrary, sustains that the matter quantum waves, solutions to the common Schrödinger equation, or to the other generalized non-linear evolution equation, are indeed real waves. They are real matter waves in the sense that they try to describe an objective reality that is observer independent. Since these waves are real, in the previous stated sense, they, evidently, cannot be normalized at will.

Once again we are before two different, even opposite, interpretations for the same quantum situation. In this case of quantum waves the problem can be summarized in the following question:

Are quantum waves real waves or just probability waves?

Most of the quantum experimental evidence accepts both interpretations. The explanation and the predictions of the outcome of the majority of the quantum experiments is the same no matter which interpretation you choose for the meaning of quantum waves. This state of things led us to seek for special situations where the predictions of the outcome of the experiments differ with the chosen interpretation for the meaning of the psi wave. This quest started in the middle of the fifties. Nevertheless, nothing really significative was produced during thirty years. It is true that much work was done on the subject, since the creation of quantum mechanics. Sill most of this work was related with the development and presentation of the so-called quantum paradoxes, like for instance, Schrödinger's cat. Nevertheless, by its very nature those were conceptual experiments impossible to be submitted to the verdict of experiment. Only in the middle of the eighties indications were presented on the possibility of devising such crucial experiments. This early work was developed under the influence of Andrade e Silva, former student of de Broglie. Immediately after, with the help of the school of Bari under the direction of Selleri, the first proposals for conceptual experiments were made. Soon, these efforts led to a breakthrough. In fact the author developed and presented some proposals of feasible concrete experiments that could test the nature of quantum waves. Once the conceptual threshold attained, the basic ingredients found, a large number of these experiments were proposed. In order to present them in a systematic way we group them in two principal categories.

The first category is related with the reduction postulate of orthodox quantum mechanics. This postulate states that when the measurement is performed all quantum waves, being probability waves without physical reality, collapse into a single wave.

The other category of experiments results from the fact that if quantum waves are indeed probability waves, when they propagate in free space, without interaction, they must keep its relative intensity unchanged. Therefore, interferometric experiments, done in free space, will keep the same visibility independently of the interferometer arms length.

5.2 A CAUSAL INTERPRETATION FOR THE TWO-SLIT EXPERIMENT

Let us now retake the most important, from the conceptual point of view, experiment in quantum physics. It is the double slit experiment we have previously discussed in the framework of the Copenhagen interpretation. Now we are going to discuss it in terms of the causal approach of de Broglie.

We recall briefly that in the model of the local causal framework of de Broglie a quantum particle that is composed of an extended wave plus an indivisible well-localized singularity. As we shall see, with this more complex model for the quantum particle a natural causal local explanation of the double slit experiment comes out easily.

When the quantum particle reaches the screen with the slits two simultaneous things happen:

1 – The extended wave being larger than the distance between the two slits crosses both at the same time giving origin to two small coherent waves.

2 – The singularity goes through one slit or the other.

In such conditions if two detectors are placed one in front of each slit, only one of them is triggered at a time. Never will the two detectors be fired at once. This is a consequence of the nature of the quantum particle that only the singularity has sufficient energy to give rise to the common quadratic detection process. The two small waves that enter the detectors at the same time do not have enough energy to trigger them.

If the detectors are removed from the slits the two waves keep going on in until they eventually mix giving origin to a composite wave at the detection region where an array of detectors is placed. The singularity follows on one or the other wave until it is immersed in the composite wave sum of the two waves. The localization of the singularity on the total wave follows the guiding principle. This principle states that the singularity is preferentially localized at the points of higher wave intensity. Under such conditions after a sufficient number of arrivals of individual particles an interference pattern starts appearing at the array of detectors.

The overall causal explanation for the double slit experiment is shown in Fig.5.1

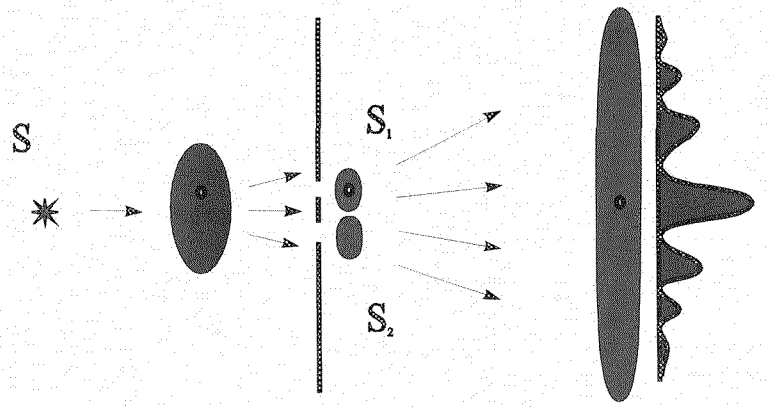

Fig.5.1– Explanation of the double slit experiment in de Broglie causal framework.

In this local causal paradigm the apparently contradictory conclusions, coming from the experiment, that the quantum particle must pass at the same time:

1 – Through one slit **or** the other slit;

2 – Through one slit **and** the other slit;

is clearly understood without having to deny the objective reality of quantum beings. In fact the two conclusions are perfectly conciliated in the following way:

1 – The singularity being indivisible passes through one slit **or** the other slit.

2 – The wave being extended passes at the same time through one slit **and** the other slit.

In this way, by devising a more ingenious model for the quantum particle, all experimental contradictions were removed. In this context no necessity arises to call for supernatural help or to deny the objective reality. The causal methodology we have inherited from the Greeks is more than sufficient to explain without ambiguities the double slit experiment.

Bohr and followers, as we have seen in chapter 2, in order to explain the same double experiment, instead of looking for a subtler local causal model for the quantum particle, chose to reject the objective reality. In the orthodox framework the potential quantum particle having no real existence crosses also potentially the two slits. The two potential waves in their potential course mix and interfere also potentially at the overlapping region. One the other hand if the detectors are placed in front of the slits, then one of the potentialities or probabilities materializes itself at one of the detectors, the other probabilities being reduced to zero.

The outcome of the double slit experiment being perfectly explained by the two opposite paradigms is no good ground to decide which is the better approach to help us understand Nature. Had the followers of de Broglie's ideas, those who seek causality and locality, the same intellectual attitude of the huge majority of the so-called revolutionary theoreticians then they would be happy with the previous results. That is, they had been able to devise a theory capable of explaining quantum phenomenology but without the major inconvenience of being experimentally testable. On the contrary, if our goal is the truth, the understanding, the clarification and confirmation of the models to give us more insight into Reality one has to seek for concrete experimental situations where the two opposite approaches predict different results.

5.3 EXPERIMENTS TO TEST THE NATURE OF THE WAVE FUNCTION

As stated at the beginning of the chapter there are at least two ways to test the true nature of quantum waves: One is based on the collapse of the wave function in a measurement process; the other based in the different physical properties of the carrying wave theta and the full wave conducing to what can be called auto reduction of the wave packet.

Let us begin with the method based on the collapse of the wave function.

5.4 EXPERIMENTS ON THE COLLAPSE OF THE WAVE FUNCTION

In order to study in a better systematic way the experiments related with the postulate of the reduction or collapse of the wave train in an orthodox quantum measurement process it is convenient to consider first the concept of the generator of theta waves.

5.4.1 Generator of Theta Waves

The fundamental idea behind the experiments related with the collapse of the wave function in a measurement is deeply connected with the concept of a generator of theta waves. This device is, as we shall see, a direct consequence of the reduction postulate of the orthodox quantum mechanics.

Orthodox quantum mechanics assumes that the wave function is a probability wave devoid of any physical meaning and therefore the quantum measurement process implies the collapse of the whole multiple probabilities into a single one.

In the causal interpretation there cannot be a collapse because we are dealing with a function representing a real entity with physical meaning and not with a mere probability. Therefore, if the initial carrying wave, in the particular experimental setup, was divided into many sub waves, the singularity following on one of them, then when the detector is triggered, at a particular location, it means that the singularity had followed that path while the other waves going through other different paths remained unaffected.

In order to develop a little more this crucial point and draw the practical and conceptual implications let us analyze the next experiment shown in Fig.5.2. In the picture S represents the monoparticle source emitting quantum particles, one at a time. This demand is very stringent. It must imperatively be met in practice because without monoparticle sources the real experiments are meaningless. Today, thanks to the development of experimental physics this basic necessity poses no problem.

In the case of massive particles such as neutrons, electrons and atoms it is relatively easy to design and build such type of sources. Still, for photons the problem is not so easy. Even if the intensity is very low, the source delivering only a few photons or less than one per second, it cannot be

considered monophotonic. The photons are usually emitted in bunches because photons are bosons and so tend to be together, the so-called bunching effect. The development of monophotonic sources was connected principally with the quantum experiments related with the EPR (Einstein, Podolsky and Rosen) paradox and Bell's theorem. The initial sources were very complex. They basically consisted of a source of atoms and a laser. The source of atoms produced one atom at a time, which was introduced in the laser field given origin to an interaction photon-atom. From this one-at-a-time interaction two photons with good angle correlation were produced. Thus the detection of one photon at one direction implied that at the other there could be found the second photon at a correlated time.

The next easier way to produce photonic monoparticle sources was developed mainly by Mandel and his group at the University of Rochester. They produced and tested these different types of monoparticle sources. These monophotonic sources are generally composed of a UV laser incident on a non-linear crystal. In the non-linear crystal a parametric down conversion occurs giving origin to a pair of correlated photons.

The reader interested in the fascinating field of monophotonic sources can consult the literature related with this subject and indicated at the end of the chapter.

Looking at Fig.5.2 one sees the monoparticle source emitting in such a way that in the whole apparatus there is only one quantum particle at a time.

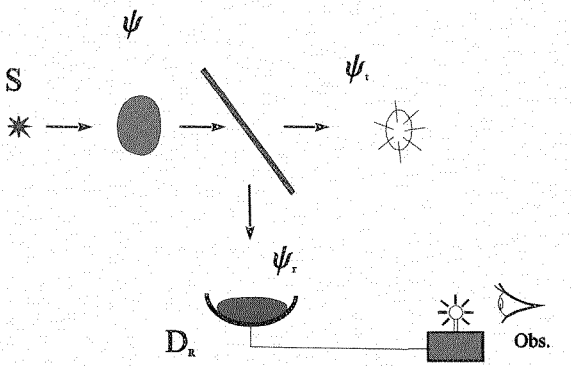

Fig.5.2 – The ψ wave emitted by the source is divided into two at the beamsplitter. If the detector D_R is activated the bulb glows and the observer sees the light.

This quantum particle is directed to a device, a beamsplitter, which splits the wave representing the particle into two waves. This quantum system is

138 *To a Nonlinear Quantum Physics*

described, in the orthodox theory, by probability wave ψ that contains all the available information on the system.

The wave ψ upon reaching the beamsplitter is divided into two small waves; one of them is reflected ψ_r, while the other ψ_t is transmitted. These two different waves follow two completely independent trajectories. When the detector placed in the path of the reflected wave ψ_r is triggered then it switches on a light that is seen by the observer.

After the measurement done, that is after the observer sees the light, what happens to the transmitted wave ψ_t?

The answer to this question depends on the theory you adopt:

(a) Orthodox approach:

The Copenhagen approach to quantum physics states that the wave function is no more than a mere mathematical probability wave which sole function is to help to predict the results of the measurements. Therefore after the beamsplitter the quantum particle can follow two ways that are described by the two probability waves. These probability waves follow the two different possible ways where, in the measurement process, the particle can be localized. In such conditions, if the particle triggers the detector, since the light is on, it implies that the particle followed the reflected path. After that, the probability of the particle being at the transmitted path turns instantly to zero, which means that the corresponding probability turns to zero, $\psi_t = 0$. This conclusion is a necessary consequence of the reduction postulate of orthodox quantum mechanics. This fundamental postulate of the orthodox quantum physics demands the collapse of the initial wave function from the multitude of possible states, in this case only two, into a single one.

Briefly, according to the orthodox interpretation of quantum mechanics, after the detection of the particle at the reflected path the probability of being in the transmitted trajectory turns to zero and consequently nothing remains there.

(b) Causal local approach:

Quite different is the answer given to this same question by causal quantum physics that assumes that the waves are real. When the source emits a quantum particle it means that a full wave $\phi = \psi$, the wave plus a

singularity, moves in direction of the beamsplitter. This device divides the physical wave into two smaller waves. The singularity following on one of the waves is reflected or transmitted. When the singularity is reflected, the case shown in Fig.5.2, it interacts with the detector in its path. This interaction detector-singularity produces an electric pulse that turns the light on. Because the two paths are independent and quite apart the transmitted real wave is submitted to no physical interaction. Since the real transmitted physical $\psi_t = \theta$ undergoes no physical interaction the conclusion we must draw is the following: After the measurement, after the detection of the singularity, the transmitted wave keeps going on its way unaffected.

As expected, the two approaches, being epistemologically quite different conduce in this particular case, contrary to what happens in the double slit experiment, to completely different predictions.

Summarizing:

– The orthodox approach states that after the measurement nothing remains in the transmission trajectory.

– The causal approach, predicts that along the transmission path follows a real physical wave carrying a negligible amount of energy.

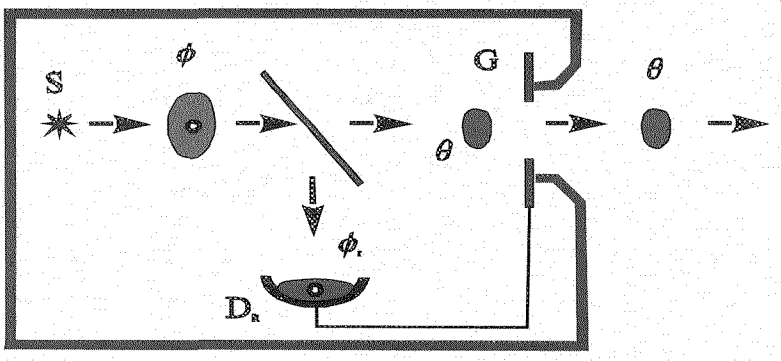

Fig.5.3 – Generator of theta waves.

This is precisely the situation we were looking for, a practical feasible experiment for which the two approaches predict different results. In this

way a concrete experimental test for two opposite theories for quantum physics looks possible.

The previous experimental setup can further be improved by a slight modification. Suppose that now the detector D_R is connected directly to a fast shutter G, as shown in Fig. 5.3

In the case shown when the singularity happens to be reflected the reduction detector D_R is triggered and sends an electric pulse to open, for a short time, the fast gate G allowing the wave without singularity to pass. When the singularity is transmitted the reduction detector is not activated because the theta wave that hits it has not enough energy to trigger the detection process. In such circumstances, since no pulse is sent to the gate it remains closed and consequently the particle remains trapped in the device.

Clearly, the whole apparatus behaves like a source, a generator of waves devoid of singularity, that is, of theta waves. Nevertheless if a common quadratic detector were placed in front of the device it would not be activated. The energy these waves carry is so small that it does not reach the detector threshold.

Quite different are the expectations of the Copenhagen school, which would claim that since the particle was seen at the reduction detector D_R, nothing more remains in the transmission path. Furthermore, this conclusion can be put to proof by placing a detector in front of the device, which of course would detect nothing.

Briefly: The orthodox school states that nothing leaves the apparatus. The causal approach, on the contrary, maintains that a physical wave with very little energy comes out from the device.

In order to settle the problem, of whether something really leaves the apparatus or not, it is necessary to find some kind of special detectors able to reveal such waves that carry such a small amount of energy.

5.4.2 Direct Detection of Theta Waves

The simplest process to reveal the existence of the waves without singularity is by direct detection. This implies that we must be able to devise a special detector with the possibility of reacting directly to the very small amount of energy that these waves carry. An ingenious process for revealing these waves practically devoid of energy was devised by Selleri in the late eighties. The idea at the heart of the process is that these waves may act akin to the vacuum fluctuations that are responsible for spontaneous emission.

Thus these waves may modify the decay probability of specially prepared unstable systems. The concrete idea is to inject a theta wave, coming out from the generator, in the cavity of a laser gain tube. There, the wave practically without energy would stimulate the emission of photons that would be revealed at a common quadratic detector. The idea is depicted in Fig.5.4

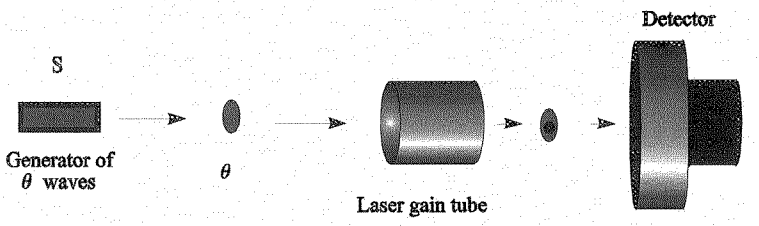

Fig.5.4 – Sketch of Selleri's experiment for direct detection of theta waves.

In the laser cavity the theta waves have the possibility of revealing their real existence by generating a practically zero energy-transfer stimulated emission. If the detector detects a distribution of photons different from the usual poissonian noise the experiment would be conclusive proving that something had come from the special generator. This experiment has been extensively discussed in the literature and the main inconvenience put forward was that it was not conclusive. This means that we are not dealing with a yes-or-no experiment. If the experiment fails it cannot be attributed for sure to the inexistence of the theta waves, it may happen that the laser cavity does not behave as expected. Nevertheless, due to the simplicity of the experiment it could eventually show the existence of de Broglie's waves by putting the laser gain tube in front of a generator of theta waves with a very high emission rate. In these circumstances if the counting rate of the detector significantly increased above the dark counting rate, it would prove the real existence of theta waves.

As we shall see in the next section, Garuccio, Rapisarda and Vigier proposed another experiment opposite to the one of Selleri. It would, in principle, work in the case one of Selleri's failed to demonstrate the existence of theta waves.

5.4.3 Detection with Coherent Sources

One other way to detect these waves without energy is by the phase information they carry. We know from the early experiments done with photons from different sources that waves from independent sources do in fact interfere. These experiments that are against Dirac's initial statement that the photon only interferes with itself were first done by Pfleegor and Mandel and since then repeated by many others experimentalists like Radloff. Under such conditions it is relatively easy to devise experiments that may manifest the existence of theta waves by the phase information. The basic idea is shown in the following picture, Fig.5.5.

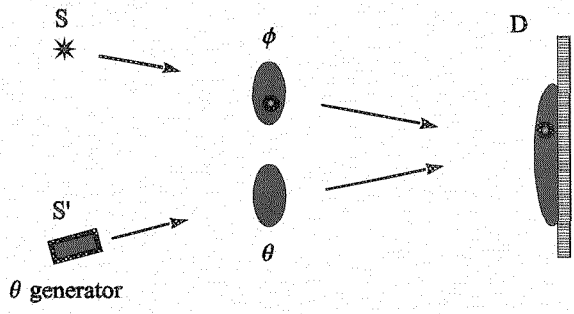

Fig.5.5 – Principle for detection of theta waves by the coherent phase information.

From the picture the underlying principle is quite easy to understand. The two coherent waves overlap at the mixing region where the detectors array is placed. Since they are coherent waves the interferometric pattern will be stable in time giving origin to an observable interference distribution of photonic counts.

The causal predictions for intensity registered at the array of detectors D is given by the squared modulus of the sum of the two overlapping coherent real waves

$$I_c = |\phi + \theta|^2 \tag{5.4.1}$$

assuming, for simplicity reasons, that the intensity of the carrying wave is equal to the intensity of the theta wave

$$|\phi| = |\theta|, \tag{5.4.2}$$

one gets

$$I_c \propto |\phi|^2 (1+\cos\delta), \tag{5.4.3}$$

where δ is the constant phase difference between the two real waves.

The prediction for this experiment outcome given by the Copenhagen school is quite different. Since the wave without singularity does not exist the intensity at the detector shall be only

$$I_o \propto |\phi|^2, \tag{5.4.4}$$

that is, no interference is expected.

The main problem with coherent phase detection is that it is very difficult to produce two single particle independent coherent sources emitting precisely at the same time. Building two independent sources able to emit single particles at the same time with the same correlation in phase is indeed a real challenge for the experimentalists.

Garuccio, Rapisarda and Vigier proposed a method for solving this experimental problem for the case of photonic sources. Their basic assumption is that, contrary to Selleri's hypothesis, the emission in the laser cavity cannot be induced by the wave devoid of singularity. Only the corpuscle can induce laser emission. The sketch of the experiment proposal of is shown in Fig.5.6

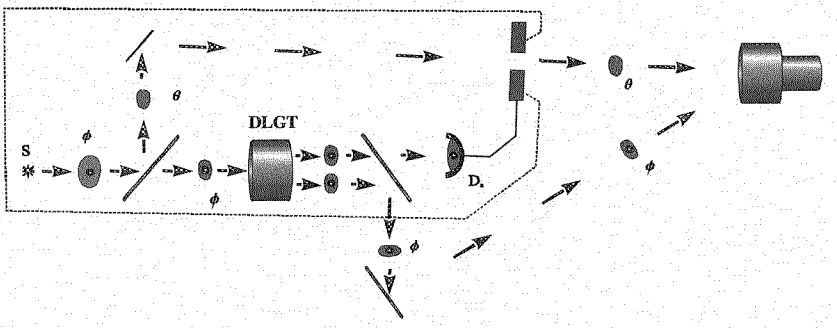

Fig.5.6 – Garrucio, Rapisarda and Vigier experiment.

In this experiment the transmitted wave carrying the singularity, instead of acting on the reduction detector enters a special duplicator laser gain tube.

There, assuming that the stimulation is only due to the presence of the singularity, two photons keeping the same phase relation with the incident one are produced. These twin photons, produced in the duplicator, DLGT, are directed to a beamsplitter. If one of them is transmitted then the photon triggers the reduction detector that opens the gate, an optical shutter, for a short time, just sufficient to allow the wave devoid of singularity to pass. In the meantime, the other quantum of light that was reflected is directed to the superposition region where a detector is placed. Therefore, at the superposition region there would be present two coherent waves one carrying the singularity and the other empty. The total wave resulting from the sum of the two present waves guides the singularity so that an interferometric pattern is to be expected if, of course, the experiment assumptions are correct. The other possibilities of the experiment, not shown in the picture, are, for al practical purposes, meaningless.

The weakness of this experiment is that it is based on unproven experimental assumptions depending much on the behavior of the laser duplicator. Furthermore the experiment is not conclusive. If it fails the fact cannot be attributed to the inexistence of the theta waves but possibly to the fact that the experimental assumptions are not valid.

In order to design truly conclusive experiments to reveal the existence of the theta waves one has to seek other open possibilities that do not require the necessity of two independent coherent monoparticle sources emitting at the same time.

5.4.4 Detection with Incoherent Sources

Since the direct and the coherent processes are not truly conclusive it is necessary to look for another conceptually clear method that could in principle avoid the stated experimental difficulties. A conclusive experiment to decide on such an important issue as the true nature of quantum waves, whether they are real or not must be conceptually very simple and above all conclusive in principle. This process was indeed developed and is known as incoherent interferometric detection of the theta waves. The early conceptual developments of this method were due to J. Andrade e Silva and M. Andrade e Silva. A short time later the author formalized and shaped the initial idea so that it could give origin to feasible concrete experiments that can be done, in principle, with any quantum particle. All incoherent wave detection experiments are conceptually variants of the same basic idea.

Because of the difficulty in building two coherent sources emitting at the same time, the idea was to use independent incoherent sources. In this case the presence of the incoherent wave is to blur the net interferometric pattern due to the superposition of coherent waves all sharing the same singularity. In practice the basic idea for the experiment is no more than a variant of the Young double slit experiment. It is a triple slit experiment that is depicted in Fig.5.7.

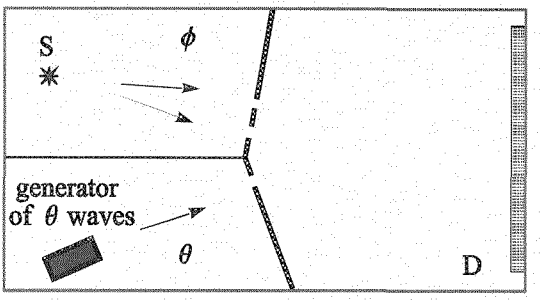

Fig.5.7 – Triple slit experiment to test the reality of quantum waves by incoherent overlapping.

In this case, shown in Fig.5.7, the expected intensity predicted at the detectors array, assuming that quantum waves are real, can be computed in the following way. Before embarking in the calculations we must stress that the method of incoherent wave mixing can be applied, in principle, to any quantum particle, neutrons, electrons, photons and so on.

From the picture we see that the position of each photon-singularity, arriving at a certain time t_i at the detector is given, according to de Broglie guiding principle, by the square modulus of the sum of the three overlapping waves

$$I_c(t_i) \propto |\theta + \phi_1 + \phi_2|^2, \tag{5.4.5}$$

which, by development gives

$$\begin{aligned} I_c(t_i) \propto |\theta|^2 + |\phi_1|^2 + |\phi_2|^2 + 2|\theta||\phi_1|\cos\delta_{\theta,\phi_1}(t_i) \\ + 2|\theta||\phi_2|\cos\delta_{\theta,\phi_2}(t_i) \\ + 2|\phi_1||\phi_2|\cos\delta_{\phi_1,\phi_2}(t_i) \end{aligned} \tag{5.4.6}$$

where $\delta_{i,j}$ is the phase difference between the respective waves. In order to simplify the calculations but without loss of physical meaning let us assume that the experiment was done in such a way that the amplitude of all the waves is the same

$$|\theta|=|\phi_1|=|\phi_2|. \tag{5.4.7}$$

In this case expression (5.4.6) can be written

$$I_c(t_i) \propto |\theta|^2 \left[3+2\cos\delta_{\theta,\phi_1}(t_i)+2\cos\delta_{\theta,\phi_2}(t_i)+2\cos\delta_{\phi_1,\phi_2}(t_i)\right]. \tag{5.4.8}$$

Since in the whole experimental apparatus there are no more than three finite waves at the same time the expected probability distribution of position at the detectors array after n single arriving photon-singularities shall be given by the sum of each individual contribution

$$I_c \propto \sum_{i=1}^{n} |\theta|^2 \left[3+2\cos\delta_{\theta,\phi_1}(t_i)+2\cos\delta_{\theta,\phi_2}(t_i)+2\cos\delta_{\phi_1,\phi_2}(t_i)\right]. \tag{5.4.9}$$

In order to proceed with the calculations we must recall that the relative phase difference between waves ϕ_1, and ϕ_2 is constant in time

$$\delta_{\phi_1,\phi_2}(t_i) = \delta = \text{constant}, \tag{5.4.10}$$

because they are coherent between themselves. This coherence condition is easily meet experimentally for the simple reason that the two partial waves result from the splitting of the same initial wave. That is, they come from the same source. Nevertheless, the relative phase difference between waves (θ,ϕ_1), which is, $\delta_{\theta,\phi_1}(t_i)$ and similarly between waves (θ,ϕ_2) which corresponds to $\delta_{\theta,\phi_2}(t_i)$, changes randomly with time since they come from incoherent independent uncorrelated sources. In such circumstances the sum (5.4.9) may be written

$$I_c \propto |\theta|^2 \left[n(3+2\cos\delta) + 2\sum_{i=1}^{n} \cos\delta_{\theta,\phi_1}(t_i) + 2\sum_{i=1}^{n} \cos\delta_{\theta,\phi_2}(t_i) \right]. \tag{5.4.11}$$

For a large number of arriving photon-singularities, large n, the summing cosines random terms average to zero. Therefore the total photon counting distribution is given by

$$I_c \propto (1+\tfrac{2}{3}\cos\delta). \tag{5.4.12}$$

This formula clearly shows that the presence of the incoherent theta wave is put in evidence by blurring of the interference pattern visibility the by a factor of
V_c = 2/3. The visibility parameter being defined, as usual, by Born and Wolf's expression

$$V = \frac{I_M - I_m}{I_M + I_m}. \tag{5.4.13}$$

If we compute the expected visibility for this experiment in the framework of orthodox quantum mechanics the result shall be quite different. In this approach the theta waves do not exist and therefore only two coherent waves of about the same amplitude superimpose, at the detection region. This overlapping gives origin to a net, clear interference pattern of visibility one. Thus, the expected intensity shall be given only by

$$I_o \propto |\phi_1 + \phi_2|^2, \tag{5.4.14}$$

that is

$$I_o \propto (1+\cos\delta), \tag{5.4.15}$$

which, as stated, corresponds to a visibility one, $V_o = 1$.

The preceding calculations lead to different predictions for expected visibility. If one accepts the orthodox framework the visibility of the interference pattern shall be one, because none but the usual coherent waves

overlap. In the causal paradigm the theta waves of de Broglie are real waves and therefore at the superposition region there shall be present three waves. Because the theta wave is incoherent with the other two the interference pattern appears blurred conducing to a reduction of the visibility by a factor of 2/3.

There is another possible variant of the previous experiment, where the causal calculations, assuming the reality of quantum waves, are quite similar conducing precisely to the same prediction for visibility. In this case, shown in Fig.5.8,

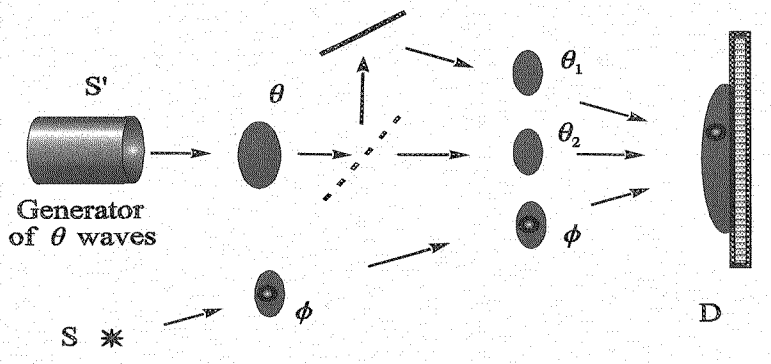

Fig.5.8 – Incoherent detection of θ waves.

the two coherent waves are now the theta waves, the full wave is added to provide for the photon-singularity and to produce noise. For this same particular experimental setup the orthodox predictions are entirely different.

Following the causal approach at the detection region three waves overlap giving origin to a resulting wave

$$\phi_T = \theta_1 + \theta_2 + \phi\,. \tag{5.4.16}$$

This total wave resulting from the superposition of three waves drives the single photon-singularity according to the guiding principle. So, the expected intensity shall be given by

$$I_c \propto |\,\theta_1 + \theta_2 + \phi\,|^2\,, \tag{5.4.17}$$

and recalling that this time the two coherent waves are the theta waves we can write

$$I_c \propto |\theta_1 + \theta_2|^2 + |\phi|^2, \tag{5.4.18}$$

because the cross terms of the incoherent waves average to zero. Developing this expression one gets

$$I_c \propto |\phi|^2 + |\theta_1|^2 + |\theta_2|^2 + 2|\theta_1||\theta_2|\cos\delta, \tag{5.4.19}$$

where, as usual δ represents the constant phase difference between the two coherent waves.

Assuming again, for calculation simplicity reasons, that all waves have the same amplitude, one gets for the expected intensity

$$I_c \propto (1 + \tfrac{2}{3}\cos\delta), \tag{5.4.20}$$

the same expression previously obtained (5.4.12) that, evidently, corresponds to the same visibility, $V_c = 2/3$.

A completely different result is predicted if one uses the Copenhagen approach. In this particular setup since the theta waves do not exist, at the detection region there shall be present only one wave and the expected intensity shall be given simply by

$$I_o \propto |\phi|^2. \tag{5.4.21}$$

This means that in view of the fact that there is no interference term, no interference pattern is to be seen, and consequently the expected visibility shall be zero, $V_o = 0$.

This experiment is in a certain sense the symmetric of the previous one. In the three-slit experiment the theta waves show their presence, by blurring the clear interference pattern, in this experiment the waves produce an interference pattern where none was expected.

A symmetric experiment more prone to practical realization can be drawn as shown in Fig.5.9.

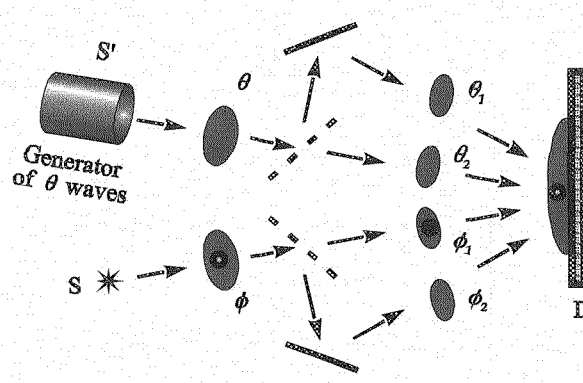

Fig.5.9 – Symmetric mixing of waves.

In this experimental scheme four waves overlap at the detection region. The waves that come from the same source are coherent between themselves and incoherent relative to the others. Again, theta waves are incoherent with the usual waves since they come from different sources. The expected intensity predicted in the causal paradigm shall be, accordingly

$$I_c \propto |\theta_1 + \theta_2|^2 + |\phi_1 + \phi_2|^2, \tag{5.4.22}$$

and the one expected in the orthodox approach

$$I_o \propto |\phi_1 + \phi_2|^2, \tag{5.4.23}$$

since theta waves do not exist.

The main experimental difficulty with this kind of experiments is related with the fact that at the mixing region of space the waves coming from different sources must always fully overlap. Only in ideal experiments the two independent sources are completely synchronous. This means that is necessary to produce real independent sources emitting precisely at the same time. Even if in principle the two sources emit particles at the same time in practice there are always unavoidable random fluctuations that if not taken in account can hide the action of the theta waves.

the singularity, the so-called coherence length is, in general, very small and therefore complete overlapping at all times is impossible.

5.4.4.1 Experiment with correction for synchronization

In order to address this crucial experimental point the following experimental methodology was developed. A scheme of the experimental process is shown in Fig 5.10.

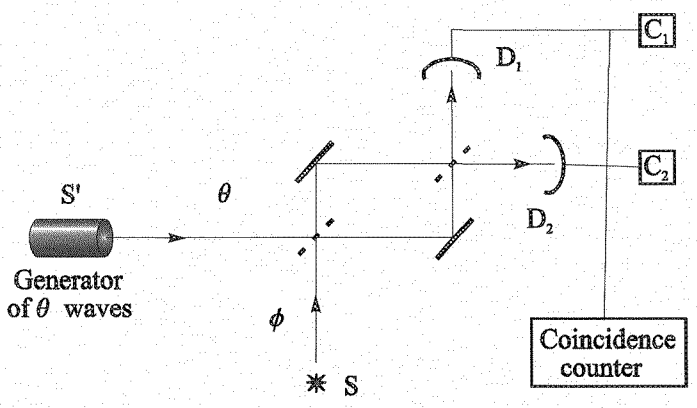

Fig.5.10 – Detection of theta waves with correction for synchronization

In the picture one can see two waves, one from the common photon source, the other from the theta waves generator, feeding the input ports of a Mach-Zehnder interferometer. The intensity registered at output ports C_1 and C_2 predicted by the orthodox approach results only from the common input single source S, and is simply given by

$$\begin{cases} I_o^1 \propto |\phi_{TR} + \phi_{RT}|^2 \\ I_o^2 \propto |\phi_{RR} + \phi_{TT}|^2 \end{cases} \tag{5.4.24}$$

Here ϕ_{TR} represents the wave that was reflected at the first beamsplitter and later transmitted at the second. Assuming the ideal case of no absorption and for 50% beam splitters we can write

$$|\phi_{TR}|^2=|\phi_{RT}|^2=|\phi_{RR}|^2=|\phi_{TT}|^2=\tfrac{1}{4}|\phi|^2, \quad I_0=\alpha|\phi|^2, \tag{5.4.25}$$

where α is a proportionality constant. After the habitual and easy calculation and by naming the relative phase shift between the two coherent waves by δ_ϕ one gets

$$\begin{cases} I_o^1 = I_0(1+\cos\delta_\phi) \\ I_o^2 = I_0(1-\cos\delta_\phi) \end{cases} \tag{5.4.26}$$

which gives, for this experimental setup, the intensities expected, at the two output ports, by the Copenhagen approach.

If one accepts the causal approach of de Broglie it is necessary to include also the theta waves coming from the special generator. In order to proceed with the calculations we assume, in a first step, that the two independent sources S and S' are perfectly synchronic. Meaning that is there is always a perfect overlapping of the waves coming from different sources. In a second step this drastic experimental requirement is somewhat relaxed.

In such circumstances, assuming that the two independent sources S and S' emit finite waves precisely at the same time, so that a perfect overlapping of the waves occurs at the mixing region, the predicted causal intensity at the two output ports of the Mach-Zehnder interferometer shall be given by

$$\begin{cases} I_c^1 \propto|\phi_{TR}+\phi_{RT}+\theta_{TT}+\theta_{RR}|^2, \\ I_c^2 \propto|\phi_{RR}+\phi_{TT}+\theta_{RT}+\theta_{TR}|^2, \end{cases} \tag{5.4.27}$$

Since the relative phase difference of the waves coming from the two different independent sources varies randomly in time one is allowed to write

$$\begin{cases} I_c^1 \propto |\phi_{TR} + \phi_{RT}|^2 + |\theta_{TT} + \theta_{RR}|^2, \\ I_c^2 \propto |\phi_{RR} + \phi_{TT}|^2 + |\theta_{RT} + \theta_{TR}|^2. \end{cases} \tag{5.4.28}$$

Assuming, as usual, for calculation simplicity reasons, that all mixing guiding waves have equal intensity

$$|\theta_{TR}|^2 = |\theta_{RT}|^2 = |\theta_{RR}|^2 = |\theta_{TT}|^2 = \tfrac{1}{4}|\phi|^2, \tag{5.4.29}$$

one gets by developing expressions (5.4.28)

$$\begin{cases} I_c^1 = \frac{1}{2} I_0 (1 + \cos\delta_\phi - \cos\delta_\theta), \\ I_c^2 = \frac{1}{2} I_0 (1 - \cos\delta_\phi + \cos\delta_\theta). \end{cases} \tag{5.4.30}$$

where δ_θ stands for the constant phase shift between the two coherent theta waves.

Now, if we set the experimental conditions so that the two independent arms of the interferometer are equal, which corresponds to a precisely identical optical path for all the waves, we may write

$$\delta_\phi = \delta_\theta = 0. \tag{5.4.31}$$

Substituting the value of the relative phase shift in the orthodox prediction formulas (5.4.26), one gets

$$\begin{cases} I_o^1 = I_0, \\ I_o^2 = 0, \end{cases} \tag{5.4.32}$$

and, for the same reason, the causal predictions, formula (5.4.30), gives by substitution

$$\begin{cases} I_c^1 = \frac{1}{2} I_0, \\ I_c^2 = \frac{1}{2} I_0. \end{cases} \tag{5.4.33}$$

The previous expressions show that for the particular choice of parameters of the experiment, given by expression (5.4.31), the overall behavior of the interferometer, according to the orthodox interpretation (5.4.32) is like a pure transmissible medium. All light coming from the common source S is transmitted, nothing is reflected. This somewhat unexpected result is a consequence of the fact that at the output port one the ϕ waves are in phase while at the output port two they are in phase opposition conducing to a null optical field.

In the causal framework since it is necessary to assume that quantum waves are real then the predictions are entirely different (5.4.33), the Mach-Zehnder interferometer behaves in this case like a perfect 50% beamsplitter.

These causal predictions, as stated, are valid only when the two independent sources emit precisely at the same time. This experimental requirement is, as we can imagine, very hard to implement in practice. In general, the two completely independent sources emit particles in a random way. Sometimes the two different waves arrive precisely at the same time, which corresponds to a complete overlapping, while other times they don't even partially mix. If it happens that the two independent waves do not overlap at the mixing region then the experiment is meaningless. In such circumstances no inference about the existence or no existence of quantum waves of de Broglie can be drawn. Between these two extreme situations there are, of course, all the intermediate cases of partial superposition.

It is relatively easy to develop a simplified model taking in consideration the true random emission nature of the two independent sources.

In order to do that let n_ϕ be the rate of particles emitted by the common source S. This rate corresponds to the number of particles that is registered per second at both output ports. Also, let n_c be the coincidence rate between the two detectors. In these circumstances, the rate, the number per second, of ϕ waves, arriving at the detection zone without the corresponding θ waves is $(n_\phi - n_c)$.

The total counting rate, assuming the reality of quantum waves, is given by two parts:

One part relates to the cases when the ϕ waves arrive alone at the beamsplitter without the corresponding theta waves $(n_\phi - n_c)$. In this case all particles are transmitted and go to detector D_1.

The other part corresponds to the situation when the waves from the independent sources arrive at the same time at the mixing region. For this case the same counting rate is obtained at the detectors.

Symbolically this can be described by

$$\begin{cases} I_c^1 = \frac{1}{2} n_c + (n_\phi - n_c), \\ I_c^2 = \frac{1}{2} n_c . \end{cases} \tag{5.4.34}$$

Let γ be a factor characterizing the mean overlapping coincidence rate of the two independent emitting sources, such that

$$n_c = \gamma\, n_\phi , \qquad 0 \le \gamma \le 1 . \tag{5.4.35}$$

by substitution into (5.4.34) one gets

$$\begin{cases} I_c^1 = (1 - \frac{1}{2}\gamma) n_\phi , \\ I_c^2 = \frac{1}{2}\gamma\, n_\phi . \end{cases} \tag{5.4.36}$$

Representing by Δ the difference between the counts per second of the two detectors we have

$$\Delta = I^1 - I^2 . \tag{5.4.37}$$

This generic expression, by substitution of the previously derived formulas, assumes different forms according to the model. The orthodox usual model predicts

$$\Delta_o = I_o^1 - I_o^2 = n_\phi , \tag{5.4.38}$$

while the causal approach conduces to

$$\Delta_c = I_c^1 - I_c^2 = (1-\gamma)n_\phi \,. \tag{5.4.39}$$

The predictions of the two approaches are shown in Fig.5.11, for the particular case of $\gamma = 1/2$.

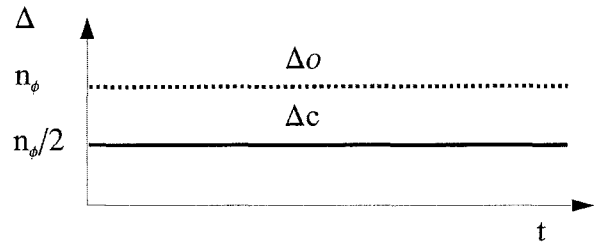

Fig.5.11 – Predictions for the two models for the particular case of = 1/2: Dotted line - orthodox model; solid line - causal model.

As can be inferred from the expression (5.4.39) the most unfavorable case corresponds to absolutely no overlapping between the wave packets emitted by the two independent sources $\gamma = 0$. In this case the predictions are precisely the same for the two models $\Delta_c = \Delta_o = n_\phi$. For different values of the mean overlapping factor $0 \le \gamma \le 1$, all intermediary situations are obtained. Considering the best overlapping situation $\gamma = 1$, the difference in the predictions of the two theories is maximal. The causal model expects that the difference between the counting rates of the two output ports is zero, $\Delta_o = 0$. The orthodox approach states that this difference is always the same, $\Delta_c = n_\phi$, since the theta waves do not exist.

The principal advantage of these experiments, of incoherent wave mixing, compared with the others is a consequence of the facts that first, they are inherently conclusive, and second, they can be put in practice with the now available technology. In the following we shall present one concrete practical execution of one of those proposals.

5.4.4.2 Mandel's experiment

These ideas were mature enough to lead about ten years ago L. Mandel and his group of Quantum Optics at the University of Rochester to make an experiment to test the nature of quantum waves. The experiment they made was based on a particular proposal of an experiment developed by J.R. Croca, A. Garuccio, V.L. Lepore and R.N. Moreira. The sketch of the proposal is shown in Fig.5.12.

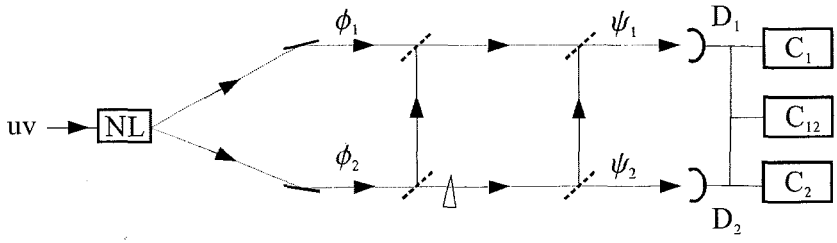

Fig.5.12 – Schematic representation of the proposal of an experiment to test the nature of quantum waves.

A uv laser beam of frequency ω_0 is directed to a non-linear crystal NL giving origin to a parametric down-conversion. For each arriving uv photon two photons ω_1 and ω_2 are produced such that $\omega_0 = \omega_1 + \omega_2$. These two photons, usually called the sign and the idler, that are produced at about the same time enter the Mach-Zehnder interferometer following the paths shown in the picture.

For this experimental setup the predictions of the causal de Broglie approach are the following: In order to proceed with the calculations it is useful to recall that the transmission and reflection coefficients satisfy the usual relation

$$\begin{aligned} |r|^2 + |t|^2 &= 1, \\ rt^* + r^* t &= 0, \end{aligned} \tag{5.4.40}$$

in such conditions the arriving waves at the detectors can be written in terms of input waves from the non-linear crystal

$$\begin{aligned} \psi_1 &= t^2\phi_1 + r^2 t\phi_2 + tr^2\phi_2\, e^{i\delta}, \\ \psi_2 &= t^2\phi_2\, e^{i\delta}, \end{aligned} \tag{5.4.41}$$

where δ represents the phase difference between the two coherent waves. This small phase shift is introduced by the phase shifting device, usually a glass slab. From the picture one sees that when the detector D_2 is triggered it means that the photon-singularity ϕ_2 followed the lower path being transmitted twice. At the other detector D_1, only the other photon-singularity can be detected. The probability of simultaneous detection at the two detectors is proportional to the product of the two expected intensities

$$P_c(D_1, D_2) \propto |\psi_1|^2 |\psi_2|^2, \tag{5.4.42}$$

which by substitution gives

$$P_c(D_1, D_2) \propto |t|^4 |\phi_2|^2 \left[|t|^4 |\phi_1|^2 + 2|r|^4 |t|^2 |\phi_2|^2 (1+\cos\delta) \right], \tag{5.4.43}$$

assuming, as usual, that the two waves have the same amplitude and for 50% lossless beamsplitters we get

$$P_c(D_1, D_2) \propto 1 + \tfrac{1}{2}\cos\delta\,. \tag{5.4.44}$$

This expression shows that if quantum waves are real and the stated assumption valid the joint probability detection depends, as expected, on the phase shift.

For the usual interpretation once the photon is detected at D_2, nothing more from ϕ_2 remains in the interferometer due to the collapse of the wave function in the whole interferometer. Therefore at detector D_1 only the wave ϕ_1 from the usual source arrives. Since the path of this wave does not cross the phase shifting device and what is more, it is a single wave that is presented at the detector there are no interferences and consequently the coincidence count does not depend on the phase.

These calculations can be made in terms of the usual quantum optics that as we shall see conduce, as expected, precisely to the same absence of interference. In order to do the quantum optical calculations for the joint probability detection at the two detectors it is useful to consider the following picture, Fig.5.13, where the relevant annihilation operators and the optical path lengths are shown.

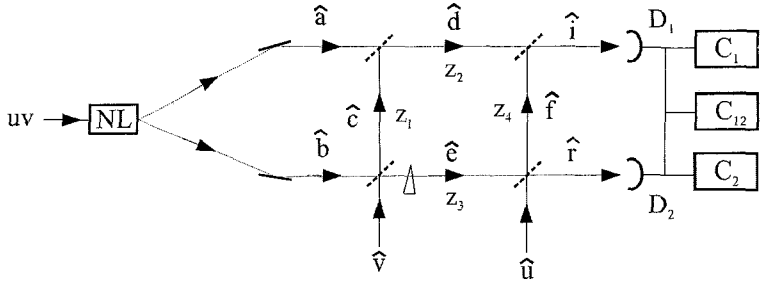

Fig.5.13 – Sketch of the proposed experiment showing the annihilation operators and the optical path lengths.

The output annihilation operators $\hat{i}$ and $\hat{r}$ can be expressed in terms of the annihilation operators $\hat{a}$ and $\hat{b}$ that stand for the signal and idler photons.

$$\begin{cases} \hat{i} = t\hat{d}e^{ikz_2} + r\hat{f}e^{ikz_4}, \\ \hat{r} = t\hat{e}e^{ikz_3} + r\hat{u}, \end{cases} \tag{5.4.45}$$

or recalling from the picture that

$$\begin{cases} \hat{d} = t\hat{a} + r\hat{c}e^{ikz_1}, \\ \hat{f} = r\hat{e}e^{ikz_3} + t\hat{u}, \end{cases} \qquad \begin{cases} \hat{c} = r\hat{b} + t\hat{v}, \\ \hat{e} = t\hat{b} + r\hat{v}, \end{cases} \tag{5.4.46}$$

the output annihilation operators can be written

$$\begin{cases} \hat{i} = t^2 e^{ikz_2}\hat{a} + tr^2\left[e^{ik(z_1+z_2)} + e^{ik(z_3+z_4)}\right]\hat{b} + \left[rt^2 e^{ik(z_1+z_2)} + r^3 e^{ik(z_3+z_4)}\right]\hat{v} + rt\, e^{ikz_4}\hat{u}, \\ \hat{r} = t^2 e^{ikz_3}\hat{b} + tre^{ikz_3}\hat{v} + r\hat{v}. \end{cases} \tag{5.4.47}$$

Now that we have the output annihilation operators expressed in terms of the input annihilation operators the calculation of the joint probability detection is only a matter of calculation. Accordingly, following Glauber, we can write the joint probability detection as the mean of the product of the four field operators

$$P_{1r}(\vec{R}_i,t_i;\vec{R}_r,t_r)=\alpha\left\langle\psi\,|\,\hat{E}_i^{(-)}(\vec{R}_i,t_i)\hat{E}_i^{(+)}(\vec{R}_i,t_i)\hat{E}_r^{(-)}(\vec{R}_r,t_r)\hat{E}_r^{(+)}(\vec{R}_r,t_r)\,|\,\psi\right\rangle, \tag{5.4.48}$$

where α is a proportionality constant. The single-mode field operators can be written the generic form

$$\hat{E}_i^{(+)}(\vec{R}_i,t_i)=i\sqrt{\frac{2\pi\hbar\omega}{V}}\,e^{i(\vec{k}_i.\vec{R}_i-\omega_i t_i)}\hat{h}. \tag{5.4.49}$$

With the input state $|\psi>$ for this particular experimental setup having the form

$$|\psi>=|1_a,1_b,0_u,0_v> \tag{5.4.50}$$

the somewhat lengthy calculations give, for the joint probability detection

$$P_{ir}\propto(|t|^2)^4, \tag{5.4.51}$$

which shows, as expected, no interference, no dependence on the phase shift.

A version of this experiment was carried out by Mandel and his group at the University of Rochester. The particulars of the experimental apparatus were a little different from the one shown previously as can be seen in the picture, Fig.5.14.

Even if the experiment is conceptually the same, nonetheless from a physical point of view is much more complex that the one presented. The physical simplicity of the first experiment where the beams were completely separated is lost here with the beams, just like in a Michelson interferometer, returning by the same path. All this complexity was introduced, according to

the authors, with the aim of obtaining an experimental apparatus with less one beamsplitter!

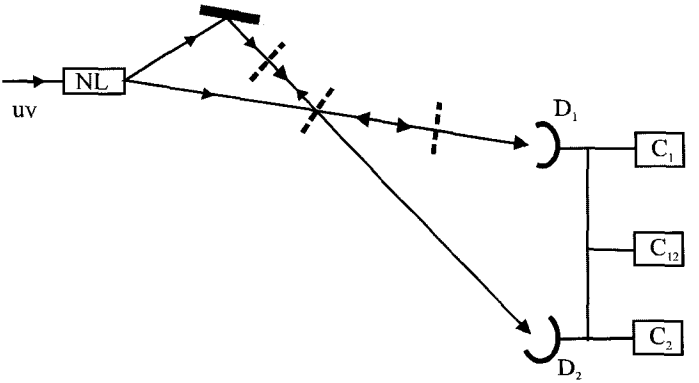

Fig.5.14 – Sketch of the experiment performed by Mandel and co-workers.

The experimental data obtained by the authors is presented in the next picture, Fig.5.15. The data in the first row of Fig.5.15 was privately provided by the authors while the data in the second row has been published.

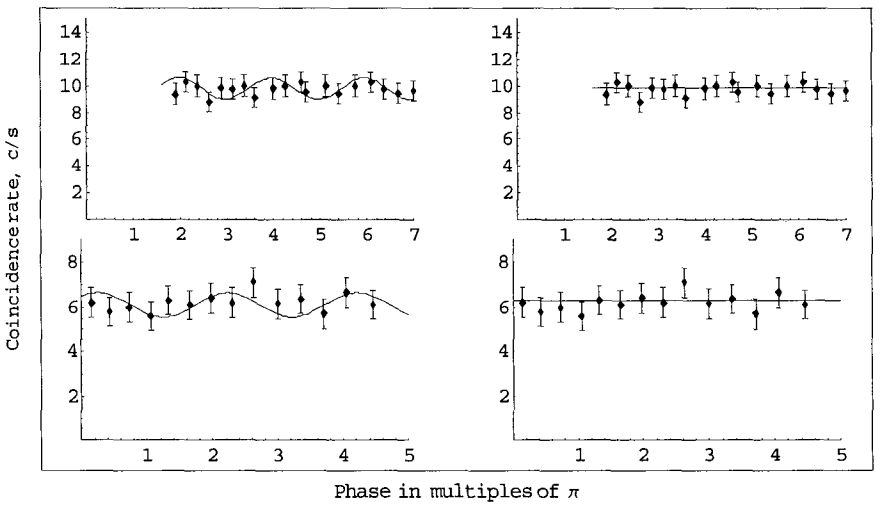

Fig.5.15 – Data obtained by Mandel et. al. fitted according to the causal de Broglie approach, first column, and fitted by the orthodox interpretation, second column.

The picture shows, in the first column, the data fitted using the causal model corresponding to an interferometric function of the type previously obtained

$$P_c(D_1, D_2) \propto 1 + V \cos\delta ,$$

with a visibility of about ten per cent $V = 0.1$. The picture shows also, in the second column, the same data fitted by a straight line.

The authors of the experiment concluded, in their paper, that the experimental data ought to be fitted by a straight line. This fit is presented in the last row of the second column. Their final conclusion was that the results of the performed experiment deny the existence of the theta waves. Their claim was made on the grounds that the theoretical visibility, predicted for the ideal case, would be of 50%.

As we can see from the picture, Fig.5.15, it is also equally possible to fit the same obtained data either by a straight line or by the interferometric expression with a visibility of about ten per cent.

The presented data shows that the statistics of the experiment were very poor with a mean coincidence rate of about six counts per second. In these cases of poor statistics the mechanical instabilities of the interferometer, imperfect alignment, temperature fluctuations, the fact that the used light is not perfectly monochromatic and other similar causes lead to the objective fact that the experimental visibility fails always to be the one predicted for the ideal case. This is precisely what happed in the case of an experiment done with the same type of equipment, by Mandel and his collaborators where they predicted a theoretical visibility of 100% and obtained an experimental value of about 30%. Naturally, to explain this notorious disagreement of the theoretical predictions with the values obtained the authors invoked the habitual arguments of temperature fluctuations, mechanical instabilities, imperfect alignment, the fact that the used light is not perfectly monochromatic and so on. Had the same type of arguments been applied to the performed experiment to reveal the existence of the theta waves and the expected experimental visibility would fall to a value of 15%, not very far from the obtained value of about 10%.

The truth is that the obtained experimental data can be fitted either by an interferometric function, with a visibility of about ten percent, or by a straight line. Since the same data can be used either to prove the existence of the theta waves or to deny it the only solid conclusion to be drawn from the

performed experiment is that it is inconclusive and therefore needs to be redone. So in order to clarify the problem the experiment must be redone in better conditions, with a more significative statistics.

It is interesting to refer that Selleri [F. Selleri, *Two-Photon Interference and the Question of the Empty waves*, in *Wave Particle Duality*, ed by F. Selleri, Plenum Press, New York, 1992] based on his model of variable detection probability obtains for the above experiment a visibility of 8%, not very far from the best fit of about ten percent.

An important point with these experiments, as was stressed before, is the necessity of perfect overlapping of the wave packets. In the performed experiment the packets temporal dimension was of about 10^{-13}s, whereas the electronics resolution time of the apparatus was of about 10^{-8}s. These figures mean that in the minimum resolution time of the apparatus it is possible to put side-by-side nearly 10^5 photon wave packets.

If one wants the experiment to be meaningful it is necessary to improve the statistics of the experiment, increase the resolution time of the system or increase the coherence length of the electronic packets.

Aiming at the solution to these experimental problems the experiment shown in Fig.5.16 was proposed by the author [J.R. Croca, *In Quest of de Broglie Waves*, in *Waves and Particles in Light and Matter*, eds. A. van der Merwe and A. Garuccio, Plenum Press, New York, 1994]

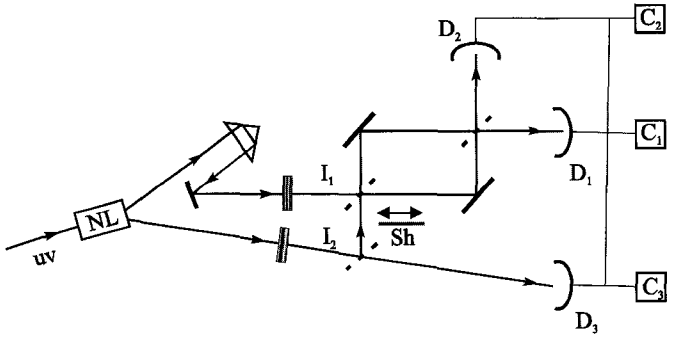

Fig.5.16 – Proposed modifications to improve the experiment done by Mandel.

In the proposed experiment, designed to improve the previous experiment done by Mandel, instead of the interferential filters we put two Fabri-Perot

Etalons with a bandwidth of about 10^{-9}s, so that the time duration of the wave packets could be of the same order of the electronic system resolving time. The fact of reducing the bandwidth of the light beams greatly diminishes the number of counts per unit time. Therefore it is necessary to devise more intense photon sources and improve the efficiency of the detectors.

The experiment, as can easily be seen, is no more than a variant of the one presented in Fig.5.10, devised precisely to take in account the problem of synchronization of the two sources. Here the role of the theta wave generator is played by the reduction detector D_3 and the electronic coincidence apparatus.

The experimental conditions must be set so that the intensity of the input beams I_1 and I_2 is equal, $I_1 = I_2$. The input port two can be blocked by placing the shutter in front of it. When the shutter is blocking the input port two all light that enters the interferometer comes from input port one. Since the interferometer was set precisely for the same conditions as the one represented in Fig.5.10, and described above, all light goes to detector D_1. When the shutter is removed then the theta waves beam feeds the interferometer modifying the counting statistics at the two output ports of the interferometer, in a way previously discussed, see section 5.4.4.1 – Experiment with correction for synchronization.

5.5 EXPERIMENTS BASED ON THE COMPLEX INTERACTION PROCESS OF THE CAUSAL QUANTUM PARTICLES

Another possibility to test the reality of quantum waves derives directly from the causal model for the quantum particle. In the causal approach of de Broglie, the quantum particle is composed of a carrying wave plus a singularity. These two real composing entities of the quantum particle have different properties when interacting with matter or with the surrounding subquantum medium resulting consequently in a complex overall interaction process.

Suppose that one has a finite wave devoid of singularity, a theta wave, hitting on a beamsplitter. Since we are dealing with a real physical localized field, part of it is reflected and part transmitted, the relative amount of reflection and transmission depending on the particular beamsplitter. In the

case of a perfect lossless 50% beamsplitter half of the wave shall be reflected and the other half transmitted.

Consider now that in front of the theta wave we place a succession of perfect lossless 50% beamsplitters as shown in Fig.5.17

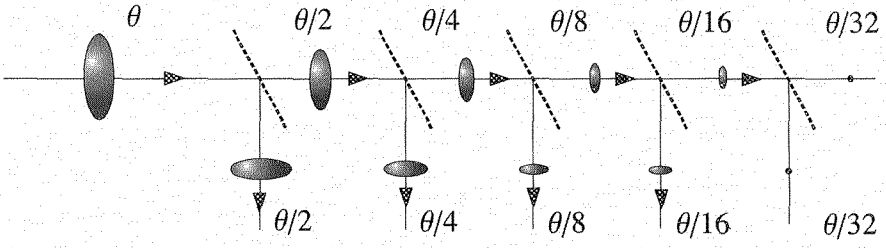

Fig.5.17 – The real theta wave progressively looses amplitude when crossing the successive beamsplitters until vanishing completely.

At each beamsplitter the transmitted real theta wave looses half of the amplitude. If the number of beamsplitters is large enough then at the end nothing of the incident wave remains.

This natural reduction of amplitude, due to the fact that the guiding wave is a real physical wave, can be represented by

$$\theta = t^n \theta_0 , \tag{5.5.1}$$

where n is the number of crossed beamsplitters, t the transmission coefficient, that in the represented case is equal to 1/2 and θ_0 the initial amplitude of the carrying wave. This expression can also be written in a more convenient form

$$\theta = \theta_0 e^{-\mu n} \tag{5.5.2}$$

where μ stands for the attenuation factor. These two factors are related by the expression

$$\mu = -\ln t . \tag{5.5.3}$$

It is natural to assume that this real guiding wave when crossing the so called "void" or "empty" space that as we know is not empty but is in reality full with the zero point field radiation, which was better and more meaningfully named by de Broglie as the subquantum medium, shall loose energy, that is, amplitude. In this case the expression (5.5.2) written for the attenuation with the beamsplitters remains essentially the same. The only modification one needs to make is to change the discrete variable n, the number of beamsplitters, by the continuous variable x standing for the path traveled by the theta wave in the free space,

$$\theta = \theta_0 \, e^{-\mu x} , \tag{5.5.4}$$

and evidently the attenuation factor μ is, accordingly, modified for the continuous subquantum medium.

For a full wave, a wave with a singularity things are rather different. Let us consider again the situation of the interaction with the beamsplitters but now with the full wave. Only the situation in which the singularity is transmitted is to be considered. The whole process shall run like this:

The wave strikes the first beamsplitter and the singularity is transmitted. Next it hits the second beamsplitter, and the singularity is again transmitted, and this process is repeated endlessly.

The question now is how can we describe this interacting process?

We know that, according to the causal model for the quantum particle, at each beamsplitter the singularity is either reflected or transmitted. The guiding wave instead is divided into two equal parts. In such circumstances if this interacting process keeps going on, after a certain number of beamsplitters the guiding wave will have completely disappeared mixed with the surrounding subquantum medium.

If we accept the last conclusion for the interacting process of the full wave then, after a sufficient number of beamsplitters, the guiding wave should have vanished completely. In such conditions we would have a pure singularity without the accompanying wave and consequently the most basic assumption of quantum physics of the duality of wave and particle would be completely broken.

To avoid this wreck and in order to preserve the dualism wave-particle contained in de Broglie's most basic statement that any quantum particle is composed of a wave and a singularity, it is necessary to assume another interacting process between the full wave and the beamsplitter.

Let us consider again the interacting process:

When the full wave interacts with the first, lossless, 50%, beamsplitter the transmitted amplitude of the wave is reduced to half and the singularity is transmitted. The transmitted singularity is guided by an accompanying wave with half the amplitude of the initial one. This process of halving the transmitted guiding wave keeps going on until a certain beamsplitter numbered $n = k$.

Had this process of halving the amplitude of the carrying wave kept going then only the singularity would remain. It is necessary to assume that from this point on this process of amplitude reduction is somehow compensated. Thus the guiding wave θ having reached the minimum level of energy, compatible with the existence of the duality wave and particle, starts regenerating itself at the expense of the singularity energy.

This point of minimum energy, compatible with the existence of the quantum particle, corresponds to the simplest fundamental state for the free particle. In this fundamental state of minimum possible energy the free theta wave has the minimum possible size. It is useful at this point to recall that the size of the guiding wave corresponds, in this context, to the region of space where it can manifest interferometric properties.

From this point on, the amplitude of the accompanying wave remains essentially constant, no matter the number of beamsplitters it crosses. The process goes on as long as the singularity has enough energy to keep feeding the accompanying wave.

$$\phi_{k-3} = \theta_{k-3} + \xi, \quad \phi_{k-2} = \theta_{k-2} + \xi, \quad \phi_{k-1} = \theta_{k-1} + \xi, \quad \phi_k = \theta_k + \xi, \quad \cdots$$
$$\cdots \quad \phi_{k+j} = \theta_k + \xi_j, \quad \phi_{k+j+1} = \theta_k + \xi_{j+1}, \quad \phi_{k+j+2} = \theta_k + \xi_{j+2},$$

This situation is illustrated in Fig.5.18

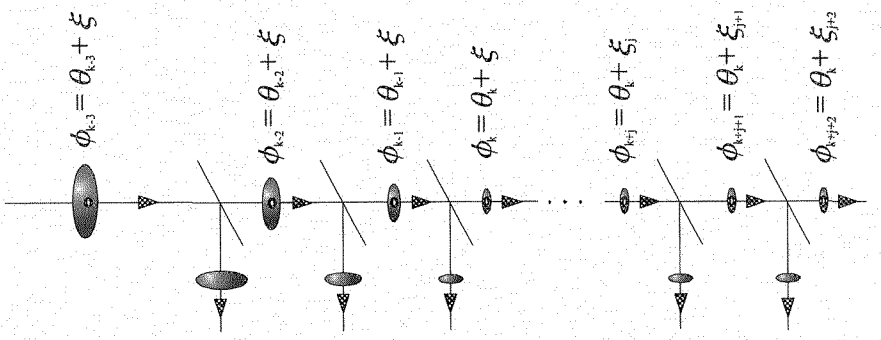
$\phi_{k-3} = \theta_{k-3} + \xi$
$\phi_{k-2} = \theta_{k-2} + \xi$
$\phi_{k-1} = \theta_{k-1} + \xi$
$\phi_k = \theta_k + \xi$
$\phi_{k+j} = \theta_k + \xi_j$
$\phi_{k+j+1} = \theta_k + \xi_{j+1}$
$\phi_{k+j+2} = \theta_k + \xi_{j+2}$

Fig.5.18 – The amplitude of the guiding wave keeps decreasing until a certain level. From this point on the amplitude of the accompanying wave remains essentially constant.

The decrease in amplitude of the accompanying wave can analytically be represented by the following relations,

$$\begin{cases} \theta = \theta_0 \, e^{-\mu n}, & n < k, \\ \theta = \theta_0 \, e^{-\mu n} = \theta_0 \, e^{-\mu k} = \text{const}, & n \geq k. \end{cases} \tag{5.5.5}$$

After having reached the minimum possible intensity, compatible with its existence, the amplitude of the guiding wave remains for all practical purposes constant. This level of minimum energy, for the accompanying wave, compatible with its very existence, corresponds to its most basic fundamental free state. Having attained this fundamental state it is possible to determine experimentally the extended size of the particle by changing the length of one of the interferometer arms until no interference is observed. From the experimentally known coherence length, that in this extreme fundamental case corresponds to the true free length of the particle, it would be easy to determine the value of the universal constant M. In the previous chapter we have seen that this constant relates the width of the extended part of the particle in the fundamental state with its wavelength by the expression $\sigma = M \lambda$.

In any case and for any quantum particle, in particular in the case of particles of light, after having crossed the necessary number of beamsplitters to reach the threshold, the energy of the photon singularity starts decreasing.

5.5.1 Experimental Test of the Tired Light Model of de Broglie for the Photon and its Implications on the Cosmological Expanding Model of the Big Bang for the Universe

The wave with the singularity as it crosses the successive beamsplitters after having reached the threshold level k maintains its energy practically constant thanks to the continuous feeding from the singularity. In such conditions from this point on the energy of the singularity starts decreasing. We know that this transfer of energy from the singularity to the accompanying wave is very small, nevertheless, if the number of beamsplitters is large enough the loss of energy can be of significance. On the other hand we know that the energy of the particle, which in this case means the energy of the singularity, is related to the frequency by the usual formula. Therefore, the very small progressive energy loss of the photon singularity, due to the feeding of the associated wave, needs to correspond to a correlated shift in the frequency. In plain English this means that light as it crosses the successive beamsplitters turns red.

If the interaction of the photon instead of being done at the beamsplitters was done with absorbers the final result would be precisely the same and the light would turn red. The same effect should occur when the light coming from the distant stars crosses the astronomical space. It is precisely because of this complex interacting mechanism of the light that de Broglie proposed his so-called tired light model to explain the observed cosmological redshift. The photon as it travels through space progressively looses energy so that its accompanying wave can survive.

We know that the same observed cosmological redshift is commonly interpreted as a consequence of the Doppler shift, implying that the heavenly bodies are running away from Earth. This is, as we know, the essence of the Big Bang model for the universe.

Still if one looks a little more carefully at the problem what do we have?

A very far heavenly source of light emits photons that travel for a very, very long time until some of them eventually reach the Earth. In this long route it happens that the photons turn to the red, the so-called redshift.

These are the observed facts.

The problem now is how to explain the observed facts in the framework of a physical theory.

If one accepts the Doppler explanation for the observed redshift then it implies that these very complex quantum entities we know under the name of photons can travel, throughout the subquantum medium, or as is usually named the zero point field, no matter how long the distance, without being disturbed. This is indeed a very strong assumption that lies at the very roots of the Big Bang model for the universe.

It seems much more reasonable to follow de Broglie, which asserts that the photons, just like any other quantum particle, are very complex entities that when traveling through the galactic space must have some kind of interaction with it.

Since it is possible to explain the observable experimental facts, the photons going to the red, without the Doppler effect, there is no logical necessity for assuming, as an inevitable, the Big Bang model. In reality it is possible to build a sound causal model where the observable redshift does not imply a whole expanding Universe.

Nevertheless even if it is possible to explain the cosmological redshift by the aging photon model of de Broglie, a practical, feasible, direct test of the model is not easy because the minimum necessary distance for the aging effect to be noticed is enormous.

Let us make a rough estimate of this distance assuming for simplicity that the cosmological redshift is due only to the complex interaction of the photon with the subquantum medium.

Recalling the previous characteristics of the photon in de Broglie's model, it is reasonable to write for the energy lost from the singularity to the accompanying wave an expression similar to the one for the loss in amplitude of the wave, that is

$$E = E_0 e^{-\alpha x}. \tag{5.5.6}$$

This formula expresses the small progressive loss of energy of the singularity, as it travels through cosmic space, due to the feeding of the accompanying wave in order to keep the minimum energy value for the guiding wave compatible with its very existence. The mean attenuating factor is represented by α and x is the distance traveled by the photon in cosmic space. Since $E = \hbar \nu$ we can also write

$$\nu = \nu_0 e^{-\alpha x}, \tag{5.5.7}$$

developing the exponential,

$$\nu = \nu_0 \left[1 - \alpha x + \tfrac{1}{2!}(\alpha x)^2 - \tfrac{1}{3!}(\alpha x)^3 + \cdots\right], \tag{5.5.8}$$

staying at the linear approximation and for $\alpha x << 1$ one gets

$$\nu \cong \nu_0 (1 - \alpha x) \tag{5.5.9}$$

or

$$\frac{\nu - \nu_0}{\nu_0} \cong -\alpha x,$$

that can be written

$$\frac{\Delta \nu}{\nu_0} \cong -\alpha x, \quad \Delta \nu = \nu - \nu_0, \tag{5.5.10}$$

or, recalling that

$$\lambda = c\nu^{-1} \quad \rightarrow \quad \Delta\lambda = (-1)c\nu^{-2}\Delta\nu$$

one can make

$$\frac{\Delta\lambda}{\lambda_0} \cong \alpha x, \tag{5.5.11}$$

where, as usual, λ represents the wavelength of the light. The fractional increase in the wavelength of the photon equivalent to the corresponding decrease in the frequency responsible for the redshift, can be expressed following Gosh, in such way that

$$\alpha \cong \frac{k}{c} \tag{5.5.12}$$

with k being the Hubble constant, which has an estimate value of about $k = 1.6 \times 10^{-18} s^{-1}$.
Substitution of the respective values of the constants into (5.5.12) gives for the approximate value of the damping parameter $\alpha \approx 10^{-26}$. Replacing the value of the attenuating parameter into (5.5.7) one gets

$$\nu = \nu_0 e^{-10^{-26} x}. \tag{5.5.13}$$

From this approximate expression it is possible to estimate the traveling distance through "empty space" necessary for a relative decrease of 10^{-5} in frequency, that is $\Delta\nu/\nu_0 \approx 10^{-5}$. The results of the calculations say that even for this small change in the frequency of light, one gets for the distance the photon needs to travel, a value of $x \approx 10^{21}$ m, which corresponds to about the diameter of our Galaxy.

These figures imply that even for this minute change in the relative frequency, and assuming that the cosmological redshift is only due to the aging of the photon, the distance light has to travel needs to be of galactic scale.

To test this complex mechanism of interaction of the photon as it travels in free space Jeffers and collaborators did an experiment. The aim of the performed experiment was to measure the eventual reduction in amplitude of the wave devoid of singularity as it travels in "empty space". Nevertheless, due to the fact that their experimental setup did not meet the basic requirements needed to the results to have any physical meaning the experiment was inconclusive.

We know that one of the most basic requirements for all this kind of experiments to be meaningful is that the sources employed must be single particle sources. This necessity arises, as we have seen, because of the collapse or non-collapse of the wave packet in a quantum measurement process. Jeffers and his group instead of using a monoparticle photon source employed a laser source. The development of single photon sources as is well known was very difficult. Building a single photon source able to deliver one photon at a time is not a trivial task. It is not by reducing the intensity of a common laser source by means of absorbers that it is possible to develop a monophotonic source. It is known, that even at very low laser beam intensities the probability of having only one single photon at a time is extremely small due to the bunching effect.

The second requirement the performed experiment failed to met is not one of basic nature it is a simple problem of scale. It is related with the minimum necessary distance for the effect to be noticeable. The free course the photon needs to travel must have a minimum value. If this minimum value is not attained no decrease in amplitude of the theta wave can be perceived. The path traveled by the photon in the experiment done by Jeffers was 258.1 cm, about two meters and half. From the previous calculation one can see that this figure looks indeed very small. Even in the case of an optical path of the kilometric order, the attenuation in the amplitude of the accompanying wave would hardly have been noticed.

These facts suggest the necessity of designing a practical, feasible experiment that although possible to run at the scale of a laboratory could also be able to perceive this very minute effect. Indeed an experiment of this type seems possible.

In this experiment instead of the subquantum medium as the natural interacting agent one uses beamsplitters or other similar absorbers to reduce in a significant way the amplitude of the accompanying wave.

For this case it is possible to rely on the developed complex interacting process of de Broglie particles and on the formulas previously obtained.

In such case and assuming for a transmission factor a value of 1% in each interacting device and according to formula (5.5.1) for only ten equal beamsplitters, the amplitude of the transmitted wave would be reduced by a factor of about 10^{-20}.

It is reasonable to expect that for such significative overall attenuation factor the threshold level k could be achieved. These facts imply that the size of the experimental apparatus could be made small enough so that it could be placed in a laboratory, not necessarily very large.

The concrete experiment shown in Fig.5.19 uses a modified Mach-Zehnder interferometer.

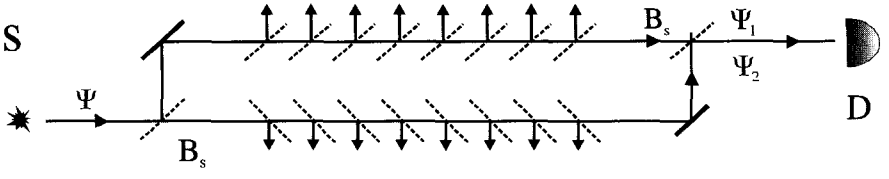

Fig.5.19 – Laboratory-scale experiment to study the complex interacting behavior of de Broglie waves.

In each arm of the interferometer is placed an equal number of similar beamsplitters, as shown in Fig.5.19. From the picture we see that the monophotonic source S emits photons one at a time that enter the input port of the Mach-Zehnder interferometer. In the two independent arms of the interferometer it was placed an equal number of similar beamsplitters so that the full amount of amplitude reduction is the same in each arm.

The prediction for the results of this experiment depends on the model we adopt:

(a) Orthodox approach:

For this experiment the Copenhagen orthodox approach predicts for the intensity seen at the detector

$$I_o = |\psi_1 + \psi_2|^2, \tag{5.5.14}$$

with

$$\psi_1 = rt\,A\psi, \quad \psi_2 = tr\,A\psi e^{i\delta}, \tag{5.5.15}$$

where r and t are respectively the reflection and transmission factors of the Mach-Zehnder interferometer beamsplitters B_s, and $A = e^{-\mu n}$ stands for the overall absorbing factor due to the presence of the attenuating beamsplitters placed in the arms of the interferometer. The relative phase difference of the two overlapping waves is, as usual, represented by δ.

Taking in consideration (5.5.15) and developing (5.5.14)

$$I_o = |rt\,A\psi + tr\,A\psi e^{i\delta}|^2 = (rt\,A)^2\,|\psi|^2\,(1+e^{i\delta})(1+e^{-i\delta}),$$

or

$$I_0 = (rt\,A)^2\,|\psi|^2\,(1+\cos\delta), \tag{5.5.16}$$

that is the usual formula,

$$I_o \propto 1+\cos\delta. \tag{5.5.17}$$

This final orthodox formula is perfectly understandable because the two probability waves ψ undergo precisely the same attenuation along the arms of the interferometer. Therefore the predicted visibility in this approach for this experiment is one, $V_o = 1$ not depending, in any way, on the overall attenuation factor.

(b) Causal approach:

The causal approach, due to the complex interaction mechanism of the quantum particles with the interacting devices, predicts quite different results.

For the sake of clarity these predictions can be divided into two parts:

$$I_c = I_c^1 + I_c^2 . \tag{5.5.18}$$

The first part is related with the fact that before attaining the threshold the accompanying wave undergoes the same attenuation in both arms of the interferometer. So in this region the predictions of both approaches are the same. This situation is expressed by the expression (5.5.2) which is valid as long as the threshold k is not attained and reads

$$I_c^1 = |\, \theta_1^1 + \theta_2^1 \,|^2 , \tag{5.5.19}$$

with

$$\theta_1^1 = \theta_0 e^{-\mu n}, \quad \theta_2^1 = \theta_0 e^{-\mu n} e^{i\delta} \tag{5.5.20}$$

which by substitution in the previous expression gives

$$I_c^1 \propto 1 + \cos\delta .$$

equal to the expression (5.5.17) obtained for the orthodox approach,

$$V_c^1 = V_o = 1 .$$

The second part is quite different from the orthodox approach and corresponds to the situation beyond the threshold k. After this point the predictions are given, recalling (5.5.5)

$$\begin{cases} \theta = \theta_0 e^{-\mu n}, & n < k, \\ \theta = \theta_0 e^{-\mu n} = \theta_0 e^{-\mu k} = \text{const}, & n \geq k. \end{cases} \tag{5.5.21}$$

and taking into consideration the cases in which the singularity goes along path two, we have for the expected intensity

$$I_c^2 = |\theta_1^2 + \theta_2^2|^2 , \tag{5.5.22}$$

with

$$\theta_1^2 = \theta_0 e^{-\mu n}, \quad \theta_2^2 = \theta_0 e^{-\mu k} e^{i\delta} \tag{5.5.23}$$

therefore by substitution in (5.5.22) we get

$$I_c^2 = |\theta_0 e^{-\mu n} + \theta_0 e^{-\mu k} e^{i\delta}|^2 , \tag{5.5.24}$$

which gives

$$\begin{aligned} I_c^2 &= |\theta_0|^2 (e^{-\mu n} + e^{-\mu k} e^{i\delta})(e^{-\mu n} + e^{-\mu k} e^{-i\delta}), \\ &= |\theta_0|^2 (e^{-2\mu n} + e^{-2\mu k} + e^{-\mu(n+k)} e^{-i\delta} + e^{-\mu(n+k)} e^{+i\delta}), \\ &= |\theta_0|^2 (e^{-2\mu n} + e^{-2\mu k} + e^{-\mu(n+k)} (e^{-i\delta} + e^{+i\delta})), \\ &= |\theta_0|^2 (e^{-2\mu n} + e^{-2\mu k} + 2e^{-\mu(n+k)} \cos\delta), \\ &= |\theta_0|^2 (e^{-2\mu n} + e^{-2\mu k})(1 + 2\frac{e^{-\mu(n+k)}}{e^{-2\mu n} + e^{-2\mu k}} \cos\delta), \\ &= |\theta_0|^2 (e^{-2\mu n} + e^{-2\mu k})(1 + 2\frac{1}{e^{-\mu(n-k)} + e^{\mu(n-k)}} \cos\delta), \end{aligned}$$

or more simply

$$I_c^2 = |\theta_0|^2 (e^{-2\mu n} + e^{-2\mu k})(1 - V_c^2 \cos\delta), \qquad (5.5.25)$$

with the expected causal visibility V_c^2 given by

$$V_c^2 = \operatorname{sech}\mu(n-k), \quad n \geq k. \qquad (5.5.26)$$

When the singularity arriving at the detector comes from the other arm of the interferometer the predictions are precisely the same.

The results of the previous calculations are shown in Fig.5.20.

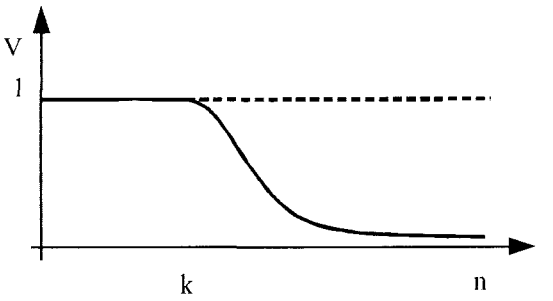

Fig.5.20 – Expected visibility for the experiment: Dashed line - usual orthodox model; Continuous line - causal model.

The plot shows the predictions for the proposed experiment. The orthodox approach predicts always the same visibility $V_o = 1$, no matter the actual length of the interferometer arms. According to the causal model the predictions are the same in the first region, with $V_c^1 = V_o = 1$. In the second zone, which starts after the level k, the expected visibility is quite different. The visibility starts decreasing until no interference is to be seen, while the orthodox approach predicts always a visibility of one.

Naturally, in order to perform the concrete real experiment some practical precautions must be taken. The reader interested in these developments should look at the works indicated in the bibliography.

5.6 REFERENCES

On monophotonic sources:

M. Dagenais and L. Mandel, Phys. Rev. A 18(1978)2217.
S. Friber, C. Hong and L. Mandel, Phys. Rev. Lett. 1(1985)2011.
P. Grangier, G. Roger and A. Aspect, Europhys. Lett. A 90(1986)173.

Some works related with experiments to test the nature of quantum waves based on the collapse of the wave function:

J. and M. Andrade e Silva, C.R. Acad. Sci. (Paris) 290(1980)501.
F. Selleri, Ann. Found. L. de Broglie, 4(1982)45.
F. Selleri, Found. Phys. 12 (1983) 1087; 17(1987)739.
A. Garuccio, V. Rapizarda and J.P. Vigier, Phys. Lett. A 90(1982)17.
J.R.Croca, in *Microphysical Reality and Quantum Formalism*, eds. A. Van der Merwe, F. Selleri, G. Tarozzi, Kluwer, Dordrecht, 1988.
J.R.Croca, Ann. Found. L. de Broglie, 14(1989)323.
J.R. Croca, *in Waves and Particles in Light and Matter*, Ed. Alwyn van der Merwe and A. Garuccio, Plenum, 1994.
J.R.Croca, A. Garuccio, V. Lepori e R.N. Moreira, Found. Phys. Lett. 3(1990)557.
R.J. Glauber, Phys. Rev. 30(1963)2529; 131(1963)2766.

Experiment based on the properties of real waves:

J.R. Croca, M. Ferrero, A. Garuccio, V.L. Lepore, Found. Phys. Letters, 10(1997)441.
J.R. Croca, Apeiron, 4(1997)41
L. de Broglie, Cahiers de Physique, **16**, 147, 429 1962; Acad. Sci. Paris, **263 B**, 9, 589, 1966.
A. Gosh, Apeiron, 9-10(1991)35.

Performed experiments and connected works:

X.Y. Zou, T. Grayson and L. Mandel, Phys. Rev. Lett. 24(1992)3667.
S. Jeffers and J. Sloan, Found. Phys. Lett. 333(1994)341.

X.Y. Zou, L.J. Wang, and L. Mandel, Phys. Rev. Lett. 67(1991)318.
F. Selleri, in *Wave Particle Duality*, ed by F. Selleri, Plenum Press, New York, 1992.

On interference with independent sources:

P.A.M. Dirac, *The principles of Quantum Mechanics*, Clarendon Press, Oxford, 1930.
R.L. Plfeegor and L. Mandel, Phys. Rev. 159(1967)1084.
W. Radloff, Ann. Phys. (Leipzig) 26(1971)178.
Z.Y. Ou and L. Mandel, Phys. Rev. Lett. 62(1989)2941.
H. Paul, Rev. Mod. Physics, 58(1986)209.

This page is intentionally left blank

CHAPTER 6

INTERFERENCE WITHOUT SUPERPOSITION OF THE WAVE PACKETS

6.1 INTRODUCTION

Lately some authors have presented, in the scientific literature, what they call weird situations where the "Magic" of quantum mechanics is put in evidence. Among these so-called strange situations we refer quantum teleportation, quantum interaction-free measurements and interference without actual spatial superposition of the wave packets. This later unexpected nonlocal interference implies, according to those authors, retroaction in time. It is a very strange situation that we are now facing in science. Most of these so-called scientific works look more like bad science fiction. At least in the good works of science fiction the purpose of the authors is in general clearly stated and developed. More important is the fact that these authors do not pretend to be making science where the logical rigor and the clarity of the ideas are of supreme importance. Nowadays the more confusing a "scientific" work can be the better. The necessity of clearly explaining the basic underlying assumptions and of following a straight rigorous line of reasoning and the search of the truth seems of no concern to most of them. Things that are essentially relatively easy are presented in such a confusing and bewildering way that any open-minded reader not working in the field is completely lost in the meaningless rhetoric. Yet what is more surprising in this unhappy general trend is that most of these authors are not even preoccupied with the rigor and clarity of the underlying ideas. On the contrary, it seems that the very aim of such researchers is the confusion and mystification of the ideas. One would say that to pretend or to look like has become more fashionable than to be. Take for instance the interaction free measurement presented some time ago in the scientific journals with fanfare, see Kwiat, Zeilinger et. al., as a great new discovery.

Nevertheless if we look back in scientific literature we see that this problem had been discussed exhaustively, as we have seen in chapter 2, by Renninger and other authors. The comprehension of such interaction free measurement has led to an improvement of the conceptual formalization of orthodox quantum mechanics.

In this chapter we will limit ourselves to the presentation of what is called in the orthodox approach the nonlocal interference. We shall show that this "Magic" interference without "physical" superposition of the wave packets can be perfectly understood in terms of a causal intuitive process without recourse to strange weird explanations like retroaction in time.

6.2 INTERFEROMETRIC EXPERIMENTS WITHOUT OVERLAPPING OF THE WAVEPACKETS

Earlier, we have seen that in order to observe interference it was mandatory that the wave packets fully or partially superimposed at the mixing region of the interferometer. For the case of two coherent waves if the overlapping was complete the visibility would be one hundred percent, as can be seen in Fig.6.1.

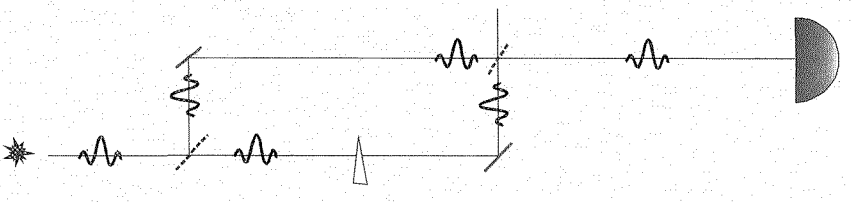

Fig.6.1 – Interference with complete overlapping of the wave packets giving 100% visibility.

When the optical path difference between the two beams is greater than the coherence length, which led to no overlapping of the two coherent wave packets, no interference is observed.

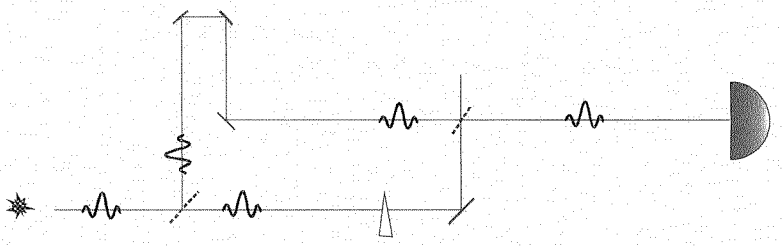

Fig.6.2 – No interference is observed because the difference of the optical path between the two beams is greater that the size of the wave packets.

In Fig. 6.2 is shown an asymmetric Mach-Zehnder interferometer with the upper arm length greater than the lower one. The difference between the two optical paths is such that it never happens that the two coherent wave packets overlap at the mixing beamsplitter. In this case since the coherent wave packets never superimpose there should not be any observable interference.

Consider that next we place a monochromator in front of the source. In practice this monochromator can assume diverse particular forms depending on the quantum particle in question. For photons the form of such monochromator can be from the simple prism, the diffraction grating, to the complex Fabri-Perot etalon. For neutrons this analysing device is made in general of a slab of silicon crystal. In any case the action of the monochromator is to increase the coherence length of the initial packet so that the two packets originated at the first beamsplitter now overlap partially at the mixing region. This mixing region, in this particular set up, corresponds to the second beamsplitter where the two wavepackets physically overlap partially. This situation is shown in Fig. 6.3.

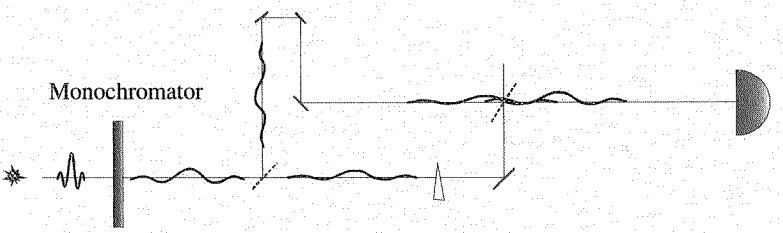

Fig.6.3 – In front of the monoparticle source a monochromator is placed to increase the coherence length of the initial packet so that now the two wave packets overlap partially at the mixing region.

In this new situation since there is superposition of the wave packets, coming from the two different arms of the interferometer, there is to be expected an interference pattern. The visibility of the interference depends, of course, on the degree of overlapping of the two wavepackets.

Till this point there are no problems. Everybody agrees with the above explanation. The problem arises when instead of placing the monochromator in front of the source and before the interferometer we place it after the interferometer, after the mixing region, before the detector as shown in Fig.6.4

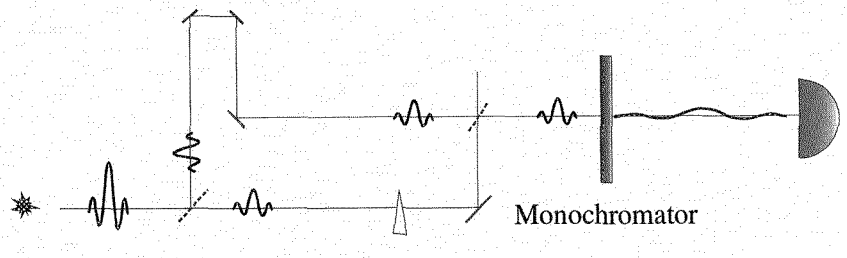

Fig.6.4 – Asymmetric Mach-Zehnder interferometer with a monochromator placed after the interferometer so that the two wave packets do not physically overlap.

In this case, as is easily seen from the picture, there is no physical superposition of the wave packets at the mixing region.

The question now is the following: For this particular experimental setup what are the predictions for the distribution of the arriving particles at the detector?

Experiments done with neutrons and photons have shown, without any margin of doubt, that the distribution of arriving particles at the detector follows in fact an interferometric pattern. That is, we do observe interference even if the wave packets do not physically overlap!

A sketch of one experiment of this type with neutrons, performed by Rauch and is group at Vienna, is shown in Fig.6.5

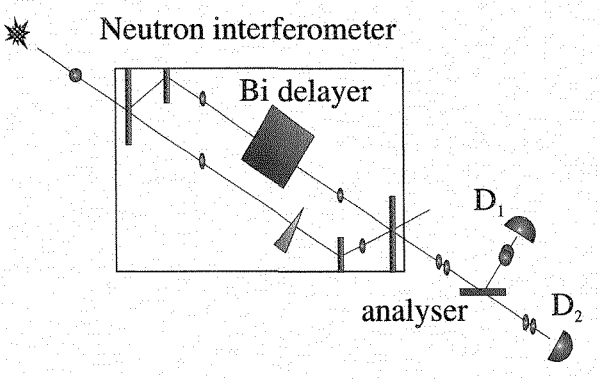

Fig.6.5 – Rauch's experiment for nonlocal neutron interferometry.

From the picture we see that at the detector D_2, arrive the neutrons with the initial coherence length that due to the delay introduced by bismuth slab Bi do not overlap at the second beamsplitter. Therefore no interference, that is no dependence on phase shift, is to be expected at this detector. The neutrons that arrive at the detector D_1 have been analysed at the crystal, which increases the coherence length of the neutron wave packets so that they now partially overlap. Even though the crystal analyser is placed after the neutron interferometer, after the region of superposition of the packets, nonetheless interference is observed.

The problem now is how to explain the observed interference of the wave packets in this very strange situation. It seems like "magic", somehow there is observable interference even without physical superposition of the two wave packets.

6.3 ORTHODOX INTERPRETATION

In orthodox quantum mechanics the experimentally observed interference causes intrinsically no problem. Since in this non-causal approach time and space play no significative role it is not contradictory to say that by placing the monochromator behind the interferometer a certain time later one makes a concrete action on the past. This particular action in the past leads to the appearance of the interference pattern. The orthodox explanation for these results would run like this:

1 – The initial small wave packet emitted by the monoparticle source interacts with the first beamsplitter and is divided into two: one reflected the other transmitted. These two wavepackets follow independent paths. The upper path is much longer than the lower. So the transmitted wave packet, following the lower path, arrives first at the second beamsplitter. The other wave packet, the reflected one, having to follow a longer path arrives at the beamsplitter at a much later time. In these circumstances they are never able to joint at the mixing beamsplitter. In this situation no interferences are to be expected.

2 – Suppose now that a monochromator is placed after the second beamsplitter. Then the "true" action of the analysing monochromator is such that everything happens as if instead of being placed after the second beamsplitter at a certain present time t_1 it had in fact be placed before the first beamsplitter backwards in time, at time t_2, with $t_2 < t_1$, so that the wave packets could later mix, interact at the second beamsplitter. Nevertheless we know for sure that the monochromator was never actually placed before the first beamsplitter. In these circumstances everything happens as if an action done at the actual present time t_1 had really an effect somewhere at time t_2, in the past.

The conclusion to infer from this type of experiments is that interferences can occur when two or more wave packets overlap either in the present, as is common, or through an action from the present into the past. Believing in this scenario, again we have a proof that with orthodox quantum mechanics man has indeed attained a higher level of consciousness acquiring one of God attributes that of omnipresence. In these circumstances the homo quanticus is consequently able to transcend the old barriers of space and time.

Let us now look at the orthodox calculations leading to the appearance of the observable interference pattern. Naturally these calculations, implying a retroaction in time are, as we shall see, a direct consequence of the nonlocal and nontemporal Fourier analysis. The reader more interested in the epistemological implications of quantum mechanics can skip the calculations confirming the previous statement without great loss.

In order to perform the calculations we assume that a source emits photons that enter an asymmetric Mach-Zehnder interferometer. These photons in the orthodox approach are built from the infinite sum of harmonic plane waves

$$\psi_0 = \int_{-\infty}^{+\infty} g(k') e^{ik'(x-ct)} dk' \tag{6.3.1}$$

that for a gaussian wave number distribution gives

$$\psi_0 = A' \int_{-\infty}^{+\infty} e^{-\frac{(k'-k)^2}{2\sigma_{Sk}^2}} e^{ik'(x-ct)} dk' \tag{6.3.2}$$

which by integration gives

$$\psi_0 = A_0 e^{-\frac{(x-ct)^2}{2\sigma_x^2}} e^{i(kx-\omega t)} \tag{6.3.3}$$

with

$$A_0 = \sqrt{2\pi} A' \sigma_{Sk} \tag{6.3.4}$$

This wave packet upon interaction with the first beamsplitter is divided into two. The reflected packet, the one that follows the longer path, upon arriving at the detector region can be written in the form

$$\psi_1 = rt\psi_0(x - c(t - \Delta t)) e^{i\pi/2} \tag{6.3.5}$$

with r and t standing for the reflected and transmitted coefficients at the first and the second beamsplitters respectively. This formula can also be written

$$\psi_1 = rt\psi_0(x - ct + \xi) e^{i\pi/2} \tag{6.3.6}$$

where we have made the larger optical path difference

$$c\Delta t = \xi \tag{6.3.7}$$

or explicitly

$$\psi_1 = rt\,A_0 e^{-\frac{(x-ct+\xi)^2}{2\sigma_x^2}} e^{i(kx-\omega t+k\xi)} e^{i\pi/2}. \tag{6.3.8}$$

The wave packet transmitted at the first beamsplitter follows the shorter path and can be written

$$\psi_2 = tr\psi_0(x-ct)e^{i\phi}e^{i\pi/2} \tag{6.3.9}$$

or

$$\psi_2 = tr\,A_0 e^{-\frac{(x-ct)^2}{2\sigma_x^2}} e^{i(kx-\omega t)} e^{i\phi} e^{i\pi/2}. \tag{6.3.10}$$

with ϕ representing the small phase change due to the phase shifting device.

For the sake of clarity these wave packets are indicated in the sketch of the experiment Fig.6.6

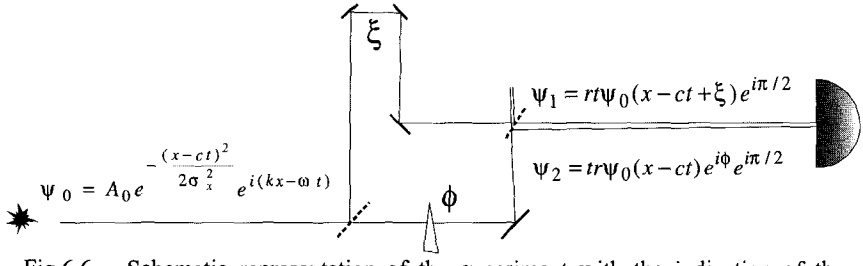

Fig.6.6 – Schematic representation of the experiment with the indication of the respective wave packets.

The output waves can also be written

$$\psi_1 = Ae^{-\frac{(x-ct+\xi)^2}{2\sigma_x^2}} e^{i(kx-\omega t)} e^{i(k\xi+\pi/2)} \tag{6.3.11}$$

and

$$\psi_2 = Ae^{-\frac{(x-ct)^2}{2\sigma_x^2}} e^{i(kx-\omega t)} e^{i(\phi+\pi/2)} \tag{6.3.12}$$

with

$$A = rtA_0 \tag{6.3.13}$$

In these conditions the output total transmitted wave is given by the sum of the two waves

$$\psi = \psi_1 + \psi_2 \tag{6.3.14}$$

and the intensity seen by the detector is the temporal average of the squared modulus of the total wave

$$I = \langle |\psi|^2 \rangle = \langle |\psi_1 + \psi_2|^2 \rangle \tag{6.3.15}$$

which by development gives

$$I = \langle |\psi_1|^2 \rangle + \langle |\psi_2|^2 \rangle + \langle \psi_1 \psi_2^* \rangle + \langle \psi_1^* \psi_2 \rangle . \tag{6.3.16}$$

Recalling the previous expressions one is allowed to write

$$|\psi_1|^2 = A^2 e^{-\frac{(x-ct+\xi)^2}{\sigma_x^2}} , \tag{6.3.17}$$

and equally

$$|\psi_2|^2 = A^2 e^{-\frac{(x-ct)^2}{\sigma_x^2}} . \tag{6.3.18}$$

The temporal average of the first wave is,

$$\langle |\psi_1|^2 \rangle = A^2 \int_{-\infty}^{+\infty} |\psi_1(t)|^2 \, dt \,, \tag{6.3.19}$$

the substitution gives

$$\langle |\psi_1|^2 \rangle = A^2 \int_{-\infty}^{+\infty} e^{-\frac{(x-ct+\xi)^2}{\sigma_x^2}} \, dt \,, \tag{6.3.20}$$

which upon integration leads to

$$\langle |\psi_1|^2 \rangle = \frac{1}{4} I_0 \,, \tag{6.3.21}$$

with

$$I_0 = 4\sqrt{\pi} A^2 \sigma_x / c \,. \tag{6.3.22}$$

For the same reason the independent contribution of the second wave is the same

$$\langle |\psi_2|^2 \rangle = \frac{1}{4} I_0 \,. \tag{6.3.23}$$

The first cross term is

$$\psi_1 \psi_2^* = A^2 e^{-\frac{(x-ct+\xi)^2 + (x-ct)^2}{2\sigma_x^2}} e^{i(k\xi - \phi)} \tag{6.3.24}$$

and the temporal mean value

$$\langle \psi_1 \psi_2^* \rangle = A^2 \int_{-\infty}^{+\infty} e^{-\frac{(x-ct+\xi)^2 + (x-ct)^2}{2\sigma_x^2}} e^{i\delta} \, dt \,, \tag{6.3.25}$$

or developing

$$\langle \psi_1 \psi_2^* \rangle = A^2 e^{i\delta} \int_{-\infty}^{+\infty} e^{-\frac{1}{2\sigma_x^2}\left[(x+\xi)^2 - 2(x+\xi)ct + c^2t^2 + x^2 - 2ctx + c^2t^2\right]} dt ,$$

$$\langle \psi_1 \psi_2^* \rangle = A^2 e^{i\delta} e^{-\frac{(x+\xi)^2 + x^2}{2\sigma_x^2}} \int_{-\infty}^{+\infty} e^{-\frac{c^2}{\sigma_x^2}t^2 + (2x+\xi)\frac{c}{\sigma_x^2}t} dt ,$$

which, by direct integration conduces to

$$\langle \psi_1 \psi_2^* \rangle = A^2 e^{i\delta} e^{-\frac{(x+\xi)^2 + x^2}{2\sigma_x^2}} \sqrt{\pi}\, \frac{\sigma_x}{c}\, e^{\frac{\left[(2x+\xi)c/\sigma_x^2\right]^2}{4c^2/\sigma_x^2}} ,$$

or, after rearranging the terms

$$\langle \psi_1 \psi_2^* \rangle = \frac{1}{4} I_0\, e^{-\frac{\xi^2}{4\sigma_x^2}}\, e^{i\delta} . \tag{6.3.26}$$

The second cross term is the conjugated of the last

$$\langle \psi_1^* \psi_2 \rangle = \frac{1}{4} I_0\, e^{-\frac{\xi^2}{4\sigma_x^2}}\, e^{-i\delta} . \tag{6.3.27}$$

In such conditions taking advantage of the above results the expected intensity at the detector can be written

$$I = \frac{1}{4} I_0 + \frac{1}{4} I_0 + \frac{1}{4} I_0\, e^{-\frac{\xi^2}{4\sigma_x^2}} \left(e^{i\delta} + e^{-i\delta} \right)$$

that finally gives

$$I = \frac{1}{2} I_0 (1 + e^{-\frac{\xi^2}{4\sigma_x^2}} \cos\delta), \tag{6.3.28}$$

with a visibility depending on the large optical path deviation

$$V = e^{-\frac{\xi^2}{4\sigma_x^2}}. \tag{6.3.29}$$

The plot of the visibility as function of the large optical path delay in σ_x units is shown in next figure, Fig.6.7

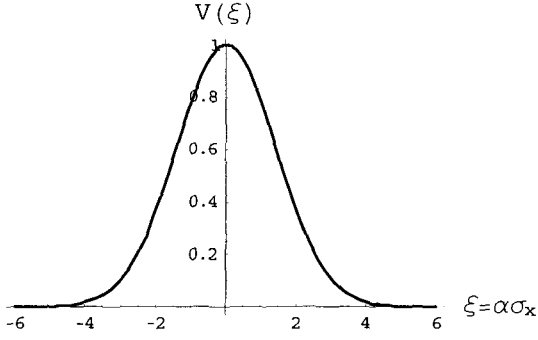

Fig.6.7 – Plot for the expected visibility as function of the optical path delay in units of the coherence length of the incident wave packet σ_x.

As can be seen from the picture, when the optical path difference is greater than five coherence lengths of the incident wave packet, no interference is to be expected. Since in the experiment the optical path difference was chosen to be much longer than the coherence length of the incident wave packets visibility zero is predicted, that is, no interference is to be expected. These theoretical predictions are, of course, well confirmed by the experiments.

Let us now see what happens when an interferential filter is placed after the interferometer precisely before the detector as shown in Fig.6.4. The practical action of this optical filter is to reduce the bandwidth of the incident wave packets increasing concomitantly the coherence length of the exit wave

packets in such a way that now this length is larger than the optical path difference.

There are diverse mathematically equivalent ways for describing the action of the filter on the incident beam as can be seen in the literature. The most common corresponds to applying the filter to each single harmonic plane wave with a well-defined frequency and then averaging over the entire spectrum of the source. This mathematical trick of building the wave packet after the monochromator, after the mixing region of space means that since the monochromatic harmonic plane waves are infinite in space they had indeed interfered, that is, superimposed at the second beamsplitter, no matter how long the optical path difference could be. In these circumstances it is no surprise that the interference could be recovered.

Accordingly, this action of the filter on single monochromatic harmonic plane waves is described by the transfer function

$$\psi_{F1} = T\psi_1, \quad \psi_{F2} = T\psi_2 \tag{6.3.30}$$

so that the wave coming out from the monochromator is the product of the incident wave by the transfer function. This transfer function is in general approached by a gaussian

$$T = e^{-\frac{(k-k_0)^2}{2\sigma_{Fk}^2}} \tag{6.3.31}$$

where σ_{Fk} is the bandwidth of the monochromator interference filter. Under these conditions the total wave beyond the monochromator is

$$\psi_F = \psi_{F1} + \psi_{F2} = T\psi_1 + T\psi_2 = T(\psi_1 + \psi_2) = T\psi, \tag{6.3.32}$$

therefore the intensity of a single incident harmonic plane wave seen by the detector after the interference filter comes

$$I_F = \langle |\psi_F|^2 \rangle = \langle |T\psi|^2 \rangle = T^2 \langle |\psi|^2 \rangle = T^2 I \tag{6.3.33}$$

because the transmission function does not depend on time.

The expression for the intensity, after the interferometer without filter, for an incident harmonic plane wave has the habitual form

$$I = \frac{1}{2} I_0 (1 + \cos\delta) .$$

This expression could also be simply inferred from the output intensity for the case of an incident wave packet

$$I = \frac{1}{2} I_0 (1 + e^{-\frac{\xi^2}{4\sigma_x^2}} \cos\delta) ,$$

when the width $\sigma_x \to \infty$ goes to infinity. Obviously, this case, according to the usual Heisenberg's relations, leads to a single harmonic plane wave. In such case we can write for the output beam after crossing the monochromator

$$I_F = \frac{1}{2} I_0 e^{-\frac{(k-k_0)^2}{\sigma_{Fk}^2}} (1 + \cos\delta) , \qquad (6.3.34)$$

or, remembering that the relative phase deviation is also a function of the spatial frequency

$$\delta = k\xi - \phi ,$$

expression (6.3.34) may be written in the explicit form

$$I_F = \frac{1}{2} I_0 e^{-\frac{(k-k_0)^2}{\sigma_{Fk}^2}} (1 + \cos(k\xi - \phi)) . \qquad (6.3.35)$$

From this expression we see that the intensity after the monochromator depends on the bandwidth on the central frequency k_0 chosen for the filter

In this conditions in order to obtain a final formula for the output intensity beam after the interference filter it is necessary to average over the power spectrum of the source

$$S(k) = \frac{A_0}{\sqrt{\pi}\sigma_{Sk}} e^{-\frac{(k-k_0)^2}{\sigma_{Sk}^2}} \tag{6.3.36}$$

that was chosen to be centred, like the monochromator, in k_0. Therefore the mean intensity seen by the detector can be expressed by

$$\bar{I}_F = \int_{-\infty}^{+\infty} S(k) I_F(k)\, dk\,. \tag{6.3.37}$$

Substituting the respective values of the functions into (6.3.37) we get

$$\bar{I}_F = \frac{A_0 I_0}{2\sqrt{\pi}\sigma_{Sk}} \int_{-\infty}^{+\infty} e^{-\frac{(k-k_0)^2}{\sigma_{Sk}^2}} e^{-\frac{(k-k_0)^2}{\sigma_{Fk}^2}} (1+\cos(k\xi-\phi))\, dk \tag{6.3.38}$$

or

$$\bar{I}_F = \frac{A_0 I_0}{2\sqrt{\pi}\sigma_{Sk}} \int_{-\infty}^{+\infty} e^{-\frac{(k-k_0)^2}{\sigma_{Tk}^2}} (1+\cos(k\xi-\phi))\, dk \tag{6.3.39}$$

where we have made

$$\sigma_{Tk}^2 = \frac{\sigma_{Sk}^2 \sigma_{Fk}^2}{\sigma_{Sk}^2 + \sigma_{Fk}^2}\,. \tag{6.3.40}$$

Developing (6.3.39) we have

$$\bar{I}_F = \frac{A_0 I_0}{2\sqrt{\pi}\sigma_{Sk}} (\sqrt{\pi}\sigma_{Tk} + \int_{-\infty}^{+\infty} e^{-\frac{y^2}{\sigma_{Tk}^2}} \cos((y-k_0)\xi - \phi)\, dy), \qquad (6.3.41)$$

with

$$y = k - k_0 \qquad (6.3.42)$$

which by integration gives

$$\bar{I}_F = \frac{A_0 I_0}{2\sqrt{\pi}\sigma_{Sk}} \left[\sqrt{\pi}\sigma_{Tk} + \sqrt{\pi}\sigma_{Tk}\, e^{-\frac{\xi^2}{4/\sigma_{Tk}^2}} \cos(k_0\xi - \phi) \right], \qquad (6.3.43)$$

or, by simplification

$$\bar{I}_F = A_F (1 + e^{-\frac{\xi^2}{4\sigma_{Tx}^2}} \cos\delta'), \qquad (6.3.44)$$

where

$$A_F = \frac{\sigma_{Tk} A_0 I_0}{2\sqrt{\pi}\sigma_{Sk}}, \quad \delta' = k_0\xi - \phi \qquad (6.3.45)$$

and we made, as habitual, in the Fourier nonlocal formalism

$$\sigma_{Tx} = \frac{1}{\sigma_{Tk}}. \qquad (6.3.46)$$

From formula (6.3.44) we see that the visibility after the interference filter is given by

$$\overline{V}_F = e^{-\frac{\xi^2}{4\sigma_{Tx}^2}}. \tag{6.3.47}$$

In order to study the behaviour of the visibility it is convenient to explicit the expression (6.3.46) in terms of known quantities. Recalling (6.3.40)

$$\sigma_{Tk}^2 = \frac{\sigma_{Sk}^2 \sigma_{Fk}^2}{\sigma_{Sk}^2 + \sigma_{Fk}^2}$$

and that the interferometric experiment is only meaningful when the bandwidth of the source is larger than the one of the filter

$$\sigma_{Sk} >> \sigma_{Fk}, \tag{6.3.48}$$

otherwise no interferences can be observed, the expression (6.3.40) can be simplified giving

$$\sigma_{Tk} \cong \sigma_{Fk}, \quad \text{and} \quad \sigma_{Tx} \cong \sigma_{Fx}, \tag{6.3.49}$$

That is, the output bandwidth of the beam is practically equal, as expected, to the one of the filter. From (6.3.46) we can write finally

$$\sigma_{Fx}\sigma_{Fk} \cong 1. \tag{6.3.50}$$

This last expression means that the product of the coherence length of the output beam, after the monochromator, by the bandwidth of the filter verify the usual uncertainty relations. Therefore, the better the filter, the shorter the bandwidth, and consequently according to (6.3.50) the larger the coherence length of the exit beam. In the limit, for a perfect monochromator $\sigma_{Fk} \cong 0$ the coherence length of the output beam would be infinite $\sigma_{Fx} \cong \infty$ conducing to a visibility one, $\overline{V}_F \cong 1$, no matter how long the optical path difference could be.

Let us suppose that in a concrete experiment the interference filter is such that the coherence length of the output beam is two times the optical path difference $\sigma_{Fx} = 2\xi$. For these concrete experimental conditions the interference visibility shall be of about 94%, which is nearly one hundred percent.

The above calculations for the outcome of this concrete asymmetric interferometric experiment do indeed conduce, as expected, to a significant interference visibility even in the case when the two wave packets do not overlap at the second mixing beamsplitter. This conclusion, as was stressed before, constitutes no surprise because is a direct consequence of the omnipresence of the monochromatic harmonic plane waves of nonlocal Fourier analysis that are the basic building blocks of the wave packets.

6.4 CAUSAL EXPLANATION

Now we are going to see how it is perfectly possible to interpret this so-called nonlocal interference in terms of a causal local rational explanation without need of invoking fussy retroactions in time and so. An explanation without mysteries and spooky actions in the past is indeed possible if one avoids the many traps laid by the abusive utilization of the common Fourier paradigm.

The first attempt to explain the nonlocal interference in a causal way was presented by Lepore in terms of the linear approach of de Broglie. Still, this explanation was done using the nonlocal Fourier epistemology implying that the guiding physical wave of de Broglie ought to be approached by a monochromatic harmonic plane wave.

A causal local explanation without spooky actions comes out naturally if one looks more careful at the physical conditions of the experiment. The orthodox standard reasoning, as usual, overlooks certain key experimental facts. This is perfectly understandable because their aim is not to present a coherent picture of the facts. On the contrary, most authors enjoy presenting a somewhat confusing, inexplicable image of the facts whenever they can.

What are these concrete key theoretical and experimental facts behind the so-called nonlocal interferometric experiment?

1 – The concrete action of the monochromator filter corresponds to a selection, from the initial large group of waves composing the incident packet, of a smaller group of waves. For an ideal monochromator only a single wave with a well-defined frequency would be selected. In this last ideal case two possibilities remain open:

(a) Fourier straight paradigm.

In this case the monochromator selects, from the initial ensemble, one single probability monochromatic harmonic plane wave with a well-defined frequency. Since this wave has an infinite spatial width no matter how large the optical path difference the two potential probability waves always overlap at the interferometer.

(b) Wavelet local paradigm.

The action of the monochromator corresponds to the selection of one finite wavelet with a well-defined frequency. In this approach as long as the optical path difference is shorter than the width of the wavelet interferences are to be seen. Nevertheless if the optical path difference between the two arms of the interferometer is greater than the length of the wavelet no overlapping occurs and consequently no interference is observed.

2 – The beam entering the Mach-Zehnder interferometer has an intensity much greater than the intensity of the output beam. This reduction in amplitude of the output beam relative to the incident one is a function of the bandwidth of the monochromator interference filter. The shorter the filter bandwidth the greater the reduction in intensity of the output beam.

3 – From the previous points one gathers that in the concrete experiment with an observable interference pattern there is always overlapping of the selected waves at the mixing region. Even in the Copenhagen paradigm this overlapping occurs contrary to what is suggested in words. The same always-present overlapping is, in general, somehow confused and shadowed by the abusive use of mathematics by most authors incorrectly using the orthodox approach.

In the nonlocal and, we must stress, nontemporal Fourier paradigm these assertions, of nonlocal interference and retroactions in time, correspond in fact to an overstatement. Since time and space play no key role in this

approach no real separation in space and time is ever possible. Any entity includes all time and is present in all space. In this sense, as we have already pointed out, separability is only a hoax, an illusion of our senses.

The local causal approach states that interference is always the result of a real physical superposition of two finite waves. These finite real physical waves, selected by the monochromator, overlap whenever the difference between the two optical paths is shorter than the length of the wavelets.

4 – Another important point to notice is the distinction between the concept of interference and visibility. Interference occurs whenever two or more finite real waves occupy at a certain time the same region of space. If two waves physically overlap they do indeed interfere, that is, interact. In this case the instantaneous visibility is different from zero. It happens that sometimes this interference is shadowed by the noise produced by other not correlated waves. When other group of waves coming from the source and arriving later at the mixing zone do not have the same phase relationship the interference pattern do not occurs at the same position. In such conditions after a large number of arrivals the interference pattern of the single pair of waves is completely cancelled out. The interference is always there, only we cannot see it. We are not able to observe the hidden interference pattern, with the usual means, because it is confused, mixed with the noise. In this case the visibility, the average visibility, shall be zero. The concept of visibility is usually associated with the average observable interference.

Having presented the principal key factors involved in any interferometric experiment the causal local explanation follows directly:

The source emits in a random way particles each one with a well-defined energy described by a finite wave. The width of these wavelets σ_0 needs always to be greater than the optical path difference between the two arms of the interferometer otherwise no interference will be observed. Nevertheless, the whole pulse of many particles emitted by the source is described by a pack of wavelets. This pack of wavelets corresponds to a kind of average over the whole ensemble of particles of the burst. The size of this average pack of wavelets has, as we have seen, a shorter width $\sigma_x \leq \sigma_0$ given by the generalized uncertainty relations

$$\sigma_x^2 = \frac{1}{\sigma_{Sk}^2 + \frac{1}{\sigma_0^2}}. \tag{6.4.1}$$

The interferometric experiment is done when the optical path difference is greater than the width of the pack of wavelets $\xi > \sigma_x$. Apparently and accordingly to what most authors lead us to believe this condition would imply that the waves do not have any possibility of physically overlapping. Nothing more wrong and farther from the truth! It is only an unfair tricky way to hide what really happens with a deviating confusing smoke curtain. The physical real waves are the wavelets with a size greater than the optical path difference $\sigma_0 > \xi$. In this situation they are able to superimpose more or less partially at the mixing region. The pack of wavelets bears no real physical meaning; it corresponds only to an average statistical description for the ensemble of individual real wavelets.

In order to recover the interference pattern out of the surrounding noise, by introducing a monochromator, it is necessary that the optical path difference be less than the size of the individual wavelets representing the particle $\xi < \sigma_0$. Only in this case the waves have possibility of overlapping and consequently of interacting, producing an interference pattern that by means of an adequate filter is rendered observable. In this circumstances when the monochromator reduces the spatial frequency bandwidth, increasing concomitantly the size of the average pack of wavelets, the practical result is a filtering with a reduction of the noise of the observable interference pattern. By selecting from the large ensemble only a small number of wavelets the interference of the single wavelets can indeed be observed.

A similar situation happens in a crowd gathering with each one talking at the same time. We cannot pick out a single intelligible conversation because of the all-present background noise. Nevertheless if by means of some device one is capable of isolating out of the mob a single person or a small number of people then we will be able to understand what they say.

Again the reader interested only in the basic concepts underlying the causal model can skip the detailed calculations supporting what was stated in words.

The calculations for the expected intensity in the causal local approach are practically the same as those using Fourier nonlocal analysis for the case when no monochromator is placed after the interferometer. The difference here is that the starting point is not the monochromatic harmonic plane wave but instead the wavelet that has a mathematical expression similar to formula (6.3.3)

$$\psi_0 = A_0 e^{-\frac{(x-ct)^2}{2\sigma_0^2}} e^{i(kx-\omega t)}. \tag{6.4.2}$$

This expression now stands for the wavelet that describes the extended size of the quantum particle entering the interferometer. The size of this finite wave is given by σ_0.

The total pack of wavelets coming from the source is described precisely by a formula similar to (6.3.3)

$$\psi_0 = A_0 e^{-\frac{(x-ct)^2}{2\sigma_x^2}} e^{i(kx-\omega t)}, \tag{6.4.3}$$

analogous calculations lead us to formally the same expected intensity

$$I_c = \frac{1}{2} I_0 (1 + e^{-\frac{\xi^2}{4\sigma_x^2}} \cos\delta), \tag{6.4.4}$$

with a visibility at the output port, without placing the filter after the interferometer,

$$V_c = e^{-\frac{\xi^2}{4\sigma_x^2}}, \tag{6.4.5}$$

which is also formally alike. Only now σ_x, stands for the size of the pack of wavelets which expression is given by the generalized uncertainty relations expressed by formula (6.4.1).

When the interference filter is placed after the interferometer things are rather different. The action of the optical filter is, in this approach, quite clear. From the large ensemble of particles coming from the source and having different energies, corresponding concomitantly to different spatial frequencies, the device selects, filters, only those that fall in its allowed bandwidth. In such circumstances the particles arriving at the detector

correspond to the sum of all particles, emitted by the source, that are able to cross the filter.

In such circumstances the action of the filter on a single particle can be expressed by

$$I_F^c = \frac{1}{2} I_0 e^{-\frac{(k-k_0)^2}{\sigma_{Fk}^2}} \left(1 + e^{-\frac{\xi^2}{4\sigma_0^2}} \cos(k\xi - \phi)\right), \tag{6.4.6}$$

and the total output beam of particles after the interference filter is given by averaging over the emission distribution of the source

$$S(k) = \frac{A_0}{\sqrt{\pi}\sigma_{Sk}^2} e^{-\frac{(k-k_0)^2}{\sigma_{Sk}^2}}. \tag{6.4.7}$$

Therefore the mean intensity seen by the detector is

$$\bar{I}_F^c = \int_{-\infty}^{+\infty} S(k) I_F^c(k)\, dk\,. \tag{6.4.8}$$

which by substitution gives

$$\bar{I}_F^c = \frac{A_0 I_0}{2\sqrt{\pi}\sigma_{Sk}} \int_{-\infty}^{+\infty} e^{-\frac{(k-k_0)^2}{\sigma_{Sk}^2}} e^{-\frac{(k-k_0)^2}{\sigma_{Fk}^2}} \left(1 + e^{-\frac{\xi^2}{4\sigma_0^2}} \cos(k\xi - \phi)\right) dk \tag{6.4.9}$$

or

$$\bar{I}_F^c = \frac{A_0 I_0}{2\sqrt{\pi}\sigma_{Sk}} \int_{-\infty}^{+\infty} e^{-\frac{(k-k_0)^2}{\sigma_{Tk}^2}} (1 + e^{-\frac{\xi^2}{4\sigma_0^2}} \cos(k\xi - \phi)) dk \quad (6.4.10)$$

where, as before, we have made

$$\sigma_{Tk} = \frac{\sigma_{Sk}\sigma_{Fk}}{\sqrt{\sigma_{Sk}^2 + \sigma_{Fk}^2}} \cong \sigma_{Fk} . \quad (6.4.11)$$

because, in the experiment, the bandwidth of the filter is smaller than the one of the source, $\sigma_{Sk} >> \sigma_{Fk}$.

The integration of (6.4.10) gives

$$\bar{I}_F^c = A_F (1 + e^{-\frac{\xi^2}{4\sigma_{Fx}^2}} \cos\delta') , \quad (6.4.12)$$

with

$$\sigma_{Fx}^2 = \frac{1}{\sigma_{Fk}^2 + \frac{1}{\sigma_0^2}} , \quad (6.4.13)$$

and, as previously, the constant parameters have the form

$$A_F = \frac{\sigma_{Tk} A_0 I_0}{2\sqrt{\pi}\sigma_{Sk}}, \quad \delta' = k_0\xi - \phi . \quad (6.4.14)$$

From formula (6.4.12) we see that the causal visibility after the interference filter is given by

$$\bar{V}_F^c = e^{-\frac{\xi^2}{4\sigma_{Fx}^2}}, \tag{6.4.15}$$

expression formally similar to the one (6.3.47) obtained in the orthodox paradigm. The difference between the two approaches lies only on the meaning of the width of the gaussian. In the orthodox approach it is related to the usual uncertainty relations $\sigma_{Fx}\sigma_{Fk} = 1$, while in the causal description of nature the width of the same gaussian is connected with the generalized uncertainty relations given by expression (6.4.13). Furthermore we gather that everything happens as if the first expression obtained for the visibility (6.3.29) without placing the monochromator after the interferometer formally holds for the two approaches needing only to change the width of the gaussian by the appropriate expression.

6.5 EXPERIMENTAL TEST FOR THE TWO APPROACHES

From the above we gather that it is perfectly possible to explain the so-called nonlocal interferences either in the Copenhagen orthodox picture or in the causal approach. Once more we are faced with two alternative opposite interpretations for the same observable facts. At this point it would be interesting to see if the experiment could be improved in such a way that it could eventually distinguish between the two approaches.

A relatively easy improvement of the experiment making it decisive seems indeed possible. The crucial experimental difference between the two approaches was already stated and comes out from the following facts:

(a) In the Copenhagen Fourier nonlocal and nontemporal approach one predicts always interference if the monochromator is good enough. For an ideal monochromator $\sigma_{Fk} \cong 0$ the optical path difference ξ can be made as large as one wishes. In this case the coherence length of the wave is infinite $\sigma_{Fx} \cong \infty$ and therefore the expected visibility is always one hundred per cent.

(b) In the causal local approach of de Broglie with finite waves interference only occurs when the real physical wavelets overlap at the second beamsplitter. The action of the ideal monochromator is to select, to isolate, one single wavelet with a well-defined spatial frequency. Yet this wavelet, contrary to the infinite monochromatic harmonic plane waves, has indeed a finite size. As a consequence, if the optical path difference is larger than the width of the wavelet no overlapping occurs and therefore no interference is to be observed.

Under these circumstances it is relatively easy to devise an in principle decisive experiment to test the two approaches.

The experiment is relatively easy to improve and it consists on introducing better and better monochromators in front of the interferometer and then compare the observed intensity with the predictions.

Writing explicitly the visibilities predicted by the two approaches in terms of known parameters we get:

Orthodox nonlocal Fourier usual visibility

$$V_o = e^{-\frac{\xi^2}{4/\sigma_{Fk}^2}}. \tag{6.5.1}$$

Causal local visibility

$$V_c = e^{-\frac{\xi^2}{4/(\sigma_{Fk}^2+1/\sigma_0^2)}}. \tag{6.5.2}$$

Recalling the meaning of the symbols we have σ_{Fk} standing for the bandwidth of the interference filter that is placed after the interferometer, σ_0 for the size of the entering wavelet, describing the extended part of the quantum particle in de Broglie causal approach, and ξ standing for the optical path difference between the two arms of the asymmetric Mach-Zehnder interferometer.

The plot of these two visibilities is shown in Fig.6.8. In the first one we see that the visibility predicted by the usual standard approach V_o when the

bandwidth of the interference filter σ_{Fk} approaches zero and remains equal to one for any value of the optical path difference.

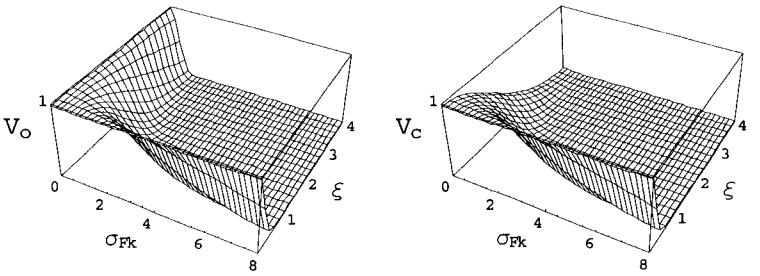

Fig.6.8 – Plot of the visibilities predicted by the two approaches.

The second plot, for the visibility predicted by the causal approach was done for an arbitrary chosen fixed value of the size of the basic wavelet.

In the next plot shown in Fig.6.9 the difference

$$\Delta = V_o - V_c \tag{6.5.3}$$

between the two predicted visibilities is shown for three different increasing values of the size σ_0 of the wavelet representing the extended part of the real causal quantum particle.

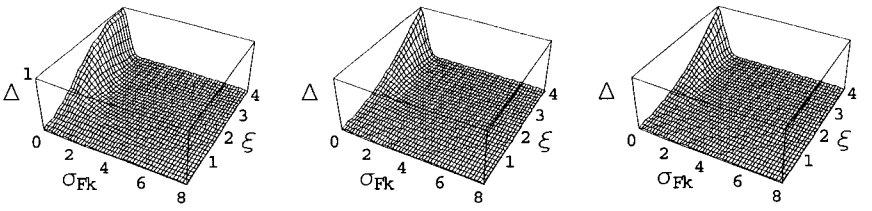

Fig.6.9 – Plot of the difference in the predictions of the two approaches for three different increasing values of the size of the wavelet.

From the plots we see that when the size of the wavelet increases the difference in the predictions tends to cancel out. This result is no surprise because as we know the general uncertainty relations approach the usual Fourier orthodox ones when the size of the basic wavelet increases.

The major inconvenience of this testing experiment is that the outcoming result could not, in any case, go against the causal approach. Since we do not know the size of the wavelet it is always possible to increase its size to fit the experimental results. Only in the case when the experimental results could not be fitted by the orthodox formula could the experiment be conclusive and furthermore it would allow us to experimentally determine the size of the wavelet.

In order to surpass this problem J. Marto has being studying the influence of spectral modifications. The differences in predictions for spectral modulation may lead to conclusive experiments.

6.6 FRANSON TYPE EXPERIMENTS

Another very interesting class of experiments where interference effects are observed without apparent overlapping of the wave packets is the one developed for the first time by Franson, and since then performed in other variants by diverse researchers. The basics of this type of experiments is shown in next figure, Fig.6.10

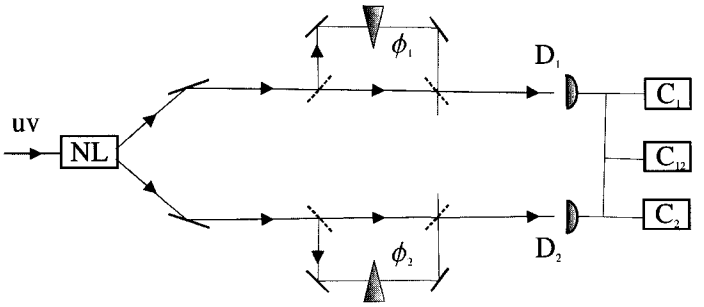

Fig.6.10 – Franson type experiment.

Two particles correlated in time are emitted from a non-linear crystal, or by some other means, and then each is directed to independent asymmetric interferometers. The optical path difference is such that the wave packets have no possibility to overlap at the mixing beamsplitter. In such conditions no second order interference is observed at detectors D_1 and D_2. Second order interference is the common interference resulting from the correlation between two fields. In plain words it means that the counting rates at the

detectors D_1 and D_2 do not depend on the phase shift. This is a consequence of the fact that since the two wave packets do not overlap at the second beamsplitter of the interferometer, no interference is expected no matter what phase shift is introduced.

Suppose now that we make coincidence counting between the outputs of the two detectors. The question that rises is whether this coincidence counting, read at C_{12} depends on the relative phase shift introduced in each independent interferometer?

In a first naïve approach we would be led to say that the counting coincidence rate would be independent on the relative phase shift. Yet every experiment of this type yields coincidence counting rate dependence on the relative phase shift.

How can we account for this kind of interference without superposition of the wave packets?

The nonlocal and nontemporal orthodox approach is perfectly able to arrive at an explanation and prediction for the outcome of the experiments.

The question is if this type of experiments can be explained in the causal local framework of de Broglie.

A local causal explanation is being developed by Marto. Nevertheless and because of it here I will limit myself only to indicate the main line of reasoning leading to the causal explanation.

A careful look at the real situation shows that this experiment is in a way much similar to the nonlocal interferometric experiment discussed earlier. In the two experiments we do observe interference without apparent superposition of the wavepackets. Yet we have shown, in the first case, that there is indeed actual physical superposition of the real physical wavelets that constitute the average pack of wavelets. The practical action of the monochromator filter is to select from among the initial large group a small subgroup of wavelets, thus eliminating the noise so that the interference can be observed. In this second type of experiments the role of the monochromator is now played by the coincidence window, which acts as a temporal filter. In these circumstances the coincidence window isolates from the large ensemble a smaller correlated subgroup having as final consequence the reduction of the noise. Experiments show that for a very large temporal coincidence window no interferences are observed.

Let us recall the former example of a large group of people each talking, almost at the same time, so that nothing can be perceived, mixed up in the general clamour. The equivalent to the monochromator filter of the first experiment would be a kind of physical device able to isolate one or few a

people, blocking them away from the crowd, so that some meaning could be picked out of their talking. The temporal coincidence window, of the Franson type of experiments, would act, in this case, as a kind of temporal selection just like a succession of very quick stroboscopic sound pictures. This action would allow, us, by an adequate selection, to isolate one or a few conversations thus eliminating the overall noise produced by the other people.

6.7 REFERENCES

On the weird "Magic" of quantum mechanics:

P. Kwiat, H. Weinfurter, T. Herzog, A. Zeilinger and M. A. Kasevich, Phys. Rev. Lett. 74(1995)4763.
P. Kwiat, H. Weinfurter and A. Zeilinger, Quantum seeing in the dark, Scientific American, November, 1996, p. 52.

On nonlocal interference:

Kaiser, R. Clothier, S. A. Werner, H. Rauch and Wölwitch, Phys. Rev. A 45 (1992)31.
H. Rauch, Il Nuovo Cimento B110, (1995) 557.
V.L. Lepore, in Waves and Particles in Light and Matter, Eds. A. Garuccio and A. van der Merwe, Plenum Press, New York, 1994.
J.R. Croca, R. Moreira and A.J. Rica da Silva, in Causality and Locality in Modern Physics, Eds. G. Hunter et al. Kluwer Academic Publishers, 1998.
W. Tiller, Appl. Opt. 23 (1994)3931.

Nonlocal nontemporal interference:

J.D. Franson, Phys. Rev. Lett. 62 (1989)2205.
J.D. Franson, Phys. Rev. A 44 (1991)4552.
Z.Y. Ou, X.Y. Zou, L.J. Wang and L. Mandel, Phys. Rev. Lett. 65(1989)321.
Z.Y. Ou and L. Mandel, J. of Optical Society of America B (1990)2127.
P.G. Kwiat, W.A. Vareka, C.K. Hong, H. Nathel and R.Y. Chiao, Phys. Rev A 41(1990)2910.

AUTHOR INDEX

Andrade e Silva, J. 35, 38, 132, 144, 178
Binning, G. 50, 56
Bohm, D. 38, 65, 70, 129
Bohr, N. 1, 2, 6, 7, 18, 23, 26, 27, 28, 32, 35, 37, 57, 65, 79, 91, 105, 119, 120, 121, 122, 128 130, 135
Born, M. 23, 39, 56
Broglie, L. de, 7, 27, 34, 38, 59, 65, 66, 68, 70, 71, 76, 77, 80, 82, 87, 94, 99, 109, 116, 122, 129, 131, 132, 133, 134, 135, 139, 141, 145, 148, 152, 154, 157, 161, 163, 164, 166, 167, 169, 170, 173, 178, 198, 206, 209
Comsa, G. 113, 130
Croca, J.R. 129, 157, 163, 178, 210
Dirac, P. 15, 24, 34, 38, 94, 131, 179
Einstein, A. 27, 34, 59, 71, 80, 131, 137
Franson, J. 208, 210,
Garuccio, A. 141, 143, 157, 163, 176
Glauber, R. 160, 178
6, J. 49, 57
Gosh, A. 171, 178
Grossmann, A. 59, 128
Gueret, Ph. 71, 76, 129
Guerra, F. 76, 129
Heisenberg, W. 4, 7, 8, 23, 27, 28, 35, 36, 37, 40, 57, 58, 79, 94, 105, 106, 108, 109, 112, 115, 116, 119, 120, 121, 122, 125, 128, 129,
Hilgevoord, J. 28, 30, 38
Jammer, M. 28, 38
Jeffers, S. 172, 173, 178
Kwiat, P. 181, 210
Lanz, M. 39, 56
Lepore, V. 157, 178, 198, 210
Mackinnon, L. 71,
Mandel, L. 137, 142, 157, 160, 161, 162, 163, 178
Marto, J. 208, 209
Meyer, 59
Moreira, R. 129, 157, 178
Morlet, J. 59, 64, 83, 95, 96, 99, 128
Neumann, J. von, 65, 129
Pfleegor, 142
Plank, M. 27
Pohl, D. 39, 53, 54, 56, 121
Popper, C. 35, 38
Pusterla, M. 76, 129
Radloff, W. 142, 179
Rapisarda, V. 141, 143

Rauch, H. 113, 130, 184, 185, 210
Renninger, W. 21, 38, 182,
2da Silva, A, 75
Roher, H: 50, 56
Scheer, J. 109, 130
Schrödinger, E. 5, 7, 68, 69, 71, 72, 76, 77, 79, 80, 82, 83, 84, 86, 95, 109, 131, 132
Selleri, F. 130, 132, 140, 143, 163, 178
Smolin, L. 76, 129
Uffink, J. 28, 30, 38
Vigier, J-P. 71, 76, 129
Wolf, E. 47, 56, 147
Zeilinger, 181, 210

SUBJECT INDEX

Abbe's rule, 39, 40, 42
amplification power, 41
analyser, 20
analysis of a function, 9, 60, 61, 62, 63
annihilation operators, 159
atomic force microscope, 51
bandwidth, 23, 24
big bang, 169, 70
Bohr's interpretation, 7, 18
carrying wave, 83, 84, 88
causal local interpretation, 59, 66, 70
causal quantum particle, 66, 68, 79, 82, 83, 85, 87
coherent detection, 142, 143, 148
collapse of the wave packet, 16
common Fourier microscope, 40
complementarity principle, 7, 18, 23, 25, 27, 57, 128
conceptual experiments, 144
constant, universal, *M*, 70
continuity equation, 74
Copenhagen interpretation, 7, 18
correspondence rules, 14
crucial experiments, 71, 132
crystal analyzer, 185
Dirac delta function, 15
Doppler effect, 170
double slit experiment, 16, 66, 133
duality wave particle, 7, 12, 13, 17
eigenfunctions,14
eigenvalues, 14
empty wave, 83
Fabri-Perot Etalon, 164
Fourier nonlocal analysis, 8, 62, 90
Fraunhofer diffraction pattern, 43, 44
frustrated total reflection, 49
fundamental state for the free particle, 133
general uncertainty relations, 94, 103, 106, 107, 108, 109, 121
generator of theta waves, 136, 139, 141
guiding formula, 70
guiding wave, 83, 84, 86
Hamilton Jacobi equation, 69, 73, 74, 81
Heisenberg's measurement space, 105, 106, 125
Heisenberg's microscope, 121
Heisenberg-Bohr's uncertainty relations, 7, 8, 23, 27
Hubble constant, 168
impossibility theorems, 65
incoherent detection, 144, 148
indeterminist
nonlocal interpretation, 7, 18, 20, 35, 37

interaction-free experiments, 181
interaction free measurements, 21, 22, 23
interferential filters, 164
local paradigm, 90, 93, 121
Mach-Zehnder interferometer, 151, 152, 157, 174, 175
matrix mechanics, 7, 79
meaning of the wave function, 131
measurements of first kind, 52, 53
measurements of second kind, 52, 53, 54
measurements without physical interaction, 21
mexican hat wavelet, 64
Michelson interferometer, 151
mind, 23
monochromator, 36, 183
monoparticle source, 136, 137, 144
Morlet, gaussian wavelet, 64, 83, 95, 96, 99
neutron interferometer, 185
no-go theorems, 65
nonlinear crystal, 137, 157
nonlinear master Schrödinger equation, 68, 77, 80
nonlocal Fourier paradigm, 116
nonlocal interference, 181
nonlocality, 7, 8, 11, 13, 20, 22, 23, 35, 59
observer, 17, 23
operators correspondence rule, 13, 14
optical ring, 110
optical stethoscopy, 39
orthodox interpretation, 7, 18, 20, 34, 35, 37, 38
parametric down conversion,137, 157
particular solutions of nonlinear equation, 80, 81
photographic camera, 42
photon ring experiment, 109
photonic condenser, 110
power spectrum, 93
probability waves, 131
quadratic detector, 67, 68, 84
quantum measurement, 14, 15, 16, 19, 20, 21, 23, 30, 35, 36, 38, 57, 110
quantum operators, 13, 14
quantum optics, 157, 159
quantum paradoxes, 59
quantum potential, 57, 72, 76
quantum teleportation, 181
Rayleigh's criteria, 39, 42, 45, 46, 48
real waves, 131, 142, 148
recovering the interference pattern, 201
rectangular function, 10
redshift, 170, 172
resolving power, resolution, 39, 40, 41, 42, 45, 47
retroaction in time, 181, 182, 186
scanning optical microscope, 53, 68
Schrödinger equation, 69, 70
singularity, particle's singularity, 68
solutions of the nonlinear equation, 80
spooky actions, 198
spreading of matter wave packets, 109, 112, 113, 114, 115

subquantum medium, 83, 87, 116, 165, 166, 167, 170, 173
superposition principle, 75
super-resolution microscopes, 49, 50, 51, 52, 54, 55, 56
super-resolution optical microscope, 55, 56, 122, 125, 127, 128
synthesis of a function, 9
theory of the double solution, 66, 76
theta wave, 82, 83, 114, 139, 140, 141, 142 144, 147, 148, 149, 150, 151, 152, 153, 155, 162, 163, 164, 165, 166, 168, 173,
tired light model, 169, 170
triple slit experiment, 145
tunnel effect, 50,
tunneling electron super-resolution microscope, 49
two-slit experiment, 16, 133
unification of classical and quantum physics, 78
visibility, 147
wave mechanics, 7, 79
wavelet local analysis, 59, 93
wavelet measurement space, 107, 128, 106
yes-or-no experiment, 140
zero point field, 166, 170

TOWARDS A NONLINEAR QUANTUM PHYSICS

The author of this book presents conceptual and experimental evidence showing that Heisenberg's uncertainty relations are not valid in all cases. Furthermore, he derives a more general set of uncertainty relations. The new relations result from the replacement of the Fourier nonlocal and nontemporal paradigm by wavelet local analysis. These results lead to a coherent and beautiful causal synthesis unifying quantum and classical physics.

World Scientific
www.worldscientific.com
5141 hc

ISBN 981-238-210-0
9 789812 382108